Vol. 30 No. 1

Science Diliman

January-June 2018

UP Diliman OVCRD ISSN 0115-7809

Office of the Vice-Chancellor for Research and Development
University of the Philippines Diliman
Lower Ground Floor, PHIVOLCS Bldg.
C.P. Garcia Ave., Diliman, Quezon City 1101, Philippines
http://www.ovcrd.upd.edu.ph

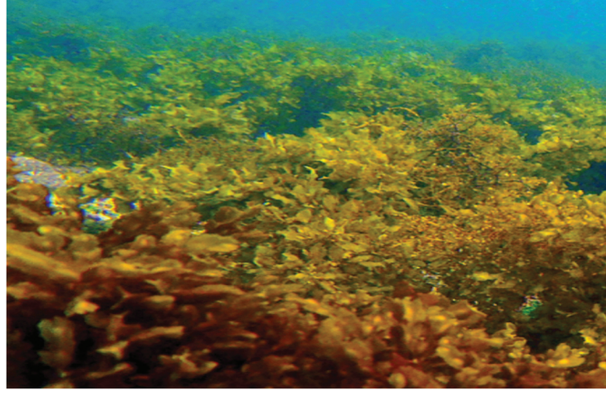

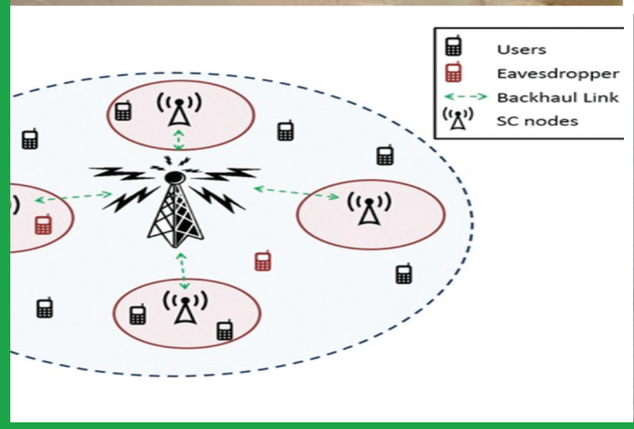

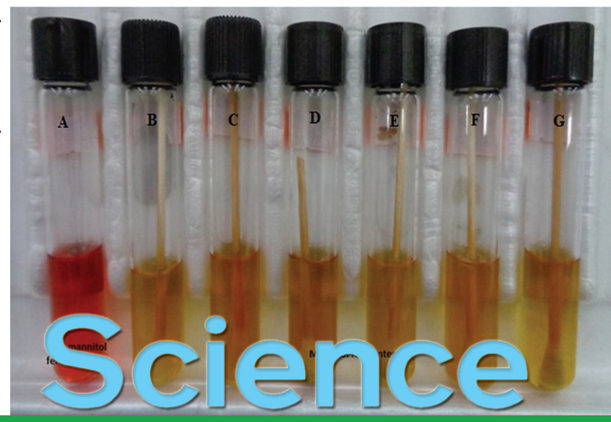

Science Diliman

A Philippine Journal of Pure and Applied Sciences • January-June 2018 • Vol. 30 No. 1

ARTICLES

Low-Complexity Physical Layer Security Scheme for Heterogeneous Cellular Networks based on Coordinated Precoding Design and Artificial Noise Generation
Neil Irwin M. Bernardo and Franz de Leon

Feeding Habits of *Mobula japanica* (Chondrichthyes, Mobulidae) in Butuan Bay, Mindano Island, Philipines
Shirlamaine Irina G. Masangcay, Ephrime B. Metillo, Ken-Ichi Hayashizaki, Satoru Tamada and Shuhei Nishida

Fucoidan Content in Philippine Brown Seaweeds
Joemark T. Narsico, Joyce A. Nieva, Alper James G. Alcaraz, Eladio G.M. Anino V, Norchel Corcia F. Gomez and Marco Nemesio E. Montaño

***Staphylococcus aureus* and Methicillin-resistant *S. aureus* (MRSA) carriage in Public Computer Service Providers and Utility Jeepneys in UP Diliman**
Jann Eldy L. Daquioag, Ricardo Benedict C. Almirol, Mary Grace G. Ayala, Ma. Socorro Edden P. Subejano and Gil M. Penuliar

SHORT COMMUNICATION

Population Structure of the Krill Prey of the Spinetail Devil Ray *Mobula japanica* (Chondrichthyes, Mobulidae) from Southeastern Bohol Sea, Philippines
Shirlamaine Irina G. Masangcay, Ephrime B. Metillo and Shuhei Nishida

Science Diliman

ISSN 0115-7809 January-June 2018 • Vol. 30 No. 1

Science Diliman is published semi-annually (June and December) by the University of the Philippines Diliman through the Office of the Vice-Chancellor for Research and Development. The journal features articles of pure and applied sciences.

On the Cover:
Images from the researches of Metillo et al., Montaño et al., Penuliar et al. and Bernardo and de Leon.

FROM THE EDITOR

Welcome to the first issue of *Science Diliman* for 2018. Let me share the good news that *Science Diliman* is now included in the ASEAN Citation Index database. *Science Diliman* is also indexed in the Emerging Sources Citation Index and is a recipient of the Journal Incentive Program (JIP) by the Commission on Higher Education.

This issue includes four main articles and a short communication. The first article by authors Bernardo and de Leon considers a cellular system design deployment called HetNets (heterogeneous network) as viable solutions to meet the demands of 5G, the next generation of cellular system. HetNets are networks connecting computers and other devices with different operating systems and/or protocols. In the second article, authors Masangcay et al. studied the feeding biology of Spinetail Devil Ray *(Mobula japanica*) belonging to the genus *Mobula*. Species of this genus are commonly called devil rays or flying rays. They feed mainly on tropical krills, locally known as *alamang*. In the short communication by the same authors, the focus of the study is on the krills and their spawning habits. The article by Narsico et al. determined that the brown macroalgae *Sargassum* spp. is the most widely distributed source of fucoidan and has higher content of partially purified fucoidan. Fucoidan is commercially available, and is known for its nutritional and health benefits. The last article by authors Daquioag et al. investigated the presence of *S. aureus* and methicillin-resistant *S. aureus* (MRSA) in computer service providers, computer peripheral, and handrails of Public Utility Jeepneys (PUJs). Interestingly, handrails of PUJs have the least carriage of *S. aureus*, while MRSA carriage is relatively low. Staph infections are treated by antibiotics and treatment becomes more complicated in MRSA infections.

Thank you to our authors and reviewers for their contributions to the increasing quality of articles in *Science Diliman*!

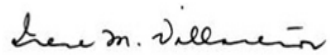

Irene M. Villaseñor, Ph.D.
Editor-in-Chief

ISSN 0115-7809 Print/ISSN 2012-0818 Online

Science Diliman (January-June 2018) 30:1, 1-3

LAYMAN'S ABSTRACTS

Low-Complexity Physical Layer Security Scheme for Heterogeneous Cellular Networks based on Coordinated Precoding Design and Artificial Noise Generation

Neil Irwin M. Bernardo and Franz de Leon

Heterogeneous Network (HetNet) deployment is a cellular system design approach in which multiple low power access nodes are underlaid in a traditional macro-cellular network. HetNets are able to provide substantial increase in cellular capacity and energy efficiency thus making it a viable solution to meet the demands in the next generation of cellular system, also known as 5G. In this study, we investigated how security can be incorporated into the downlink transmission (i.e. from telecommunications network to mobile phones) of HetNets while still maintaining their high cellular capacity and high energy efficiency properties. Our approach is to integrate information security, user data rate requirement, and power consumption of the HetNet's downlink transmission into a computationally-tractable convex optimization model. From the formulated model, we propose a security technique with suboptimal performance but with a computational complexity that is feasible for real-time implementation.

Feeding Habits of *Mobula japanica (Chondrichthyes,* Mobulidae) in Butuan Bay, Mindanao Island, Philippines

Shirlamaine Irina G. Masangcay, Ephrime B. Metillo, Ken-Ichi Hayashizaki, Satoru Tamada and Shuhei Nishida

We studied the feeding habits of the Spinetail Devil Ray *Mobula japanica*, locally known as Pantihan, from Butuan Bay, Eastern Bohol Sea from January to May 2016 using data on its stomach contents, and carbon and nitrogen stable isotope analyses. Small shrimp-like krill *Pseudeuphausia latifrons*, known locally as Alamang, contributed almost 100% to the devil ray's ingested food. Stable isotope analysis confirmed the specialized feeding and assimilation of the krill food. This study is the first to identify the swarming krill *P. latifrons* as the major food of the Spinetail Devil Ray in Butuan Bay.

ISSN 0115-7809 Print / ISSN 2012-0818 Online

Fucoidan Content in Philippine Brown Seaweeds

Joemark T. Narsico, Joyce A. Nieva, Alper James G. Alcaraz, Eladio G.M. Anino V, Norchel Corcia F. Gomez and Marco Nemesio E. Montaño

The Philippines is home to hundreds of seaweed species that serve as sources of high-value natural products, such as fucoidan. Fucoidan is a sulfated polysaccharide that can be extracted from the cell walls of brown seaweeds and is reported to have a wide range of bioactivities for possible medicinal applications. In this study, we assessed Philippine brown seaweeds as sources of fucoidan by determining which species or genera among local brown algae has the highest content of partially purified fucoidan and where these species can be found within the country. Fucoidan content from different species of brown seaweeds were determined in fifty sites across fourteen provinces in Northern Luzon (Cagayan, Ilocos), West Luzon (Pangasinan), the Eastern seaboard of Luzon (Quezon Province, Camarines, Sorsogon), Central and Eastern Visayas (Bohol, Cebu, Negros Oriental, Negros Occidental), and Northern Mindanao (Camiguin, Lanao del Norte, Misamis Oriental, Misamis Occidental). *Sargassum* spp., the most abundant in all sites, and *Turbinaria ornata*, found only in 11 sites, both have significantly higher content compared to the other samples. Similarly, higher content of semi-pure fucoidan were observed in brown seaweeds from Bohol, Cebu, Pangasinan, Quezon Province, Camiguin, and Cagayan.

Staphylococcus aureus and Methicillin-resistant *S. aureus* (MRSA) carriage in Public Computer Service Providers and Utility Jeepneys in UP Diliman

Jann Eldy L. Daquioag, Ricardo Benedict C. Almirol, Mary Grace B. Ayala, Ma. Socorro Edden P. Subejano and Gil M. Penuliar

Staphylococcus aureus is a bacterium that can cause serious infections. It is often found in solid objects, such as computer peripherals of computer service providers (CSPs) and handrails of public utility jeepneys (PUJs). *S. aureus* infections are often treated without complications, except

in cases where a particular strain called methicillin-resistant *S. aureus* (MRSA) is involved. In this study, the prevalence of *S. aureus* and MRSA in CSPs, computer peripherals, and handrails of PUJs inside UP Diliman, and associated risk factors for contamination were determined. *S. aureus* and MRSA were identified using morphological, biochemical, and molecular methods from 162 computer peripherals from 27 CSPs, and 196 PUJ handrails. *S. aureus* was identified in 92.6% of CSPs, 36.4% of computer peripherals, and 7.1% of PUJs, whereas MRSA was present in 3.1% of CSPs and 2% of PUJs. No significant associations between *S. aureus*/ MRSA and the assessed risk factors were observed ($p > 0.05$). Results indicate that, while *S. aureus* prevalence is relatively high, MRSA carriage is low in CSPs and PUJs in UP Diliman.

Population Structure of the Krill Prey of the Spinetail Devil Ray *Mobula japanica* (Chondrichthyes, Mobulidae) from Southeastern Bohol Sea, Philippines

Shirlamaine Irina G. Masangcay, Ephrime B. Metillo and Shuhei Nishida

While investigating the feeding habits of the Spinetail Devil Ray *Mobula japonica* in Butuan Bay, we found true krill (known locally as Alamang) as the main, often the only food item in the stomach of the ray. We identified the krill species as *Pseudeuphausia latifrons*. Information about the population of this krill species is very limited, thus this study was aimed at analyzing the size-composition of individuals collected from the stomach of the ray from January to May 2016. The total lengths of intact krill ranged between 4.0–6.9 mm for juveniles and 7.0–10.9 mm for adults. In general, males were larger than females. Juveniles were dominant until late March, and adults dominated by April and May. The largest male and egg-carrying female individuals also appeared during the warm months of April and May, indicating spawning during these months. This study provides evidence that individuals of the krill *P. latifrons* eaten by rays grow from juveniles to adults from January to May in Butuan Bay.

Science Diliman (January-June 2018) 30:1, 5-23

Low-Complexity Physical Layer Security Scheme for Heterogeneous Cellular Networks based on Coordinated Precoding Design and Artificial Noise Generation

Neil Irwin M. Bernardo*
Electrical and Electronics Engineering Institute
University of the Philippines

Franz de Leon
Electrical and Electronics Engineering Institute
University of the Philippines

ABSTRACT

The undertaking for higher capacity and seamless wireless connectivity in next-generation mobile networks while maintaining an energy-efficient transmission requires a fundamental redesign of the existing cellular architecture. Heterogeneous network (HetNet) deployment is a promising architectural framework for meeting these design goals. However, an increase in cellular capacity and device connectivity would also result in an increase of sensitive data and classified information being exchanged over the network, thus making security another critical aspect in cellular network design. In this study, a convex optimization model was formulated that minimizes the total power consumption of the network while satisfying certain level of per-user data rate requirement and information secrecy at the physical layer. From this model, a low-complexity physical layer security scheme was developed that exploits coordinated precoding design, artificial noise generation, and a suboptimal sleep mode strategy in HetNets. Simulation results show that joint optimization of coordinated precoding scheme and artificial noise generation is an effective approach for increasing cellular capacity while simultaneously lowering the transmit power of the base stations and risk of eavesdropping attacks. Incorporating sleep mode mechanism in physical layer security transmission scheme of HetNets also reduced the total power consumption while maintaining a

*Corresponding Author

ISSN 0115-7809 Print / ISSN 2012-0818 Online

secured and reliable communication during low traffic periods. Furthermore, our proposed physical layer security scheme exhibited significant reduction in computational complexity, but at the expense of slight performance degradation in terms of energy efficiency.

Keywords: Physical Layer Security, Heterogeneous Networks, Small Cells, 5G

INTRODUCTION

The rapid growth of the number of mobile devices and data traffic created a demand for cellular technologies that can provide extremely high data throughput and seamless wireless coverage. One approach to meet this demand is through the dense deployment of multiple low-power small cell access nodes (SCAs) in order to complement the performance of high-power base stations (BS), thus forming a heterogeneous network (HetNet) (Nigam et al. 2014). SCAs can be deployed on hot spots with high throughput demand to offload the traffic from the macro-cell BS or on coverage holes to ensure uninterrupted connectivity. This results in large cellular capacity improvement. Several studies have also shown that, with proper coordinated transmission and interference mitigation schemes, heterogeneous network deployment is an energy-efficient alternative to traditional macro-cell-only cellular architecture in meeting the data rate requirement of future wireless applications (Bjornson et al. 2013; Tang et al. 2015; Nguyen et al. 2016; Vu et al. 2016). Due to these advantages, several regulatory bodies, as well as some major players in telecommunication industry, have acknowledged heterogeneous network deployment as an enabler for fifth generation mobile networks or 5G (International Telecommunication Union 2014; Samsung Electronics Co. 2015).

Aside from improvements in energy and spectral efficiency, cellular network security has also become a significant concern in mobile networks. The increase in data traffic and number of connected device had increased the risk of data theft and eavesdropping as more and more confidential data are being exchanged over the network (Yang et al. 2015). Furthermore, the growth of Internet-of-Things (IoT) would also require a sufficient security scheme that is both computationally-efficient and energy-efficient for low-power IoT devices (Trappe 2015). Security solutions for wireless devices are traditionally implemented at the application layer in the form of cryptography. However, the performance of these cryptographic protocols is highly dependent on the assumption of limited computational power of the eavesdropper, thus introducing potential vulnerabilities to network's data confidentiality (Mukherjee et al. 2014).

An alternative approach to encryption strategies is to implement security at the physical layer (PHY) of the network. PHY security can provide a quantifiable and information-theoretic security to the network by exploiting the random characteristics of wireless channel. HetNets are able to provide reliable security at the physical layer using coordinated precoding design (Lv et al. 2015; Bernardo and De Leon 2016), resource allocation strategy (Shiqi et al. 2016), and artificial noise (AN) generation (Deng et al. 2015; Wang et al. 2016) in fending off eavesdropping attacks. However, most studies on PHY security performance of HetNets assume that SCAs are always in active mode. In an energy efficiency perspective, time periods with low user density and low traffic would leave multiple SCAs idle, thus resulting in wasted energy. In practice, SCAs have sleep mode mechanism to adapt with high spatiotemporal variations in user density and mobile data traffic (Hoydis et al. 2011). Furthermore, PHY security approaches presented in the work of Lv et al. (2015) and Bernardo and De Leon (2016) have very high computational complexity, making them infeasible to implement in multi-tier cellular networks with dense layer of SCAs. As such, there is a need to implement computationally-efficient PHY security solutions for HetNets that consider sleep mode capabilities of SCAs.

This study presents a low-complexity PHY security scheme for heterogeneous cellular networks. We formulate an optimization model that solves for the optimal precoding vectors and AN signals which minimize the total power consumption of a heterogeneous network, while satisfying the Quality-of-Service (QoS) requirement of every user, the transmit power limitations of macro-cell BS and SCAs, and a certain degree of secrecy against eavesdropping attacks. Moreover, an algorithm that incorporates the sleep mode capability of SCAs in precoding and an AN design to further reduce the total power consumption is proposed. To the best of our knowledge, no prior study has been done with regards to the development of fast and low-power PHY security techniques for HetNets that consider their sleep mode capability.

SYSTEM MODEL AND ALGORITHM FORMULATION

System Model for Heterogeneous Networks

We consider a single cell downlink scenario of a two-tier heterogeneous cellular network serving K authorized single-antenna user equipment (UE) (Figure 1). The macro-cell BS and SCAs are connected via a high capacity backhaul network which enables joint spatial soft-cell resource allocation (Parkvall et al. 2011; Bjornson et al. 2013). The backhaul network facilitates the information exchange and

interference coordination of the network. Furthermore, the BS and SCAs allow spatial multi-flow transmission so that a UE can be served by multiple BS. In spatial multi-flow transmission, the BS and SCAs convey the same information symbol for *k*th UE, denoted by S_k, but independently apply precoding on the information symbol before transmission (Holma and Toskala 2012). In addition, the macro-cell BS also transmits an AN signal to degrade eavesdropper reception. AN signals do not carry any user information and are only emitted for the sole purpose of disrupting the eavesdroppers. The transmitted signals of the macro-cell BS and SCAs are given by:

$$\mathbf{x_0} = \sum_{k=1}^{K} \mathbf{w_{k,0}}\, s_{k,0} + \mathbf{v_0} \quad \text{and} \quad \mathbf{x_j} = \sum_{k=1}^{K} \mathbf{w_{k,j}}\, s_{k,j} \tag{1}$$

where $w_{k,0} \in C^{N_{BS}X1}$ and $w_{k,0} \in C^{N_{SC}X1}$ are the precoding vectors of the BS and *j*th SCA, respectively. N_{BS} denotes the number of antennas at the macro-cell BS and N_{SC} denotes the number of antennas at each SCAs. $v_0 \in C^{N_{BS}X1}$ is the AN vector transmitted by the macro-cell BS.

K_{eve} single-antenna eavesdropping terminals are placed within the macro-cell and try to listen to the transmit signals x_0 and x_j. Furthermore, the eavesdroppers are assumed to be colluding; that is, an eavesdropper can share its observation of x_0 and x_j with other eavesdroppers. Collusion of eavesdroppers was modeled as a single eavesdropper with multiple antennas located at different locations in the cell

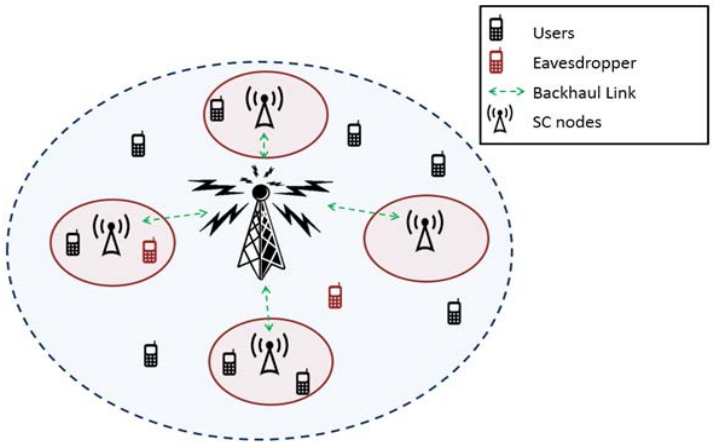

Figure 1. Illustration of a generic heterogeneous network: a macro-cell base station with NBS antennas and multiple small-cell access points communicate with *K* single-antenna UEs uniformly distributed over the macro-cell area.

(assuming that the received signals can be processed by a central node). This is similar to the colluding eavesdropper model presented in the work of Goel and Negi (2005).

The downlink transmission received by the *k*th UE can be expressed as:

$$y_k = \mathbf{h}_{k,0}^{H}\mathbf{x}_0 + \sum_{j=\text{all SC}} \mathbf{h}_{k,j}^{H}\mathbf{x}_j + n_k \quad (2)$$

where $h_{k,0}^{H} \in C^{1xN_{BS}}$ represents the channel from the macro-cell BS to *k*th UE and $h_{k,j}^{H} \in C^{1xN_{SC}}$ represents the channel from the *j*th SCA to *k*th UE. n_k is a zero mean circularly-symmetric complex Gaussian noise with variance σ_k^2. The signals received by the K_{eve} eavesdroppers are stored in a K_{eve}x1 vector y_{eve} given by:

$$\mathbf{y}_{eve} = \mathbf{H}_{eve,0}^{H}\mathbf{x}_0 + \sum_{j=\text{all SC}} \mathbf{H}_{eve,j}^{H}\mathbf{x}_j + \mathbf{n}_{eve} \quad (3)$$

The matrices $h_{eve,\,j}^{H} \in C^{KevexN_{BS}}$ and $h_{eve,\,j}^{H} \in C^{KevexN_{SC}}$ denote the channels from macro-cell BS to the eavesdroppers and from *j*th SCA to the eavesdroppers, respectively. n_{eve} is a K_{eve}x1 random vector that accounts for the noise at the eavesdroppers. The *kth*-element of vector y_{eve} denotes the received signal *kth* eavesdropper.

The Radio Frequency (RF) propagation model parameters are listed in Table 1, which mainly follow the works of Vu et al. (2016), Bernardo and De Leon (2016), and the RF propagation model presented in Small Cell Forum Release 7.0 document (Small Cell Forum 2012). The radio transmission from the BS and SCAs to the UE is a multi-carrier modulation scheme with a system bandwidth of 10 MHz and

Table 1. List of channel propagation parameters used to model the downlink transmission of Heterogenous Network

	Macro-cell	Small-cell
Cell Coverage	500m	40m
Distance-dependent Path Loss at distance d (in km) [NLOS]	151.1 + 42.8log(*d*) *dB*	145.4 + 37.5log(*d*) *dB*
Distance-dependent Path Loss at distance d (in km) [LOS]	123.4 + 24.2log(*d*) *dB*	103.8 + 20.9log(*d*) *dB*
LOS Probability	*Refer to Table 2-1 of Small Cell Forum Release 7.0 Document (2012)	
Std Dev for Log-normal Shadowing	4 dB (NLOS) , 3 dB (LOS)	
Carrier Frequency/Number of Subcarriers	2 GHz/600	
System Bandwidth/Subcarrier Bandwith	10 MHz/ 15 kHz	
Noise Power Density	-174 dBm/Hz (@ 5dB NF)	

subcarrier bandwidth of 15 kHz (similar to what is currently used in 4G cellular systems). Furthermore, it was also assumed that the separation between antenna elements is wide enough, such that users and eavesdroppers experience independent and identically distributed Rayleigh fading.

FORMULATION OF THE OPTIMIZATION MODEL

As a starting point in the formulation of the optimization model, the objective function presented in our previous work (Bernardo and De Leon 2016) was modified. The objective is to optimize the power consumption of the network, while satisfying the QoS constraints and PHY security requirement of each UE. The objective function in the model is the total power consumption, denoted as $P_{TOTAL} = P_{dynamic} + P_{static}$, where

$$P_{static} = \sum_{j=0}^{M} \left(P_{cir,j} N_{SC} + P_{idle,j} \right) \tag{4}$$

$$P_{dynamic} = \sum_{j=0}^{M} \rho_j \sum_{k=1}^{K} \left\| \mathbf{w_{k,j}} \right\|^2 + \rho_0 \left\| \mathbf{v_0} \right\|^2 \tag{5}$$

ρ_j

P_{static} is the static power consumption which models the total power dissipation due to RF circuitry of the macro-cell BS and *M* SCAs. $P_{cir,j}$ and $P_{idle,j}$ denote the per-antenna circuit power consumption and non-transmission power consumption of the *j*th BS, respectively. The dynamic power consumption, denoted as $P_{dynamic}$, accounts for the aggregated emitted power of the macro-cell BS and M SCAs. The parameter $1/\rho_j \leq 1,\ j \in [0, M]$ models the power amplifier efficiency at *j*th transmitter. Higher value of means lower power amplifier efficiency, thus resulting in higher transmit power. Since the amplitude of signal transmission at each antenna element is controlled by the precoding vectors, the dynamic power consumption is proportional to the power allocated to each precoding vectors. Furthermore, the model for the dynamic power consumption presented in this work also accounts for the power allocated by the macro-cell BS in generating the AN signals.

To limit the maximum allowable transmission power of the macro-cell BS and SCAs, transmit power constraints should be imposed on the optimization model. These transmission power limits can be represented using the following inequality constraints:

$$\sum_{k=1}^{K} \mathbf{w}_{\mathbf{k,j}}^{\mathbf{H}} \mathbf{Q}_{\mathbf{j,l}} \mathbf{w}_{\mathbf{k,j}} \leq q_{j,l} \quad \forall j \neq 0, \forall l = 1, \ldots, N_{SC} \tag{6}$$

$$\sum_{k=1}^{K}\left(\mathbf{w}_{k,0}^{H}+\mathbf{v}_{0}^{H}\right)\mathbf{Q}_{0,l}\left(\mathbf{w}_{k,0}+\mathbf{v}_{0}\right)\leq q_{0,l}\quad\forall l=1,\ldots,N_{BS}\qquad(7)$$

where (6) denotes the transmit power limit for each SCAs and (7) denotes the transmit power limit for the macro-cell BS. The terms $q_{j,l}$ and $q_{0,l}$ denote the transmit power limit imposed on the *l*th antenna element at the *j*th SCA and macro-cell BS, respectively. The main difference between the (6) and (7) is the inclusion of the AN signal term in the inequality. $\mathrm{Q}_{j,1}\in \mathrm{C}^{N_{SC}\times N_{SC}}$ and $\mathrm{Q}_{0,1}\in \mathrm{C}^{N_{BS}\times N_{BS}}$ are weighting matrices for the constraints. Since per-antenna transmit power limits are desired, the weighting matrices are only non-zero at the *l*th diagonal element and zero elsewhere.

In addition to transmit power constraints, data rate requirement of each user should be defined. As such, Quality-of-Service constraints are included in the optimization model which specifies a minimum target for the information rate (in bits/s/Hz). These constraints can be defined as follows:

$$\log_2(1+\mathrm{SINR}_k)\geq\gamma_k,\quad\forall\, k=\{0,1,\ldots,K\}\qquad(8)$$

where γ_k is the minimum information rate that the *k*th UE must satisfy; and SINR_k is the signal-to-interference and noise ratio at the kth UE, and can be expressed as:

$$\mathrm{SINR}_k=\frac{\sum_{j=0}^{M}\left|\mathbf{h}_{k,j}^{H}\mathbf{w}_{k,j}\right|^2}{\sum_{i\neq k}^{K}\left(\sum_{j=0}^{M}\left|\mathbf{h}_{k,j}^{H}\mathbf{w}_{i,j}\right|^2\right)+\left|\mathbf{h}_{k,0}^{H}\mathbf{v}_{0}\right|^2+\sigma_k^2}\qquad(9)$$

σ_k^2 denotes the noise power at the *k*th UE. Information symbols not intended to the *k*th UE, as well as non-information bearing AN signals, are treated as interference. The inequality constraint for the QoS is based from the well-known Shannon's capacity formula (Shannon 1948) which relates the theoretical limit for information rate to the received signal quality. This QoS constraint formulation has also been adopted in several research works (Bjornson et al. 2013; Lv et al. 2015; Bernardo and De Leon 2016; Nguyen et al. 2016).

Finally, a set of PHY security constraints that limits the signal quality at the eavesdroppers should be incorporated to the optimization model. This set of constraints can be expressed as:

$$\begin{aligned} &\mathrm{SNR}_{\mathrm{eve,k}} \le \delta_k \quad \forall \mathrm{k} \\ &where \ \ \mathrm{SNR}_{\mathrm{eve,k}} = \frac{\sum_{\mathrm{j=0}}^{\mathrm{M}} \left\| \mathbf{H}^{\mathbf{H}}_{\mathbf{eve,j}} \mathbf{w}_{\mathbf{k,j}} \right\|^2}{\left\| \mathbf{H}^{\mathbf{H}}_{\mathbf{eve,0}} \mathbf{v}_{\mathbf{0}} \right\|^2 + \sigma^2_{\mathrm{eve}}} \end{aligned} \tag{10}$$

δ_k is the maximum allowable signal-to-noise ratio (SNR) that the eavesdropper can detect from the downlink transmission of the *k*th UE. $\mathrm{SNR}_{\mathrm{eve,k}}$ describes the combined signal quality of the signals intended to the *k*th UE at the colluding eavesdroppers' side. $\mathrm{SNR}_{\mathrm{eve,k}}$ excludes the interference terms from signals intended to other UE, and is only degraded by the transmitted AN signal and eavesdropper noise power σ^2_{eve}. This was implemented to assume the worst-case scenario, wherein the eavesdropper can decouple the information for multiple UE. PHY security constraint in (10) is derived from the secrecy capacity formula given as:

$$C_s = \log_2(1 + \mathrm{SINR}_{\mathrm{k}}) - \log_2(1 + \mathrm{SNR}_{\mathrm{eve,k}}) \tag{11}$$

which follows the work of Lv et al. (2015). Secrecy capacity is the highest information rate at which the transmitter and the intended receiver can communicate while the eavesdroppers receive an arbitrarily small amount of information. Equation (11) also relates the secrecy capacity of the communication channel to the received signal quality of the eavesdroppers. Reduction of the signal quality at the eavesdroppers would increase the secrecy capacity. By setting a target secrecy capacity C_s and minimum QoS target γ_k, the lower bound value for δ_k can be obtained using the following expression:

$$\delta_k = 2\,\hat{}\,(\log_2(1+\gamma_k) - C_s) - 1 \tag{12}$$

Using the total power consumption in (4) and (5) as the objective function and inequalities (6), (7), (8), (10) as constraints, the optimization model can be formulated as:

$$\begin{aligned} &\min_{\mathbf{v_0}, \mathbf{w_{k,j}} \forall \mathrm{k,j}} \quad \mathrm{P}_{\mathrm{dynamic}} + \mathrm{P}_{\mathrm{static}} \\ &\mathrm{s.t.} \quad \log_2(1 + \mathrm{SINR}_{\mathrm{k}}) \ge \gamma_{\mathrm{k}} \quad \forall \mathrm{k}, \\ &\quad \sum_{\mathrm{k=1}}^{\mathrm{K}} \mathbf{w}^{\mathbf{H}}_{\mathbf{k,j}} \mathbf{Q}_{\mathbf{j,l}} \mathbf{w}_{\mathbf{k,j}} \le q_{j,l} \quad \forall j \ne 0, l, \\ &\quad \sum_{\mathrm{k=1}}^{\mathrm{K}} \left(\mathbf{w}^{\mathbf{H}}_{\mathbf{k,0}} + \mathbf{v}^{\mathbf{H}}_{\mathbf{0}} \right) \mathbf{Q}_{0,\mathbf{l}} \left(\mathbf{w}_{\mathbf{k,0}} + \mathbf{v}_{\mathbf{0}} \right) \le q_{0,l} \quad \forall l, \\ &\quad \mathrm{SNR}_{\mathrm{eve,k}} \le \delta_k \quad \forall \mathrm{k} \end{aligned} \tag{13}$$

The above optimization model is not a convex optimization problem due to the QoS constraints and PHY security constraints. As such, the model must be reformulated in order to be computationally tractable. Semi-definite relaxation trick, similar to what was used in the work of Bjornson et al. (2016), was applied to the model. By letting $W_{k,j} \in S_+^N = W_{k,j} W_{k,j}^H$, $V_0 \in S^N{}_+ = V_0 V_0^H$, and ignoring the requirement that $W_{k,j}$ and V_0 should be rank-1 matrices, the original optimization model is transformed to:

$$
\begin{aligned}
\min_{\mathbf{w}_{k,j} \forall k,j} \quad & \sum_{j=0}^{M} \rho_j \sum_{k=1}^{K} \mathrm{tr}(\mathbf{W_{k,j}}) + \rho_0 \mathrm{tr}(\mathbf{V_0}) + P_{\mathrm{static}} \\
\mathrm{s.t.} \quad & \sum_{j=0}^{M} \mathbf{h_{k,j}^H} \left(\left(1 + \frac{1}{\tilde{\gamma}_k} \right) \mathbf{W_{k,j}} - \sum_{i=1}^{K} \mathbf{W_{i,j}} \right) \mathbf{h_{k,j}} \geq \sigma_k^2 + \mathbf{h_{k,0}^H V_0 h_{k,0}}, \forall k \\
& \sum_{k=1}^{K} \mathrm{tr}\left(\mathbf{Q_{j,l}} \mathbf{W_{k,j}} \right) \leq q_{j,l}, \quad \forall l, 1 \leq j \leq M \\
& \sum_{k=1}^{K} \mathrm{tr}\left(\mathbf{Q_{0,l}} \left(\mathbf{W_{0,j}} + \mathbf{V_0} \right) \right) \leq q_{0,l}, \quad \forall l \\
& \sigma_{\mathrm{eve}}^2 + \mathrm{tr}\left(\mathbf{H_{eve,0}^H V_0 H_{eve,0}} \right) \geq \sum_{j=0}^{M} \mathrm{tr}\left(\mathbf{H_{eve,j}^H} \left(\left(\frac{\mathbf{W_{k,j}}}{\delta_k} \right) \right) \mathbf{H_{eve,j}} \right), \forall k
\end{aligned}
\tag{14}
$$

where $\tilde{\gamma}_k = 2^{\gamma_k} - 1$. The removal of rank constraint implies that multiple transmitters can serve a UE, which is justified since spatial multi-flow transmission is allowed in our system model. Furthermore, the constraints were transformed into linear matrix inequalities (LMI) which inherently have a convex structure. Thus, the resulting optimization model is a convex semi-definite program (SDP) and the global optimum solution can be solved numerically using convex solvers.

Design of Low Computational Complexity Algorithm for PHY security

The solution obtained from the derived optimization model in the previous section is our benchmark for the achievable performance of heterogeneous network. The solution to the benchmark model can be calculated in polynomial time. However, the problem becomes infeasible to implement in real-time if N_{BS} and N_{SC} have large values. Thus, it is necessary to develop an alternative optimization model with complexity independent on N_{BS} and N_{SC}. This is achieved by assuming that the precoding vectors and AN vector can be expressed as:

$$
\mathbf{w_{k,j}} = \sqrt{p_{k,j}} \mathbf{u_{k,j}} \quad \text{and} \quad \mathbf{v}_0 = \sum_{p=1}^{P} \sqrt{r_p} \mathbf{f}_p \tag{15}
$$

where $p_{k,j}$ is the power allocated to $w_{k,j}$, and $u_{k,j}$ is the unit vector that specifies the direction of the $w_{k,j}$. The expression for the regularized zero-forcing (RZF) precoding presented in the work of Bjornson et al. (2013) is used to compute $u_{k,j}$. The RZF precoding expression is given as:

$$\mathbf{u_{k,j}} = \frac{\left(\sum_{i=1}^{K} \frac{1}{\sigma_i^2} \mathbf{h_{i,j}} \mathbf{h_{i,j}^H} + \frac{K}{\gamma_k q_{j,l}} \mathbf{I} \right)^{-1} \mathbf{h_k}}{\left\| \left(\sum_{i=1}^{K} \frac{1}{\sigma_i^2} \mathbf{h_{i,j}} \mathbf{h_{i,j}^H} + \frac{K}{\gamma_k q_{j,l}} \mathbf{I} \right)^{-1} \mathbf{h_k} \right\|} \tag{16}$$

v_0 is expressed as a linear combination of the P column vectors $f_0, \ldots, f_P$. The unit AN vector components f_p are chosen such that

$$\mathbf{H_0^H f_p} = \mathbf{0} \forall p, \text{ where } \mathbf{H_0} = \sum_{i=1}^{K} \mathbf{h_{i,0}} \mathbf{h_{i,0}^H} \tag{17}$$

i.e. the AN vector components should lie on the null space of H_0. This AN generation scheme is known as the null space method (Goel and Negi 2005; Zhou and McKay 2010). P denotes the nullity of matrix H_0. r_p is the power allocated to f_p. To ensure that the nullity is nonzero, N_{BS} is set to be greater than *K*.

Since the direction of the precoding vectors and AN vector components are known, the optimization model can be formulated as a power allocation strategy problem. The proposed low-complexity algorithm is implemented as follows:

1) Each transmitter j=0 to M computes the following quantities in parallel:

$$g_{k,i,j} = \left| \mathbf{h_{k,j}^H u_{i,j}} \right|^2 \quad g_{eve,k,j} = \left\| \mathbf{H_{eve,j}^H u_{k,j}} \right\|^2 \quad d_{eve,p} = \left\| \mathbf{H_{eve,0}^H f_p} \right\|^2 \tag{18}$$

2) The jth SCA sends the scalar values $g_{k,i,j}$ and $g_{evek,j}$ to the macro-cell BS. The macro-cell BS solves the convex optimization problem in (19) to obtain the optimal power allocation strategy, denoted by $p_{k,j}^*$ and r_p^*.

$$
\begin{aligned}
\min_{\substack{p_{k,j}\forall\, k,j \\ r_p \forall p}} \quad & \sum_{j=0}^{M} \rho_j \sum_{k=1}^{K} p_{k,j} + \rho_0 \sum_{p=1}^{P} r_p + P_{\text{static}} \\
s.t. \quad & \sum_{j=0}^{M} \left(g_{k,k,j}\, p_{k,j} \left(1 + \frac{1}{\widetilde{\gamma}_k} \right) - \sum_{i=1}^{K} g_{k,i,j}\, p_{i,j} \right) \geq \sigma_k^2, \forall\, k \\
& \sum_{k=1}^{K} p_{k,j} \left\| \mathbf{u}_{k,j} \right\|_{\infty}^2 \leq q_j, \quad \forall\, j \neq 0 \\
& \sum_{p=1}^{P} r_p \left\| \mathbf{f}_p \right\|_{\infty}^2 + \sum_{k=1}^{K} p_{k,0} \left\| \mathbf{u}_{k,0} \right\|_{\infty}^2 \leq q_0 \\
& \sigma_{eve}^2 + \sum_{p=1}^{P} r_p d_{eve,p} \geq \sum_{j=0}^{M} \frac{g_{eve,k,j}\, p_{k,j}}{\delta_k} \quad \forall\, k \\
& p_{k,j} \geq 0 \quad \forall k,\, j \\
& r_p \geq 0 \quad \forall p
\end{aligned}
$$

3) The optimal values $p_{k,j}^{*}$ that satisfy (19) are sent to the *j*th SCA. The precoding vectors and AN vector can now be computed by the macro-cell BS and SCAs using equation (15).

The optimization model presented in (19) is a linear problem (LP) which can be efficiently solved by convex solvers. Moreover, the unknown quantities are real-valued variables instead of complex-valued semi-definite matrices. The interference term caused by the AN signal to the UE is removed since AN signals are orthogonal to all UE channel vectors. The use of Chebyshev norm ($\left\| \cdot \right\|_{\infty}$) for the transmit power constraints provides an upper bound value on the per-antenna transmit power. This was done to remove the dependency of the optimization model on the total number of antenna elements.

Modifications to Incorporate Sleep Mode Capabilities in Proposed Algorithm

Sleep mode mechanism of HetNets is essential in order to reduce power consumption at low traffic periods. To include the sleep mode capability of SCAs in the optimization model given in (19), Boolean variables that determine the state of the *j*th small cell node, denoted as λ_j, were incorporated in the optimization model. A value of '1' indicates that the small cell is in active mode and a value of '0' indicates that the small cell is in sleep mode. With this, the optimization model can be stated as follows:

$$
\begin{aligned}
\min_{\substack{p_{k,j}\ \forall k,j \\ r_p\ \forall p \\ \lambda_j\ \forall j}} \quad & \sum_{j=0}^{M} \rho_j \sum_{k=1}^{K} p_{kj} + \rho_0 \sum_{p=1}^{P} r_p + P_{static,0} + \sum_{j=1}^{M} \left(\lambda_j P_{static,j} + (1-\lambda_j) P_{sleep,j} \right) \\
s.t. \quad & \sum_{j=0}^{M} \left(g_{k,k,j} p_{kj} \left(1 + \frac{1}{\tilde{\gamma}_k} \right) - \sum_{i=1}^{K} g_{k,i,j} p_{ij} \right) \geq \sigma_k^2, \ \forall k \\
& \sum_{k=1}^{K} p_{kj} \left\| \mathbf{u}_{k,j} \right\|_\infty^2 \leq \lambda_j q_j, \quad \forall j \neq 0 \\
& \sum_{p=1}^{P} r_p \left\| \mathbf{f}_p \right\|_\infty^2 + \sum_{k=1}^{K} p_{k0} \left\| \mathbf{u}_{k,0} \right\|_\infty^2 \leq q_0 \\
& \sigma_{eve}^2 + \sum_{p=1}^{P} r_p d_{eve,p} \geq \sum_{j=0}^{M} \frac{g_{eve,k,j} p_{kj}}{\delta_k} \quad \forall k \\
& p_{kj} \geq 0 \quad \forall k, j \\
& r_p \geq 0 \quad \forall p \\
& \lambda_j \in \{0,1\} \quad \forall j \neq 0
\end{aligned}
\tag{20}
$$

where $P_{static,0}$ and $P_{static,j}$ are the static power consumption of the macro-cell BS and jth SCA, respectively. $P_{static,j}$ is the power consumption of the jth SCA when it is in sleep mode. The last term in the objective function indicates that an SCA can only be either in sleep mode or in active mode, and that its static power consumption will depend on its state. The introduction of the Boolean variable λ_j makes the problem intractable due to loss of convexity. LP relaxation can be applied in order to obtain an approximate solution to the problem. This is done by replacing the Boolean variables by continuous variables (i.e. $0 \leq \lambda_j \leq 1 \ \forall j$). Replacing the Boolean constraints in (20) provides a convex structure to the model. The resulting optimization model can be used to determine an approximate value of λ_j that lies within the interval [0, 1]. Decision on whether the jth SCA should be in sleep state or active state can be determined by comparing the approximate value of λ_j with some threshold τ. λ_j assumes a value of '1' if the approximate value is greater than τ and '0' if otherwise. Once a decision on the states of SCAs has been made after solving optimization model (20), the proposed low-complexity algorithm in (19) can be used to calculate the precoding and AN vectors, wherein SCAs in sleep mode are ignored in the power allocation strategy. Although the proposed PHY security algorithm which incorporates sleep mode mechanism of HetNets has a suboptimal power allocation strategy due to constraint relaxations, it is shown in the next section that it outperforms the achievable performance of HetNets without sleep mode mechanism when QoS requirement is low.

RESULTS AND DISCUSSION

The total power consumption of the proposed low-complexity algorithm is analyzed for varying per-user QoS requirement. The optimal solution of the model derived

in (14) serves as a baseline for performance assessment. The HetNet consists of one macro-cell BS placed at the center and 18 SCAs strategically deployed as shown in Figure 2. The HetNet serves 10 UE, while 10 eavesdroppers uniformly distributed within the macro-cell coverage area try to intercept the data intended for each UE. The positions of UE and eavesdroppers are taken from a uniform distribution with lower and upper bound distances from the macro-cell BS of 35m and 500m, respectively. Furthermore, a constraint was added that the minimum distance between a mobile terminal and an SCA is 5m. These distance constraints are necessary to ensure the validity of the channel model parameters in Table 1. The value of δ_k is fixed at $2^{0.1}$-1 = 0.0717 for all users. Hardware parameters used in the simulation are listed in Table 2, which mainly follow those used in the works of Nguyen et al. (2016) and Tang et al. (2015).

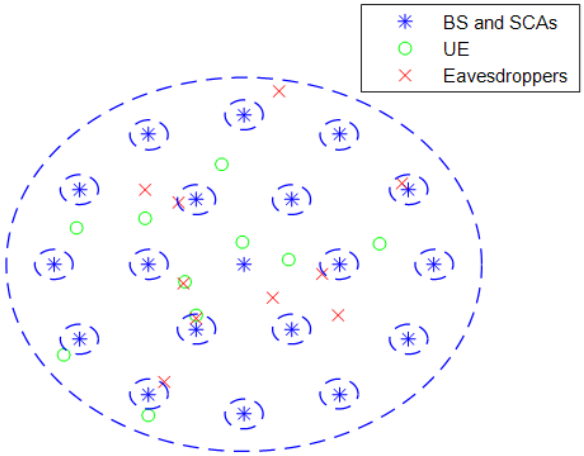

Figure 2. Illustration of a single-cell downlink scenario. BS and SCAs are fixed, while UE and eavesdroppers are uniformly distributed within the cell.

Table 2. List of hardware parameters used in simulation

	Macro-cell	Small-cell
Number of Antennas	16	4
Max Transmit Power	$P_{0,max}$ = 43 dBm $q_{0,l} = P_{0,max}/N_{BS}$	$P_{j,max}$ = 30 dBm $q_{j,l} = P_{j,max}/N_{SC}$
Per-antenna Circuit Power	189 mW	5.6 mW
Power Amplifier Efficiency	38.8%	5.2%
Non-transmission Power	30 dBm	20 dBm
Sleep Mode Power	-	5 dBm

Average total power consumption per 15 kHz subcarrier for different values of per-user QoS target is depicted in Figure 3. The optimization models presented in the previous section were implemented using a MATLAB-based modeling system for convex optimization called CVX (2010). The simulation results show that progression in average total power consumption is observed as per-user QoS target is increased. Although the proposed scheme enables fast precoding and AN vector design, deviation from the baseline performance is observed. The discrepancy in performance can be attributed to the heuristic structure of RZF precoding scheme, as discussed in the work of Bjornson et al. (2014). In the derivation of the RZF precoding structure, an assumption that the Lagrange multipliers for each user are of equal value was made, in order to reduce the complexity of the problem. However, this assumption causes a slight degradation in performance – a necessary trade-off to achieve practical implementation. RZF precoding is discussed in detail in the work of Bjornson et al. (2014). Nevertheless, the performance gap between the proposed algorithm and the optimal solution is small, with less than 1 dB (or 25%) difference in power consumption of the whole network at γ_k = 3.0 bits/s/Hz.

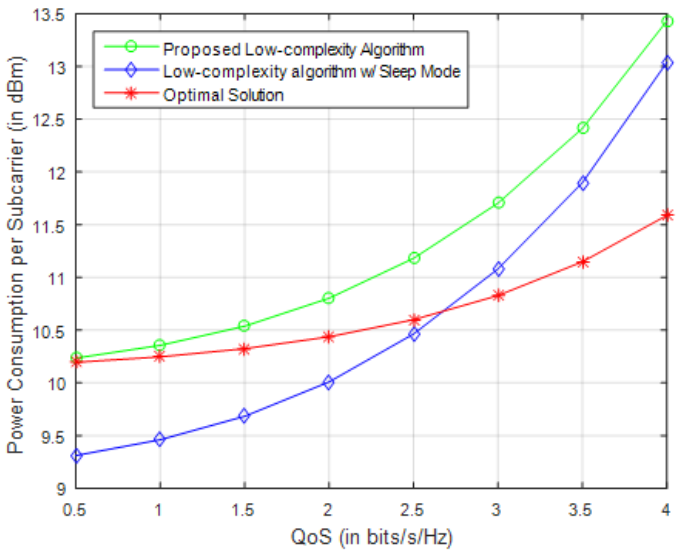

Figure 3. Average total power consumption of proposed low-complexity algorithm, low-complexity algorithm with sleep mode, and optimal solution for different QoS target.

The performance of the proposed algorithm allowing sleep mode in SCAs was also investigated. The total power consumption of the proposed algorithm allowing sleep mode is lower compared to the optimal performance of HetNets without sleep mode mechanism at γ_k < 2.5 bits/s/Hz. This shows that incorporating sleep mode capability to SCAs can reduce the power consumption at low traffic periods, while still maintaining a reliable and secure downlink transmission. At high per-user QoS requirement, the power consumption of the proposed algorithm allowing sleep mode approaches that of the proposed algorithm without sleep mode mechanism.

The impact of eavesdropper presence on the generated solution of the proposed algorithms was also analyzed and is depicted in Figure 4. Parameters used for this simulation experiment are similar to those used in Figure 3, but the per-user QoS targets γ_k are fixed at 2.0 bits/s/Hz and K_{eve} is varied instead of γ_k. The sudden jump on the average total power consumption in Figure 4 was caused by the AN signal.

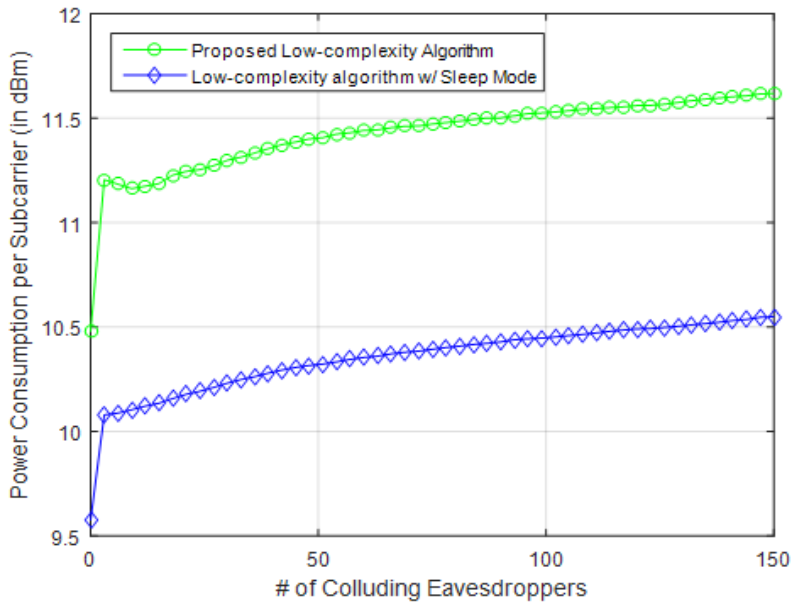

Figure 4. Average total power consumption of proposed low-complexity algorithm and low-complexity algorithm with sleep mode for varying eavesdropper count.

Since the purpose of the AN signal is to degrade the performance of the eavesdroppers, the AN signal will only have a non-zero power allocation if the eavesdroppers are present. In addition, the average total power consumption has a steadily increasing trend as the number of eavesdroppers grows. This result is not entirely unexpected due to the assumption that the eavesdroppers are colluding. Placement of additional eavesdroppers at random locations exploits receive spatial diversity which improves the quality of eavesdropped signals. As such, a more secured transmission strategy is required to degrade their signal reception. This is achieved by increasing the AN signal power or increasing the power allocation in RZF precoding.

The average runtimes of solving the benchmark performance and the proposed low-complexity schemes for different number of SCAs are listed in Table 3. The hardware used in conducting the simulation is an Intel Core i7-4770 with 3.40 GHz processing speed and 4 GB RAM. This hardware runs a Windows 7 64-bit Operating system with MATLAB 2015a installed. Runtime measurements were acquired using the built-in timeit function of MATLAB. Measured runtime in solving the benchmark performance exponentially increases as more SCAs are added to the simulation setup. This is expected since the matrix dimensions of the unknown semidefinite matrices $\mathbf{W}_{k,j}$ scale up drastically with the addition of more SCAs. Meanwhile, runtime performances of the proposed PHY security schemes were not significantly affected by the addition of SCAs. However, the runtime of the proposed PHY security scheme doubled when sleep mode was considered. This is because the algorithm needs to solve two linear optimization problem: first is to determine whether the SCAs are in the active state or in sleep state using (20), and then solve the precoding vectors of all active SCAs using (19).

Table 3. List of average runtimes in solving the original optimization model and the proposed low-complexity physical layer security schemes

Number of SCA	Runtime of Benchmark Performance (in seconds)	Runtime of Proposed Scheme (No Sleep mode) (in seconds)	Runtime of Proposed Scheme (No Sleep mode) (in seconds)
3 SCAs	2.534	0.165	0.337
6 SCAs	5.258	0.175	0.358
9 SCAs	10.227	0.187	0.382
12 SCAs	20.4917	0.198	0.404
15 SCAs	37.415	0.2083	0.425
18 SCAs	66.338	0.217	0.442

CONCLUSION

In this study, an optimization model which solves for the optimal values of the precoding vectors and an AN vector that minimizes the total power consumption, while satisfying certain level of data rate requirement and secrecy performance at the PHY layer, was developed. Using the formulated optimization model, a low-complexity algorithm which determines the optimal power allocation strategy for the precomputed AN vector and precoding vectors was designed. The performance of the proposed algorithm was analyzed by comparing it with the derived benchmark performance. Despite the decrease in computational complexity, deviation from the achievable performance was observed. However, the small increase in power consumption is an acceptable trade-off for the feasibility of real-time implementation. The algorithm was also extended to take into account the sleep mode capability of SCAs. Allowing SCAs to sleep during idle/low traffic periods could lessen the power consumption without sacrificing secrecy of communication—even outperforming the optimal solution for HetNets without sleep mode at low data rate requirement. Increase in eavesdropper also resulted in an increase in total power consumption. Finally, we note that, although perfect knowledge of UE and eavesdropper channel state information (CSI) was assumed in this study, modification of the proposed algorithm to be robust against imperfect CSI knowledge is considered for future work.

ACKNOWLEDGEMENTS

The authors would like to acknowledge the UP Wireless Communications Engineering Laboratory for their support to the study.

REFERENCES

Bernardo NI, De Leon F. 2016. On the trade-off between physical layer security and energy efficiency of massive MIMO with small cells. In: International Conference on Advanced Technologies for Communications (ATC); Hanoi, Vietnam: IEEE Computer Society. p.135-140.

Bjornson E, Kountouris M, Debbah M. 2013. Massive MIMO and small cells: Improving energy efficiency by optimal soft-cell coordination. In: 20th International Conference on Telecommunications. p. 1-5.

Bjornson E, Bengtsson M, Ottersten B. 2014. Optimal multiuser transmit beamforming: A difficult problem with a simple solution structure [Lecture Notes]. IEEE Signal Processing Magazine. 31:142-148.

CVX Research Inc. 2010. CVX: MATLAB software for disciplined convex programming version 2.1.

Deng Y, Wang L, Wong K, Nallanathan A, Elkashlan M, Lambotharan S. 2015. Safeguarding massive MIMO aided HetNets using physical layer security. In: International Conference on Wireless Communications and Signal Processing (WCSP). IEEE Computer Society. p.1-5.

Goel S, Negi R. 2005. Secret communication in presence of colluding eavesdroppers. In: IEEE Military Communications Conference. 3:1501-1506.

Holma H, Toskala A. 2012. LTE Advanced: 3GPP Solution for IMT Advanced. 1st edition. New Jersy (US): John Wiley & Sons.

Hoydis J, Kobayashi M, Debbah M. 2011. Green small-cell networks. IEEE Vehicular Technology Magazine. 6:37-43.

[ITU] International Telecommunications Union. 2014. Future technology trends of terrestrial IMT systems. M-series.

Lv T, Gao H, Yang S. 2015. Secrecy transmit beamforming for heterogeneous networks. IEEE Journal on Selected Areas in Communications. 33:1154-1170.

Mukherjee A, Fakoorian SAA, Huang J, Swindlehurst AL. 2014. Principles of physical layer security in multiuser wireless networks: A survey. IEEE Communications Surveys and Tutorials. 16:1550-1573.

Nguyen LD, Tuan HD, Duong TQ. 2016. Energy-efficient signaling in QoS constrained heterogeneous networks. IEEE Access. 4:7958-7966.

Nigam G, Minero P, Haenggi M. 2014. Coordinated multipoint joint transmission in heterogeneous networks. IEEE Transactions on Communications. 62:4134-4146.

Parkvall S, Dahlam E, Jongren G, Landstrom S, Lindbom L. 2011. Heterogeneous network deployments in LTE–the soft-cell approach. Ericsson Review.

Samsung Electronics Co. 2015. White paper on 5G Vision [Internet]. [cited 2017 October 1]. Available from: http://www.samsung.com/global/business-images/insights/2015/Samsung-5G-Vision-0.pdf.

Shannon CE. 1948. A mathematical theory of communication. Bell Systems Technical Journal. 27:379-423.

Shiqi G, Chengwen X, Zesong F, Jingming K. 2016. Resource allocation for physical layer security in heterogeneous network with hidden eavesdropper. China Communications. 13:82-95.

Small Cell Forum. 2012. W-CDMA Open Access Small Cells: Architecture, Requirements, and Dependencies.

Tang J, So DKC, Alsusa E, Hamdi KA, Shojaeifard A. 2015. Resource allocation for energy efficiency optimization in heterogeneous networks. IEEE Journal on Selected Areas in Communications. 33:2104-2117.

Trappe W. 2015. The challenges facing physical layer security. IEEE Communications Magazine. 53:16-20.

Vu QD, Tran LN, Farrell R, Hong EK. 2016, Energy-efficient zero-forcing precoding design for small-cell networks. IEEE Transactions on Communications. 64:790-804.

Wang HM, Zheng TX, Yuan J, Towsley D, Lee MH. 2016. Physical layer security in heterogeneous cellular networks. IEEE Transactions on Communications. 64:1204-1219.

Yang N, Wang L, Geraci G, Elkashlan M, Yuan J, Di Renzo M. 2015. Safeguarding 5G Wireless communication networks using physical layer security. IEEE Communications Magazine. 53:20-27.

Zhou X, McKay MR. 2010. Secure transmission with artificial noise over fading channels: achievable rate and optimal power allocation. IEEE Transactions on Vehicular Technology. 59:3831-3842.

_____

Neil Irwin Bernardo <neil.bernardo@eee.upd.edu.ph> is an Assistant Professor of the Electrical and Electronics Engineering Institute, University of the Philippines Diliman. He received both his M.S. degree in Electrical Engineering and B.S. degree in Electronics and Communications Engineering from the same institute. His research interests include communication signal processing, software-defined radios, and MIMO.

Franz de Leon <franz.de.leon@eee.upd.edu.ph> received both his B.S. degree in Electronics and Communications Engineering in 2003 and M.S. degree in Electrical Engineering in 2005 from the University of the Philippines Diliman. He received his Ph.D. degree in Electrical and Electronic Engineering in 2014 from the University of Southampton, United Kingdom. He is an Assistant Professor in the Electrical and Electronics Engineering Institute, UP Diliman, whose interests include applications of digital signal processing in audio and communications.

Science Diliman (January-June 2018) 30:1, 24-44

Feeding Habits of *Mobula japanica* (Chondrichthyes, Mobulidae) in Butuan Bay, Mindanao Island, Philippines

Shirlamaine Irina G. Masangcay
Caraga State University

Ephrime B. Metillo*
Mindanao State University-Iligan Institute of Technology

Ken-Ichi Hayashizaki
Kitasato University

Satoru Tamada
Kitasato University

Shuhei Nishida
University of Tokyo

ABSTRACT

The diet of the Spinetail Devil Ray *Mobula japanica* Müller and Henle 1841 from Butuan Bay, Philippines was investigated from January to May 2016 using data on its stomach contents, and C and N stable isotope analyses, in order to contribute to the scarce information on the feeding biology of the threatened tropical populations of the *Mobula* species. Examination of 16 *M. japanica* stomachs revealed ingestion of the euphausiid *Pseudeuphausia latifrons*, sergestid shrimps *Acetes intermedius* and *Lucifer* spp., copepods, and other rare prey items. The tropical krill *P. latifrons* was the most common, often the sole food, that increases body length of individuals towards the warmer months of April and May, which coincide with the peak season of *M. japanica* fisheries. Results from $\delta^{13}C$ and $\delta^{15}N$ stable isotope analysis are consistent with the assimilation of large zooplankton and micronektonic crustaceans. This study is the first report on the feeding of *M. japanica* in tropical waters and the identification of euphausiid *P. latifrons* as its dominant prey.

Keywords: Stomach content, *Mobula, Pseudeuphausia latifrons*, population structure, tropical

*Corresponding Author

ISSN 0115-7809 Print / ISSN 2012-0818 Online

INTRODUCTION

The Spinetail Devil Ray *Mobula japanica* from the family Mobulidae is a large marine fish with cartilaginous skeleton (Couturier et al. 2012). Locally known as Pantihan, mobulids or devil rays are pelagic fishes found in shallow and deep waters in the tropical and temperate regions (Cortes and Blum 2008; Bizzarro et al. 2009; Scacco et al. 2009; Canese et al. 2011; Metillo and Masangcay 2015; Croll et al. 2016; Francis and Jones 2016). In New Zealand, the species is a common bycatch in skipjack tuna purse seine fisheries (Francis and Jones 2016). Most *Mobula*, particularly *M. japanica,* vary in size with disk width ranging 1 – 3 meters (Paulin et al. 1982; Notarbartolo di Sciara 1987; White et al. 2006b), and are commonly known to be very fast swimmers that feed on zooplankton (Couturier et al. 2012). They have low natural rate of mortality, slow-growth with long life span, late sexual maturation, and have few but large offspring (Dulvy et al. 2003; Musick and Ellis 2005; Garcia et al. 2008; Croll et al. 2016). *Mobula japanica* is currently listed as near-threatened by the International Union for Conservation of Nature (IUCN) Red List of Threatened Species (White et al. 2006a), yet they are still being actively fished in Bohol Sea, central Philippines via the traditional harpoon and purse seine methods for sale and local consumption in the coastal area (Alava et al. 2002; Rayos et al. 2012; Acebes 2013; Freeman 2014; Croll et al. 2016). Fishermen (Galdo and Sanchez, personal communication) confirmed that *M. japanica* are seasonally observed in Butuan Bay, Mindanao Island during the Northeast monsoon when coastal enrichment is highest in eastern Bohol Sea (Cabrera et al. 2011).

Mobula species are pelagic megafauna yet they subsist on a primary diet of zooplankton and ichthyoplankton (Couturier et al. 2012). They grow very large due to the direct feeding on abundant zooplankton and ichthyoplankton in the second trophic level much closer to abundant primary producers (Shwenk 2000). Zooplanktivorous devil rays are indispensable in the marine ecosystem since they tap the lower trophic levels (Couturier et al. 2012; Jaine et al. 2012), and become important indicator species of climate change, as their planktonic food source is highly susceptible to environmental changes (e.g., ocean acidification and warming waters) (Hays et al. 2005; Richardson 2008; Weeks et al. 2015).

Studies on the biology and ecology of Mobulidae started since the 17th century, but information on its feeding habits is limited (Willoughby 1686; Stewart et al. 2016). Aggregations of devil rays are generally linked with local productivity and food availability (Celona 2004; Sleeman et al. 2007; Dewar et al. 2008; Marshall et al. 2009; Anderson et al. 2011; Couturier et al. 2011; Marshall et al. 2011*)*. Zooplanktivory is their generic feeding habit (Weeks et al. 2015), but species-

specific differences occur. For instance, *M. thurstoni* is known to feed on mysid shrimps and euphausiids, and dwells in non-overlapping microhabitats with other species (Notarbartolo di Sciara 1988). Examination of the stomach contents, and C and N stable isotope techniques have shown varying feeding habits among subtropical and temperate sub-populations under the genus *Mobula*, such as *M. mobular, M. hypostoma, M. rochebrunei, M. tarapacana, M. birostris, M. alfredi, M. japanica*, and *M. munkiana*, which generally feed on small fishes and crustaceans like krill (*Meganyctiphanes norvegica, Nyctiphanes simplex*), the mysid *Mysidium* sp., and other planktonic organisms (Notarbartolo di Sciara 1988; Sampson et al. 2010; Couturier et al. 2012). The diets of the near threatened species *M. kuhlii* and *M. eregoodootenkee* are unknown thus far (Pierce and Bennett 2003; Bizzarro et al. 2009).

Current knowledge of the prey preference of the tropical *Mobula japanica* based on its stomach contents is limited to the studies of Notarbatolo di Sciara (1988) and Sampson et al. (2010) conducted off the coast of California, USA. Analyzing feeding habits of tropical populations will determine diet preference and allow inference on habitat use and feeding behavior, which are both very important to the conservation and management of the ray (Stewart et al. 2016). Hence, this work investigated the feeding habits of *M. japanica* in Butuan Bay, northeastern part of Mindanao Island, Philippines with specific aims of analyzing the composition of its stomach contents, and indirectly inferring its feeding habits using C and N stable isotope analysis.

MATERIALS AND METHODS

Study area

Butuan Bay is located in the northeastern area of Mindanao (Figure 1). Its coastline is connected to the north with Bohol Sea or Mindanao Sea, which is known to have extreme southwest movement of surface currents coming from the Pacific Ocean (Cabrera et al. 2011). The entire bay has an average depth of 100 meters and a maximum depth of 800 meters (NGA Nautical Chart 1996). Numerous river tributaries flow directly into the bay, including the Agusan River, the third longest river in the Philippines, carrying water discharges from interconnecting rivers, channels, and lakes (Primavera and Tumanda 2008). A biologically enriched estuarine frontal plume usually occurs near the mouth of the large Agusan River in the bay (Cabrera et al. 2011). Climatic condition in Butuan Bay includes significant amount of rainfall throughout the year even in the driest month. The bay is exposed to strong trade winds and storms during the northeast monsoon (December-April).

Buenavista is a fishing coastal municipality located at the Southern portion of the bay (Figure 1) (Indab and Suarez-Aspilla 2004). The area is considered as a major fishing ground with rich fishery resources (BFAR 2015). Personal interviews in the locality validated the regular landing of *Mobula* in Buenavista, but fisherfolks report catching of rays at other locations in the bay, particularly off the coast of Carmen, Nasipit, Cabadbaran, and Tubay (Figure 1) (Metillo and Masangcay 2015).

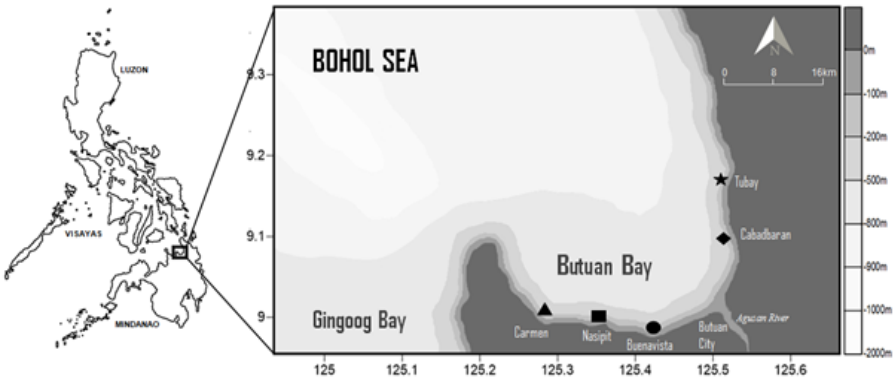

Figure 1. Geographical location of Butuan Bay in Northeastern Mindanao, and collection sites of landed *Mobula japanica* and plankton samples off the municipality of Carmen (triangle), Nasipit (square), Buenavista (dot), Cabadbaran (diamond), and Tubay (star) in the Province of Agusan del Norte. Inset is the map of the Philippines with the study site enclosed in a square.

Field sampling of ray stomach, muscle tissue, and prey items

Field collection of ray stomach samples, potential prey, and tissues for C and N stable isotopes was conducted from 18 January to 13 May 2016 to coincide with the fishing season in Butuan Bay. Sixteen specimens of *M. japanica* (Table 1) were purchased from local fishermen who caught the fish as bycatch from sardine and skipjack tuna gill net fishing during the day in five locations in Butuan Bay (Figure 1). Fishermen from Buenavista and other locations in Butuan Bay consistently stressed that their devil ray collection sites are just within the Bay (Metillo and Masangcay 2015). During specimen collections of this study, a standard procedure of asking fishermen where they captured the rays revealed that they can be found in the deep portions of Butuan Bay. The digestive tract of the 16 individuals was removed by cutting the most anterior end of the esophagus and the most posterior end of the intestine. The length and outer diameter of the stomach were measured to estimate the stomach volume that will be used in the stomach content analysis.

Afterwards, the stomach and intestine (Figure 2) were longitudinally dissected, spread apart, and the stomach contents were thoroughly flushed into clean plastic containers and preserved in 10% buffered formalin in filtered seawater. Muscle tissue samples from five *Mobula japanica* individuals were obtained near the ventro-posterior area of the pectoral fins using a sharp scalpel, and were immediately placed in a clean vial and labeled properly. Tissue samples were brought to the laboratory in an ice chest, and immediately dried in an oven at a temperature of 60°C for 48 hours.

Table 1. Body measurements (cm) of the 16 *Mobula japanica* individuals collected in Butuan Bay, Northeastern Mindanao, Philippines

#	Sex	Disk width (D_w)	Disk length (C_F)	Cephalic fin length (C_F)	Tail length (T_L)	Date collected	Site collected
a	Female	148	72	19	166	18-Jan-16	-
b	Male	130	68	23	160	25-Jan-16	-
c	Male	120	55	5	148	12-Feb-16	-
d	Male	137	67	16.4	146	27-Feb-16	Buenavista Area
e	-	-	-	-	-	11-Mar-16	Buenavista Area
f	Male	134	60	8	143	18-Mar-16	Buenavista Area
g	Male	-	-	-	-	18-Mar-16	Cabadbaran Area
h	-	-	-	-	-	30-Mar-16	Cabadbaran Area
i	Male	129	59	17	150	31-Mar-16	Buenavista Area
j	Male	146	69	22	142	31-Mar-16	Tubay Area
k	-	-	-	-	-	02-Apr-16	Buenavista Area
l	Female	135	60	18	154	09-Apr-16	Carmen Area
m	-	-	-	-	-	10-Apr-16	Carmen Area
n	Male	130	66	12	140	09-May-16	Buenavista Area
o	Male	134	63	17	148	11-May-16	Buenavista Area
p	Male	157	73	22	178	13-May-16	Buenavista Area

Note: "-", undetermined

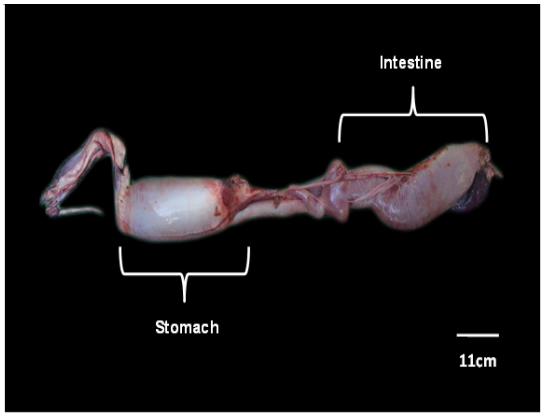

Figure 2.The digestive tract of *Mobula japanica* from Butuan Bay, Philippines.

Plankton samples were collected on 25 January 2016 at the location where *M. japanica* were caught (Table 2), particularly off Buenavista. Conical nets with mesh sizes of 100 µm and 20 µm were towed horizontally at sub-surface depths to collect zooplankton and particulate organic matter (POM), respectively (Metillo et al. 2015). Night sampling involving several 3-minute tows was performed until the desired amounts of plankton and POM triplicate samples were collected. Zooplankton samples were size-fractionated using a series of sieves with nylon gauzes of different mesh sizes (<100 µm, 100–200 µm, 200–335 µm, 335–1000 µm, >1000 µm), and were viewed under a dissecting stereo microscope to remove any debris in the sample. Zooplankton taxa (e.g. crab megalopa, decapod shrimp, hydrozoa) were sorted from the bulk samples to represent extra-large zooplankton (ZXL). Samples from the 20-µm mesh plankton net were filtered, and particles trapped in the 20-µm sieve were regarded as POM (Table 3). Large zooplankton samples (ZXL, ZL, ZM) were carefully handpicked using fine forceps, placed in foil, and dried in an oven at a temperature of 60°C for 48 hours. Smaller size fractions (ZS) of zooplankton and POM samples were separately filtered onto pre-combusted glass fiber filters (GF/F), dried in the same manner as large zooplankton, and placed inside Eppendorf tubes until stable isotope analysis.

Table 2. Tabulated coordinates of each plankton tow for stable isotopes analysis collected on 2016 January 25 in Butuan Bay, Northeastern Mindanao, Philippines

Tow No.	Net mesh size µm	Coordinates	
		Longitude	Latitude
1	100	125.401405°	8.987764°
2	100	125.399261°	8.988452°
3	100	125.397559°	8.988784°
4	100	125.396298°	8.988920°
5	20	125.394506°	8.989511°
6	20	125.393166°	8.989122°
7	20	125.391468°	8.988398°
8	20	125.389072°	8.988368°
9	20	125.386612°	8.988413°
10	20	125.384991°	8.988234°
11	20	125.383185°	8.988025°

Table 3. List of specimens used for C and N stable isotope analysis.

Sampling dates	Taxa/size group	Code	Period of collection	No. of specimen*	Source
18-Jan-16	*Mobula japonica* (female)	MJ	Day	1	Fish landing
18-Jan-16	*Pseudeuphausia latifrons*	KA	N/A	30	Net towing
25-Jan-16	*M. japonica* (male)	MJ	Day	1	Fish landing
12-Feb-16	*M. japonica* (male)	MJ	Day	1	Fish landing
27-Feb-16	*M. japonica* (male)	MJ	Day	1	Fish landing
18-Mar-16	*M. japonica* (male)	MJ	Day	1	Fish landing
25-Jan-16	*Lucifer* spp.	LU	Night	6	Net towing
25-Jan-16	*Acetes intermedius*	AC	Night	15	Net towing
25-Jan-16	Clupeidae	FJ	Night	4	Net towing
25-Jan-16	Exocoetidae	FJ	Night	1	Net towing
25-Jan-16	Blennidae	FL	Night	4	Net towing
25-Jan-16	Carangidae	FL	Night	6	Net towing
25-Jan-16	Gobidae	FL	Night	4	Net towing
25-Jan-16	Crab megalopa	ZXL	Night	2	Net towing
25-Jan-16	Decapod shrimp	ZXL	Night	2	Net towing
25-Jan-16	Hydrozoa	ZXL	Night	1	Net towing
25-Jan-16	*Macrosetella* sp.	ZXL	Night	2	Net towing
25-Jan-16	*Acartia* sp.	ZL	Night	18	Net towing
25-Jan-16	*Labidocera* sp.	ZL	Night	7	Net towing
25-Jan-16	Calanid copepods	ZL	Night	22	Net towing
25-Jan-16	*Parthenope* sp. (zoea)	ZL	Night	3	Net towing
25-Jan-16	*Paracalanus* sp.	ZM	Night	18	Net towing
25-Jan-16	Copepods (200-335 µm)	ZM	Night	1 g	Net towing
25-Jan-16	mesozooplankton (100-200 µm)	ZS	Night	1 g	Net towing
25-Jan-16	particulate matter (20-100 µm)	POM	Night	1 g	Net towing

Legend: *specimen means individual organism, except the bottom three rows where specimen is expressed in gram (g)

Stomach content analysis

The stomach content of each individual ray was removed and placed in a beaker for subsampling. The entire sample was divided into 10 parts with each tenth regarded as a subsample. Three sub-samples were then thoroughly identified using a stereomicroscope for large particles and a compound microscope for smaller ones. The contents of the intestine were also inspected, but the materials were already heavily digested and unidentifiable; hence, they were not included in the analysis. The index of relative importance (IRI) of each food item category was computed using the formula of Pinkas et al. (1971): IRI = $(Cn + Cv) \times F$, where Cn is the percentage numerical count of each food item relative to the total count of all food items; C_v is the percentage volume (assuming cylindrical shape of the ray cardiac stomach) of each food item (estimated from the product of the proportion

of space occupied by each food item and the volume of the cylindrical cardiac stomach) relative to the volume of all food item combined; and *F* is the percentage occurrence of each food item in the stomachs of all fish individuals analyzed. The use of the IRI (Pinkas et al. 1971) reduces biased description of animal dietary data. This method has been widely used in studying diet composition of large marine animals and proved efficient in determining a snapshot view of prey items in the stomach (Notarbatolo di Sciara 1988; Alonso et al. 2001; Moura et al. 2008; Schluessel et al. 2010).

Analysis of C and N stable isotopes

Dried samples were pulverized using acid-washed mortar and pestle. Powdered samples were aseptically placed in Eppendorf tubes and properly labelled. All samples were analyzed through dual C and N stable isotopes technique using the Thermo Stable Isotopes Analyzer coupled with the Thermo Finnigan DELTA plus XP isotope ratio mass spectrometer via a ConFlo-III continuous flow interface (Metillo et al. 2015). Samples with elemental C and N ratio > 4 were corrected for effects of lipids (Post 2002).

Data treatment

Isotopic values between the two *M. japanica* individuals were compared using Student homoscedastic t-test (SPSS 2002). Results of the stable isotope analysis (SIA) were plotted and interpreted using OmniGraphSketcher version 1.1.4. Relationships between prey and predator were calculated using the trophic enrichment factor values 3.2±0.43‰ for $\delta^{15}N$ and 1.8±0.29‰ for $\delta^{13}C$ (McCutchan et al 2003). Trophic levels (TL) of all samples were determined based on nitrogen isotopic values using the equation (Vander Zanden and Rasmussen 2001): $TL_{consumer} = [(\delta^{15}N_{consumer} - \delta^{15}N_{baseline})/3.4 + 2]$, where $\delta^{15}N_{consumer}$ is the mean value of the predator, $\delta^{15}N_{baseline}$ is the isotopic $\delta^{15}N$ values from the microplankton (Z1,100–200 µm) samples, and a trophic efficiency factor value of 3.4.

RESULTS

Stomach content

The state of the 16 *M. japanica* individuals only allowed sexing 12 which comprised ten males and two females (Table I). Body size as disk width (D_w) ranged from 120–157 cm, while disk length (D_L) ranged from 55–73 cm. The stomach of all 16

individuals examined contained ingested food composed of intact identifiable prey items mixed with few digested food items. Prey organisms identified were mostly planktonic euphausiids, sergestid shrimps, copepods, and other categories as minor food items (Table 4). Stomach contents from all rays consisted almost exclusively of adult and eggs of the krill *Pseudeuphausia latifrons* G.O. Sars 1883, which exhibited IRI values of 15,180.28 and 4,537.11, respectively. The other prey items in decreasing order of IRI values were the sergestoid shrimp *Lucifer* > sergestid shrimp *Acetes intermedius* > copepods > flatworm > plant fragments > polychaete larvae = mollusc veligers. Although *A. intermedius* was found to have a low IRI value of 10.65, it dominated the stomach content of one *M. japanica*.

Table 4. Diet analysis of *Mobula japanica* based on 9 prey types collected from the stomachs of 16 individuals. N, Number; V, Volume; FO, Frequency of occurrence; IRI, Index of relative importance

Prey	Number	% N	% V	% FO	IRI	% IRI
Pseudeuphausia latifrons	588,413	76.594	75.209	100.00	15,180.28	76.66
Krill egg	175,866	22.893	22.479	100.00	4,537.11	22.91
Lucifer sp.	3,348	0.436	0.638	68.75	73.85	0.37
Acetes intermedius	540	0.070	1.634	6.25	10.65	0.05
Copepods	47	0.006	0.017	31.25	0.72	0.00
Flatworm	5	0.001	0.018	6.25	0.12	0.00
Mollusc veligers	1	0.000	0.001	6.25	0.01	0.00
Polychaete larvae	1	0.000	0.001	6.25	0.01	0.00
Plant fragments	1	0.000	0.003	6.25	0.02	0.00

C and N stable isotope values

We obtained muscle tissues from five *M. japanica* individuals with sizes ranging from 130–147 cm (D_w) (Table 5). Individual values of C and N stable isotopes for these individuals were not significantly different (t = 1.56, df = 3, p = 0.22). Mean isotopic values for the five *M. japanica* were -16.07±0.52‰ for $\delta^{13}C$ and 10.69± 0.34‰ for $\delta^{15}N$. The $\delta^{15}N$ isotopic values were accordingly used to calculate and determine the trophic positions of *M. japanica* and its potential prey types. The 3.27 (female) and 3.16 (male) TL for the five *M. japanica* fall within those of secondary consumers. The stable isotope biplot displays the TL and carbon source of each taxon (Figure 3). On the other hand, isotopic signals of *M. japanica* show an enriched ^{13}C compared to potential preys which have mean values ranging from -19.46‰ (medium size zooplankton) to -17.15‰ (juvenile fish), with the exception of fish larvae (-13.83‰). Mean $\delta^{13}C$ values for ichthyoplankton (juvenile and larvae) differed with more depleted values for juveniles than those of larvae. Sergestid

shrimps *A. intermedius* had more enriched mean values (-18.47‰ for $\delta^{13}C$ and 7.89‰ for $\delta^{15}N$) than those of *Lucifer* spp (-19.03‰ for $\delta^{13}C$ and 6.29‰ for $\delta^{15}N$). The mean $\delta^{13}C$ values of both large zooplankton (ZL 335-1000 µm, and ZXL >1000µm) are more enriched at -18.65‰ to -18.40‰ in comparison to the value of smaller zooplankton (Z1 100–200 µm: -19.27‰). The krill *P. latifrons* exhibited a mean $\delta^{13}C$ value (-17.96‰) which is roughly similar to those of large zooplankton.

Table 5. $\delta^{13}C$ and $\delta^{15}N$ isotopic values (mean±standard deviation) and trophic position of *M. japanica* and its potential prey. Numbers in the species codes represent the replicate used for analysis.

Taxa	Code	Mean $\delta^{13}C$	Mean $\delta^{15}C$	n	Trophic position (TP)
M. japanica (female)	MJ1	-16.20±0.16	10.69± 0.04	1	3.27
M. japanica (male)	MJ2	-15.68±0.35	10.44±0.25	4	3.16
Acetes intermedius	AC	-18.45±0.10	7.89±0.23	3	2.44
Lucifer spp.	LU	-19.03±0.27	6.29±0.30	3	2.44
P. latifrons	KA	-17.96±0.48	8.34±0.08	3	2.34
Fish juvenile	FJ	-17.15±0.55	7.37±1.00	2	2.29
Fish larvae	FL	-13.83±4.67	7.11±0.47	2	2.22
Macrozooplankton (>1000µm)	ZXL	-18.40±1.36	6.40±0.19	3	2.01
Mesozooplankton (100-200µm)	ZS	-19.27±0.24	6.38±0.10	3	2.00
Mesozooplankton (200-335µm)	ZM	-19.46±0.12	6.71±0.12	3	2.10
Mesozooplankton (335-1000µm)	ZL	-18.65±0.21	6.47±0.80	3	2.03
Microzooplankton (20-100µm)	POM	-15.96±1.32	2.78±0.80	3	1.82

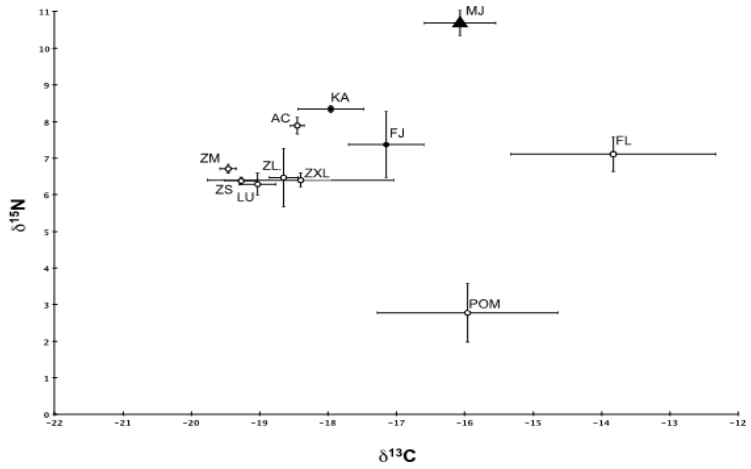

Figure 3. Isotopic values of ^{13}C and ^{15}N for *Mobula japanica* (MJ) and potential prey from Butuan Bay, Northeastern Mindanao, Philippines. ZS, zooplankton (100–200 µm); ZM, zooplankton (200–335 µm); ZL, zooplankton (335–1000 µm); ZXL, zooplankton (> 1000 µm); FJ, fish juvenile; FL, fish larva; POM, particulate organic matter; AC, *Acetes intermedius*; KA, adult *Pseudeuphausia latifrons*; LU, *Lucifer* spp.

DISCUSSION

Diet of *M. japanica*

All collected *M. japanica* (D_w = 120–157 cm) in this study were immature (Notarbatolo Sciara 1988; White et al. 2006b) and dominated by males. According to Sampson et al. (2010), *M. japanica* individuals that are <205 cm (D_w) are considered immature. The sizes of the *M. japanica* of the present study were definitely smaller compared to those of the New Zealand population with individuals showing an average of 200 cm (D_w) and 100 cm (D_L) (Francis and Jones 2016). The predominance of immature individuals may reflect the movement of larger rays to other areas (White et al. 2006b). These rays were caught by fishermen during the day, which validates the findings of Croll et al. (2012) that *M. japanica* is commonly observed at the surface waters (<5 m) during daytime and goes to deeper waters (>50 m) at night in search for food. Devil rays in general are surface water dwellers that spend long periods in the surface during the day (Gadig et al. 2003). It is suggested that surface aggregation of this species may be attributed to the daytime swarming of the krill prey *P. latifrons* (Wilson et al. 2001) and *Nyctiphanes simplex* (Gendron 1992).

Generally, stomach content analysis (SCA) provides information on prey items in limited time scales (e.g. hours to days). In this study, SCA results confirmed *M. japanica* to have a strong feeding affinity with planktonic organisms, which may be associated with its gill morphology (Paig-Tran et al. 2011). Rays are efficient in capturing zooplanktonic prey by funnelling microscopic plankton into their mouth and trapping them onto the gills which are made up of filter-like mesh of small bones (Paig-Tran et al. 2013). All 16 *M. japanica* actively fed since their stomachs contained quantifiable prey. By contrast, Notarbatolo di Sciara (1988) reported only 19 (24%) out of 78 *M. japanica* individuals had food in their stomach.

In this study, the predominance of the tropical krill *P. latifrons* in almost all of the stomach contents of *M. japanica* was observed (Masangcay et al. 2018). By comparison, the subtropical populations of *M. japanica* and *M. thurstoni* exclusively feed on the subtropical krill *N. simplex*, while *M. munkiana* feed on the mysid *Mysidium* sp. (Notarbatolo di Sciara 1988; Sampson et al. 2010). *Mobula thurstoni* primarily feeds on euphausiids (Gadig et al. 2003), but it was also observed to intensively feed on mysid shrimps (Notarbartolo di Sciara, 1988). *Manta birostris* (Wilson et al. 2001) and *Rhincodon typus* (Wilson and Newbound 2001; Jarman and Wilson 2004) are also reported to prey on *P. latifrons* at daytime. These findings are in close agreement with our study, which identifies the krill species *P. latifrons*

as the most important prey of *M. japanica* from Butuan Bay. In addition, our local plankton net tows did yield a few *P. latifrons* at the locations off Buenavista where fishermen capture devil rays. The few *P. latifrons* collected is attributable to the inefficiency of the conical plankton net in catching micronektonic krill (Nemoto 1983; Wiebe et al. 2005).

Aside from adult krill, other prey items include krill eggs, whose abundance is due to the large number of egg-carrying female *P. latifrons* that can bear up to 164 eggs or more per individual (Wilson et al. 2003a). Although it is possible that the eggs would have been ingested as freely suspended eggs in the water column, we believe these were most likely dislodged from the mother krill's brood pouch as a result of the peristalsis of the ray stomach. Interestingly, the shallow water sergestid shrimp *A. intermedius* dominated one stomach of *M. japanica*, indicating ingestion of other shallow water/estuarine micronektonic crustaceans (Jarman and Wilson 2004) and a possible switch to alternative prey (Notarbatolo di Sciara 1988; Wetherbee and Cortés 2004). Past studies on ray stomach content report the importance of pelagic micronektonic crustaceans like euphausiids (true krill), sergestid shrimps like *Acetes* spp., and other planktonic species (Couturier et al. 2012). Micronektonic crustaceans form dense swarms and filter-feeding devil rays might have evolved to track large aggregations of micronektonic crustaceans whose sizes ensure energy to support the activities of these pelagic megafauna (Sampson et al. 2010; Couturier et al. 2013).

Population structure analysis of *P. latifrons* showed changes in the size-structure, reflecting individual growth from January to May (Masangcay et al. 2018). Breeding season of this species appears to be during the warm and dry months of March to May, which coincides with the decrease in number of juvenile individuals and the increase in abundance of large egg-carrying females during these months. Incidentally, the fishing season of *M. japanica* in Bohol Sea (Alava et al. 2002; Acebes 2013; Freeman 2014) and Butuan Bay (Metillo and Masangcay 2015) is from September to May with the peak season lasting from February to April. However, sightings and fishing of devil rays could extend up to June in Butuan Bay (Metillo and Masangcay 2015) and Bohol Sea (Freeman 2014). We are convinced that the preponderance of *M. japanica* individuals during these months could be linked with the availability of swarms of *P. latifrons*.

High primary production in Butuan Bay drives the abundance of *P. latifrons*, which prefer habitats with high abundance of zooplankton depending on dense phytoplankton (Wilson et al. 2003b). However, *P. latifrons* are reported to also feed on detritus (Hirota and Nemoto 1989). The peak of surface chlorophyll α is often observed in Butuan Bay at around 20–30 m depth (Villanoy, personal

communication). The primary production in Butuan Bay is at maximum during December to February when heavy rainfall causes highest river discharge (as indicated by highest chromophoric dissolved organic matter or CDOM) (Figure 4 in Cabrera et al. 2011) and a pronounced plume from Agusan River, the second largest river in the Philippines (Villanoy et al. 2011). Another primary production enhancement mechanism in Butuan Bay is the "double estuarine type circulation", which is mostly driven by the large inflow of waters from the Pacific Ocean passing through Surigao Strait and entrains large amounts of deep, nutrient-rich waters to the surface (Cabrera et al. 2011). This mechanism is strongest during the months of December to March when the northeast monsoon winds generate the westbound surface current Bohol Jet in the Bohol Sea (Cabrera et al. 2011). This regular circulation pattern, together with the highest freshwater discharge from the large Agusan River, eventually leads to nutrient enrichment and phytoplankton bloom, which in turn fuel high zooplankton abundance that feed the *P. latifrons* population.

C and N stable isotope values

Stable isotope analysis allowed the determination of a consumer-food relationship between *M. japanica* and its potential prey in Butuan Bay. The isotopic signature of $\delta^{15}N$ reflects an organism's trophic position, while isotopic differences among $\delta^{13}C$ values can trace the original dietary carbon source of the consumer, whether it originated from a marine, freshwater, or terrestrial environment (Shiffman et al. 2012). Furthermore, $\delta^{13}C$ gradients may also reflect the food web relationship between coastal or benthic, and offshore or pelagic regions (Dahl et al. 2003; Hussey et al 2011). Depleted $\delta^{13}C$ values (-22‰ to -17‰) denote pelagic feeding, whereas enriched $\delta^{13}C$ values (> -17‰) imply coastal and/or benthic foraging (France 1995).

Here, we report the C and N stable isotopes values of one female and four male *M. japanica* individuals from Butuan Bay. Values among *M. japanica* individuals did not differ, which agrees with the study of Sampson et al. (2010) who reported no difference in $\delta^{13}C$ and $\delta^{15}N$ values between stage of maturity, between sex, among monthly values, and between species (*M. thurstoni* and *M. japanica*). Similarly, Couturier et al. (2013) found similar $\delta^{13}C$ and $\delta^{15}N$ stable isotopes in *Manta alfredi* from both Lady Elliot Island and North Stradbroke Island in Queensland, Australia. Less stable isotope variation in these large organisms may be explained by the long-term (months) turnover rates of C and N stable isotopes in muscle tissues of mobulids (Sampson et al. 2010). The low variability in stable isotope values (0.16—

0.35 for $\delta^{13}C$ and 0.04—0.25 for $\delta^{15}N$ in this study) is also indicative of a highly specialized diet (Sweeting et al. 2005).

Mean $\delta^{13}C$ isotopic value (-16.07‰) of *M. japanica* falls within the enriched category which implies that its diet would most likely be composed of prey from offshore marine and planktonic habitat (France 1995). The present study reports comparable $\delta^{13}C$ values reported in other Mobulidae studies: *M. thurstoni* (-16.74‰) and *M. japanica* (-16.78‰) (Sampson et al. 2010); *M. diabolus* (-16.02‰) (Borell et al. 2011); and *M. alfredi* (-17.4‰) (Couturier et al. 2013). ^{13}C values of potential prey are enriched. The difference in values for juvenile and larval fishes may be related with migration, wherein larvae are spawned in deep spawning ground (more enriched ^{13}C signature) but juveniles move to shallow nursery habitats (more depleted ^{13}C signature) (Tanaka et al. 2008). Therefore, the ^{13}C values of the juvenile fish *Acetes* spp., *P. latifrons*, and zooplankton are reflective of shallow neritic and estuarine organisms.

The stomach content analysis in this study reveals that *M. japanica* preys on zooplankton, particularly micronektonic shrimps euphausiid (*P. latifrons*) and sergestid (*A. intermedius*) in Butuan Bay. The calculated trophic position based on mean values of *M. japanica* suggests the species is a low trophic level secondary consumer that assimilates nitrogen of primary consumers, concurring with the findings of the stomach analysis. However, following the mean trophic enrichment factors (3.2‰ for $\delta^{15}N$ and 1.8±0.29‰ for $\delta^{13}C$) of McCutchan et al. (2003), *M. japanica* would primarily eat not only the krill *P. latifrons* and the sergestid *Acetes intermedius*, but also juvenile fish. This is not surprising as other mobulids are reported to ingest ichthyoplankton, proving plasticity in its feeding habits (Stewart et al. 2016).

CONCLUSION

Stomach contents of 16 *M. japanica* individuals were dominated by adults and eggs of *Pseudeuphausia latifrons* euphausiid, followed by a much lesser amount of sergestid shrimps (*Lucifer* sp. and *Acetes intermedius*), copepods, and planktonic remains. Larger female *P. latifrons* was observed to be the most dominant in the diet of *M. japonica*, which coincided during the peak of the reproductive cycle of the krill. Stable isotopes of C and N in muscle tissues of five *M. japanica* individuals and potential preys confirm the strong feeding affinity of *M. japanica* with micronektonic crustaceans. This study is the first formal report on the feeding of *M. japanica* in tropical Philippine waters. Although the current findings are useful

input to local conservation and management of *M. japanica*, we recommend that longer period of study should be made to include other ray species in the Philippines.

ACKNOWLEDGEMENTS

The authors gratefully acknowledge the Department of Research, MSU-Iligan Institute of Technology; Department of Science and Technology (DOST)-Advance Science and Technology Human Resources Development Program; Department of Science and Technology (DOST)-Science Education Institute (SEI); and the Japan Society for the Promotion of Science (JSPS) (the Asian CORE and the Core-to-Core Programs) for their financial and technical support. We also thank Dr. MTRD Sanchez-Metillo for copyediting the manuscript.

REFERENCES

Acebes JMV. 2013. Hunting "Big Fish": A marine environmental history of a contested fishery in the Bohol Sea [doctoral dissertation]. Perth, Western Australia: Murdoch University.

Alava MNR, Dolumbalo ERZ, Yaptinchay AA, Trono RB. 2002. Fishery and trade of whale sharks and manta rays in the Bohol Sea, Philippines. In: Fowler SL, Reed TM, Dipper FA, editors. Elasmobranch biodiversity, conservation and management: Proceedings of the international seminar and workshop; July 1997; Sabah, Malaysia. Gland, Switzerland: IUCN Species Survival Commission no. 25. p 132-148.

Alonso MK, Crespo EA, García NA, Pedraza SN, Mariotti PA, Vera BB, Mora NJ. 2001. Food habits of *Dipturus chilensis* (Pisces: Rajidae) off Patagonia, Argentina. ICES Journal of Marine Science. 58:288-297.

Anderson RC, Adam MS, Goes JI. 2011. From monsoons to mantas: seasonal distribution of *Manta Alfredi* in the Maldives. Fisheries Oceanography. 20:104-113.

Bizzarro J, Smith W, White WT, Valenti SV [Internet]. 2009. *Mobula kuhlii*. The IUCN Red List of Threatened Species 2009: e.T161439A5424139; [cited 2015 November 10]. Available from http://www.iucnredlist.org.

Borrell A, Cardona L, Kumarran RP, Aguilar A. 2011. Trophic ecology of elasmobranchs caught off Gujarat, India, as inferred from stable isotopes. ICES Journal of Marine Science. 69:357-1371.

Brinton E. 1975. Euphausiids of the Southeast Asian waters. Scientific results of marine investigations of the South China Sea and the Gulf of Thailand 1959-1961. Naga Report. 4:1-287.

[BFAR] Bureau of Fisheries and Aquatic Resources [Internet]. 2015. Comprehensive National Fisheries Industry Development Plan (CNFIDP); [cited 2015 December 2]. Available from http://www.bfar.da.gov.ph/files/img/photos/CNFIDP.

Cabrera OC, Villanoy CL, David LT, Gordon AL. 2011. Barrier layer control of entrainment and upwelling in the Bohol Sea, Philippines. Oceanography. 24:130-141.

Canese S, Cardinali A, Romeo T, Giusti M, Salvati E, Angiolillo M, Greco S. 2011. Diving behavior of the giant devil ray in the Mediterranean Sea. Endangered Species Research. 14:171-176.

Celona A. 2004. Caught and observed giant devil rays *Mobula mobular* (Bonnaterre, 1788) in the Strait of Messina. Annales Series Historia Naturalis. 14:11-18.

Cortes J, Blum S. 2008. Life at 450 m depth to Isla del Coco, Costa Rica. International Journal of Tropical Biology. 56:189-206.

Couturier LIE, Jaine FRA, Townsend KA, Weeks SJ, Richardson AJ, Bennett MB. 2011. Distribution, site affinity and regional movements of the manta ray, *Manta alfredi* (Krefft, 1868), along the east coast of Australia. Marine and Freshwater Research. 62:628-637.

Couturier LIE, Marshall AD, Jaine FRA, Kashiwagi T, Pierce SJ, Townsend KA, Weeks SJ, Bennet MB, Richardson AJ. 2012. Biology, ecology and conservation of the Mobulidae. Journal of Fish Biology. 80:1075-1119.

Couturier LIE, Rohner CA, Richardson AJ, Marshall AD, Jaine FRA, Bennet MB, Townsend KA, Weeks SJ, Nichols PD. 2013. Stable isotope and signature fatty acid analyses suggest reef manta rays feed on demersal zooplankton. PLoS ONE. 8:e77152.

Croll DA, Newton KM, Weng K, Galván-Magaña F, Sullivan JO, Dewar H. 2012. Movement and habitat use by the spine-tail devil ray in the Eastern Pacific Ocean. Marine Ecology Progress Series. 465:193-200.

Croll DA, Dewar H, Dulvy NK, Fernando D, Francis MP, Galvan-Magana F, Hall M, Heinrichs S, Marshall A, McCauley D, Newton K, Notarbartolo-di-Sciara G, O'Malley M, O'Sullivan J, Poortvleit M, Roman M, Stevens G, Tershy B, White WT. 2016. Vulnerabilities and fisheries impacts: the uncertain future of manta and devil rays. Aquatic Conservation: Marine and Freshwater Ecosystems. 26:562–575.

Dahl TM, Falk-Petersen S, Gabrielsen GW, Sargent JR, Hop H, Millar RM. 2003. Lipids and stable isotopes in common eider, black-legged kittiwake and northern fulmar: A trophic study from an Arctic fjord. Marine Ecology Progress Series. 256:257-269.

DeNiro MJ, Epstein S. 1978. Influence of diet on the distribution of carbon isotopes in animals. Geochimica et Cosmochimica Acta. 42:495-506.

Dewar H, Mous P, Domeier M, Muljadi A, Pet J, Whitty J. 2008. Movements and site fidelity of the giant manta ray, *Manta birostris*, in the Komodo Marine Park, Indonesia. Marine Biology. 155:121-133.

Dulvy NK, Sadovy Y, Reynolds JD. 2003. Extinction vulnerability in marine populations. Fish and Fisheries. 4:25-64.

France RL. 1995. Carbon-13 enrichment in benthic compared to planktonic algae: Food web implications. Marine Ecology Progress Series. 124:307-312.

Francis MP, Jones EG. 2016. Movement, depth distribution and survival of spinetail devil rays (*Mobula japanica*) tagged and released from purse-seine catches in New Zealand. Aquatic Conservation: Marine and Freshwater Ecosystems. 27(1):219-236.

Freeman AL. 2014. Mobulidae fishery in Bohol, Philippines: An assessment of its sustainability [MRes thesis]. UK: Swansea University.

Gadig OBF, Namora RC, dos Santos Motta F. 2003. Occurrence of the bentfin devil ray, *Mobula thurstoni* (Chondrichthyes: Mobulidae), in the western Atlantic. Journal of the Marine Biological Association of the UK. 83:869-870.

Garcia VB, Lucifora LO, Myers RA. 2008. The importance of habitat and life history to extinction risk in sharks, skates, rays and chimaeras. Proceedings of the Royal Society B: Biological Sciences. 275:83-89.

Gendron D. 1992. Population structure of daytime surface swarms of *Nyctiphanes simplex* (Crustacea: Euphausiacea). Marine Ecology Progress Series. 87:1-6.

Hanamura Y, Saito N, Hayashi KI. 2003. Shore stranding of the neritic euphausiid *Pseudeuphausia latifrons* (GO Sars, 1883) in western Japan. Crustaceana. 76:1147-1152.

Hays GC, Richardson AJ, Robinson C. 2005. Climate change and marine plankton. Trends in Ecology and Evolution. 20:337-344.

Hirota Y. 1987. Vertical distribution of euphausiids in the western Pacific Ocean and the eastern Indian Ocean. Bulletin of Japan Sea Regional Fisheries Research Laboratory. 37:175-224.

Hirota Y, Nemoto T. 1989. Relationship between feeding and vertical distribution of euphausiids in the western Pacific Ocean. Bulletin of the Plankton Society of Japan. 36:127-135.

Hussey NE, Dudley SFJ, McCarthy ID, Cliff G, Fisk AT. 2011. Stable isotope profiles of large marine predators: Viable indicators of trophic position, diet, and movement in sharks? Canadian Journal of Fisheries and Aquatic Sciences. 68:2029-2045.

Indab JD, Suarez-Aspilla PB. 2004. Community-based marine protected areas in the Bohol (Mindanao) Sea, Philippines. NAGA, WorldFish Center Quarterly. 27:4-8.

Jaine FRA, Couturier LIE, Weeks SJ, Townsend KA, Bennett MB, Fiora K, Richardson A.J. 2012. When giants turn up: Sighting trends, environmental influences and habitat use of the manta ray *Manta alfredi* at a Coral Reef. PLoS ONE. 7:e46170.

Jarman SN, Wilson SG. 2004. DNAbased species identification of krill consumed by whale sharks. Journal of Fish Biology. 65:586-591.

Marshall AD, Compagno LJV, Bennett MB. 2009. Redescription of the genus *Manta* with resurrection of *Manta alfredi* (Krefft, 1868) (Chondrichthyes; Myliobatoidei; Mobulidae). Zootaxa. 2301:1-28.

Marshall AD, Dudgeon CL, Bennett MB. 2011. Size and structure of a photographically identified population of manta rays *Manta alfredi* in southern Mozambique. Marine Biology. 158:1111-1124.

Masangcay SIG. 2016. Feeding biology of devil rays (Mobulidae, Chondrichthyes) in Butuan Bay, Northeastern Mindanao, Philippines [MSc Thesis]. Iligan City, Philippines: Mindanao State University-Iligan Institute of Technology.

Masangcay SIG, Metillo EB, Nishida S. 2018. Population structure of the krill prey of the Spinetail Devil Ray *Mobula japanica* (Chondrichthyes, Mobulidae) from Southeastern Bohol Sea, Philippines. Science Diliman. 30(1):74-81.

McCutchan JH, Lewis WM, Kendall C, McGrath CC. 2003. Variation in trophic shift for stable isotope ratios of carbon, nitrogen, and sulfur. Oikos. 102:378-390.

Metillo EB, Cadelinia E, Hayashizaki K, Tsunoda T, Nishida S. 2015. Feeding ecology of two sympatric species of *Acetes* (Decapoda: Sergestidae) in Panguil Bay, the Philippines. Marine and Freshwater Research. 67:1420-1433.

Metillo EB, Masangcay SIG. 2015. Rapid assessment of rays (Mantas and Mobulids) in Sulu Sea and Bohol Sea. Technical Report submitted to the Manta Trust Fund, UK; Save Our Seas and Mindanao State University-Iligan Institute of Technology.

Mintenbeck K, Brey T, Jacob U, Knust R, Struck U. 2008. How to account for the lipid effect on carbon stable-isotope ratio (δ13C): sample treatment effects and model bias. Journal of Fish Biology. 72(4):815-830.

Moura T, Figueiredo I, Farias I, Serra-Pereira B, Neves A, Borges MDF, Serrano Gordo L. 2008. Ontogenetic dietary shift and feeding strategy of *Raja undulata* Lacepède, 1802 (Chondrichthyes: Rajidae) on the Portuguese continental shelf. Scientia Marina. 72(2): 311-318.

Musick JA, Ellis JK. 2005. Reproductive evolution of chondrichthyans. In: Hamlett WC, editor. Reproductive Biology and Phylogeny of Chondrichthyes: Sharks, Batoids and Chimeras. Enfield, NH: Science Publishers. p.45-79.

Nemoto T. 1983. Net sampling and abundance assessment of euphausiids. Biological Oceanography. 2(2,3,4):211-226.

NGA Nautical Chart. 1996. Asia Philippines central part bathymetric chart (6th Ed.); [cited 2016 August 16]. Available from http://www.oceangrafix.com/chart/zoom?chart=91005.

Notarbartolo di Sciara G. 1987. A revisionary study of the genus *Mobula rafinesque*, 1810 (Chondrichthyes: Mobulidae) with the description of a new species. Zoological Journal of the Linnean Society. 91(1):1-91.

Notarbartolo di Sciara G. 1988. Natural history of the rays of the genus *Mobula* in the Gulf of California. Fishery Bulletin. 86(1):45-66.

O'Reilly CM, Hecky RE, Cohen AS, Plisnier PD. 2002. Interpreting stable isotopes in food webs: recognizing the role of time averaging at different trophic levels. Limnology and Oceanography. 47(1):306-309.

Paig-Tran EM, Bizzarro JJ, Strother JA, Summers AP. 2011. Bottles as models: predicting the effects of varying swimming speed and morphology on size selectivity and filtering efficiency in fishes. Journal of Experimental Biology. 214:1643-1654.

Paig-Tran EWM, Kleinteich T, Summers AP. 2013. The filter pads and filtration mechanisms of the devil rays: variation at macro and microscopic scales. Journal of Morphology. 274:1026-1043.

Paulin CD, Habib G, Carey CL, Swanson PM, Voss GJ. 1982. New records of *Mobula japanica* and *Masturus lanceolatus*, and further records of *Luvaris imperialis* (Pisces: Mobulidae, Molidae, Louvaridae) from New Zealand. New Zealand Journal of Marine and Freshwater Research. 16:11-17.

Pierce SJ, Bennett MB. 2003. *Mobula eregoodootenkee*. The IUCN Red List of Threatened Species 2003: e.T41832A10575938; [cited 2016 June 26]. Available from http://www.iucnredlist.org.

Pinkas LM, Oliphant S, Iverson ILK. 1971. Food habits of albacore, bluefin tuna and bonito in Californian waters. California Fish and Game. 152:1-105.

Post DM. 2002. Using stable isotope to estimate trophic position: models, methods and assumptions. Ecology. 83:703-718.

Primavera J, Tumanda Jr MI. 2008. The Agusan marsh: a situationer with focus on scientific aspects. Proceedings of the First Scientific Conference on the Agusan Marsh; 2007 May 21-23; Butuan City, Agusan del Norte, Philippines. UNESCO Jakarta Office: Philippine Council for Aquatic and Marine Research and Development. p. 5-14.

Rayos JCC, Santos MD, Barit NC. 2012. Devil ray resources in Bohol Sea, Philippines. In: Fish for the People, editors. Fish for the People, 44. Bangkok: SEAFDEC; [cited 2017 August 27]. Available from http://www.seafdec.org/download/fish-for-the-people-vol-10-no-1/.

Richardson AJ. 2008. In hot water: zooplankton and climate change. ICES Journal of Marine Sciences. 65:279-295.

Sampson L, Galván-Magaña F, De Silva-Dávila R, Aguíñiga-García S, O'Sullivan JB. 2010. Diet and trophic position of the devil rays *Mobula thurstoni* and *Mobula japanica* as inferred from stable isotope analysis. Journal of the Marine Biological Association of the United Kingdom. 90:969-976.

Scacco U, Consalvo, Mostarda E. 2009. First documented catch of the giant devil ray *Mobula mobular* (Chondrichthyes: Mobulidae) in the Adriatic Sea. Marine Biodiversity Records. 2:e93.

Schluessel V, Bennett MB, Collin SP. 2010. Diet and reproduction in the white-spotted eagle ray *Aetobatus narinari* from Queensland, Australia, and the Penghu Islands, Taiwan. Marine and Freshwater Research. 61:1278-1289.

Shiffman DS, Gallagher AJ, Boyle MD, Hammerschlag-Peyer CM, Hammerschlag N. 2012. Stable isotope analysis as a tool for elasmobranch conservation research: a primer for non-specialists. Marine and Freshwater Research. 63:635-643.

Shwenk K. 2000. Feeding. Form, function and evolution in tetrapod vertebrates. California: Academic Press. p 493-494.

Sleeman JC, Meekan MG, Wilson SG, Jenner CKS, Jenner MN, Boggs GS, Steinberg CC, Bradshaw CJA. 2007. Biophysical correlates of relative abundances of marine megafauna at Ningaloo Reef, Western Australia. Marine and Freshwater Research. 58:608-623.

SPSS. 2002. SPSS for Windows version 11. Chicago, IL: SPSS Inc.

Stewart JD, Hoyos-Padilla EM, Kumli KR, Rubin RD. 2016. Deep-water feeding and behavioral plasticity in *Manta birostris* revealed by archival tags and submersible observations. Zoology. 119(5):406-413.

Sweeting CJ, Jennings S, Polunin NVC. 2005. Variance in isotopic signatures as a descriptor of tissue turnover and degree of omnivory. Functional Ecology. 19:777–784.

Tanaka H, Takasuka A, Aoki I, Ohshimo S. 2008. Geographical variations in the trophic ecology of Japanese anchovy, *Engraulis japonicus*, inferred from carbon and nitrogen stable isotope ratios. Marine Biology. 154:557-568.

Vander Zanden M, Rasmussen JB. 2001. Variation in $\delta^{15}N$ and $\delta^{13}C$ trophic fractionation: implications for aquatic food web studies. Limnology and Oceanography. 46:2061-2066.

Villanoy C, Cabrera O, Yniguez A, Camoying M, de Guzman A, David L, Flament P. 2011. Monsoon-driven coastal upwelling off Zamboanga Peninsula, Philippines. Oceanography. 24:156-165.

Weeks SJ, Magno-Canto MM, Jaine FRA, Brodie J, Richardson AJ. 2015. Unique sequence of events triggers manta ray feeding frenzy in the Southern Great Barrier Reef, Australia. Remote Sensing. 7:3138-3152.

Wetherbee BM, Cortés E. 2004. Food consumption and feeding habits. In: Carrier JC, Musick JA, Heithaus MR, editors. Biology of Sharks and their Relatives. Florida: CRC Press. p. 225-246.

White WT, Clark TB, Smith WD, Bizzarro JJ. 2006a. *Mobula japanica*. The IUCN Red List of Threatened Species 2006: e.T41833A10576180; [cited 2016 June 15]. Available from http://www.iucnredlist.org.

White WT, Giles J, Potter IC. 2006b. Data on the bycatch fishery and reproductive biology of mobulid rays (Myliobatiformes) in Indonesia. Fisheries Research. 82:65-73.

Wiebe PH, Ashian CJ, Gallager SM, Davis CS, Laweson GL, Copley NJ. 2004. Using a high powered strobe light to increase the catch of *Antarctic krill*. Marine Biology. 144:493-502.

Willoughby F. De historia piscium Ray J, editor. Oxonii: Royal Society; 1686.

Wilson SG, Newbound DR. 2001. Two whale shark faecal samples from Ningaloo Reef, Western Australia. Bulletin of Marine Science. 68:361-362.

Wilson SG, Pauly T, Meekan MG. 2001. Daytime surface swarming by *Pseudeuphausia latifrons* (Crustacea, Euphausiacea) off Ningaloo Reef, Western Australia. Bulletin of Marine Science. 68(1):157-162.

Wilson SG, Carleton JH, Meekan MG. 2003a. Spatial and temporal patterns in the distribution and abundance of macrozooplankton on the southern North West Shelf, Western Australia. Estuarine, Coastal and Shelf Science. 56:897-908.

Wilson SG, Meekan M, Carleton J, Stewart T, Knott B. 2003b. Distribution, abundance and reproductive biology of *Pseudeuphausia latifrons* and other euphausiids on the southern North West Shelf, Western Australia. Marine Biology. 142:369-379.

Shirlamaine Irina G. Masangcay is a graduate of B.S. Marine Biology from Mindanao State University-Iligan Institute of Technology. She graduated M.S. Marine Biology from Mindanao State University-Iligan Institute of Technology on time as a DOST-ASTHRDP scholarship in 2016, and was hired immediately after graduation as Instructor at the Caraga State University, Butuan City, Philippines.

Ephrime B. Metillo <ephrime.metillo@g.msuiit.edu.ph> is B.S. Zoology graduate at the Mindanao State University Marawi City. He was University Research Assistant at the Marine Science Institute of the University of the Philippines Diliman before doing a straight Ph.D. Program at the University of Tasmania at Hobart, Australia under the Australian International Development Assistance Bureau (AIDAB) Equity and Merit Scholarship Scheme. He is now Professor at the Mindanao State University-Iligan Institute of Technology, Iligan City, Philippines.

Ken-Ichi Hayashizaki is a marine scientist, an expert on stable isotope analysis and currently Associate Professor at Kitasato University, Sagamihara, Japan.

Satoru Tamada is a recent graduate of Master of Science Marine Bioscience at Kitasato University, Japan with focus on the use of stable isotope analysis in the ecology of the Japanese flounder.

Shuhei Nishida is a recently retired Professor at the Atmosphere and Ocean Research Institute of the University of Tokyo, Japan. He has published more than 110 papers in the field of marine biology and became Editor of the Springer journal Marine Biology. His main field of interest is marine zooplankton biology and ecology.

Science Diliman (January-June 2018) 30:1, 45-59

Fucoidan Content in Philippine Brown Seaweeds

Joemark T. Narsico
Hokkaido University

Joyce A. Nieva
Alfred Wegener Institute Helmholtz Centre for Polar and Marine Research

Alper James G. Alcaraz
University of Saskatchewan, Canada

Eladio G.M. Anino V
University of the Philippines Manila

Norchel Corcia F. Gomez
Marco Nemesio E. Montaño*
Marine Science Institute
University of the Philippines Diliman

ABSTRACT

This study aims to determine which brown macroalgae in the Philippines has the highest content of partially purified fucoidan. Percent fucoidan content of brown seaweeds *Sargassum* spp., *Padina* sp., *Hydroclathrus* sp., *Turbinaria ornata* J. Agardh, *Hormophyza cuneiformis* PC Silva, and *Dictyota dichotoma* Lamouroux were determined in fifty sites across 14 provinces in Northern Luzon (Cagayan, Ilocos), West Luzon (Pangasinan), the eastern seaboard of Luzon (Quezon Province, Camarines, Sorsogon), Central and Eastern Visayas (Bohol, Cebu, Negros Oriental, Negros Occidental), and Northern Mindanao (Camiguin, Lanao del Norte, Misamis Oriental, Misamis Occidental). Crude and semi-pure fucoidan were extracted through acid hydrolysis and ethanol precipitation using 50 grams of dried and milled seaweed biomass. Extracts were verified using infrared spectroscopy with fucoidan from *Fucus vesiculosus* as standard. *Sargassum* spp. is the most widely distributed source of fucoidan found in all sites. *T. ornata* was found in only 11 sites. Both have significantly higher percent

*Corresponding Author

ISSN 0115-7809 Print / ISSN 2012-0818 Online

content ($p \geq 0.05$) of fucoidan than other sampled seaweeds. Higher percent content of semi-purified fucoidan were observed in *D. dichotoma* from Bohol (1.53%), *H. cuneiformis* from Cebu (2.17%), *Hydroclathrus* sp. from Pangasinan (2.23%), *Padina* sp. from Quezon Province (3.69%), *Sargassum* spp. from Camiguin (4.30%), and *T. ornata* from Cagayan (7.03%).

Keywords: Brown seaweeds, distribution, fucoidan, fucoidan yield

INTRODUCTION

The Philippines is known for its diverse marine flora, particularly seaweeds. The country contains 966 taxa of macroalgae, with 893 species in 82 families. Brown macroalgae (Order Ochrophyta, Phaeophyceae) are represented in 171 taxa with 153 species in 10 families (Ang et al. 2013). Brown algae contain fucoxanthin, a xanthophyll pigment responsible for its distinguishing brown color. Their cell walls are composed of cellulose, alginic acid, and other algal polysaccharides (Trono 1997).

Fucoidan is a sulfated polysaccharide commonly found in brown seaweeds, as well as in marine invertebrates (Mak et al. 2013). Fucoidan is absent in green algae (Chlorophyceae) and red algae (Rhodophyceae) (Berteau and Molloy 2003). Fucoidans are structurally diverse macromolecules with a backbone of a (1,3)- and (1,4)-linked α(1,4)-bonded α-L-fucopyranose residues. The polysaccharide may be arranged in stretches of alternating α(1,3)- and α(1,4)-bonded L-fucopyranose residues or through (13)-α-fucan (Ale et al. 2011).

Fucoidans have been extensively studied due to their biological activity which includes anti-inflammatory, antioxidant, anticoagulant, antitumor, antiangiogenic, antithrombotic, antiviral, and immunomodulatory properties. It is widely studied because it comes from different inexpensive sources, and has a potential for drug development or as a functional food resource (Li et al. 2008).

Despite the diverse potential applications of fucoidans, information on the fucoidan content of seaweeds in the Philippines remain limited. This information is necessary to guide manufacturers and researchers on which species and sites should be utilized for the maximization of the extraction of the algal polysaccharide. In this study, we determined the fucoidan content of brown seaweeds collected from different

provinces all over the Philippines through acid hydrolysis extraction and fractional ethanol precipitation. We further compared which among the species has the highest content of fucoidan.

MATERIALS AND METHODS

Sample collection

Gratuitous permits were issued by the different regional offices of the Bureau of Fisheries and Aquatic Resources (BFAR). Fresh seaweed thalli were collected from the intertidal zones across fifty sites in fourteen provinces in the Philippines (Figure 1, Table 1): Northern Luzon (Cagayan, Ilocos); West Luzon (Pangasinan); the eastern seaboard of Luzon island (Quezon, Camarines, Sorsogon); Central and Eastern Visayas Islands (Bohol, Cebu, Negros Oriental, Negros Occidental); and Northern Mindanao Island (Camiguin, Lanao del Norte, Misamis Oriental, Misamis Occidental). One-time sampling was conducted in all the sites. Not all species were found in

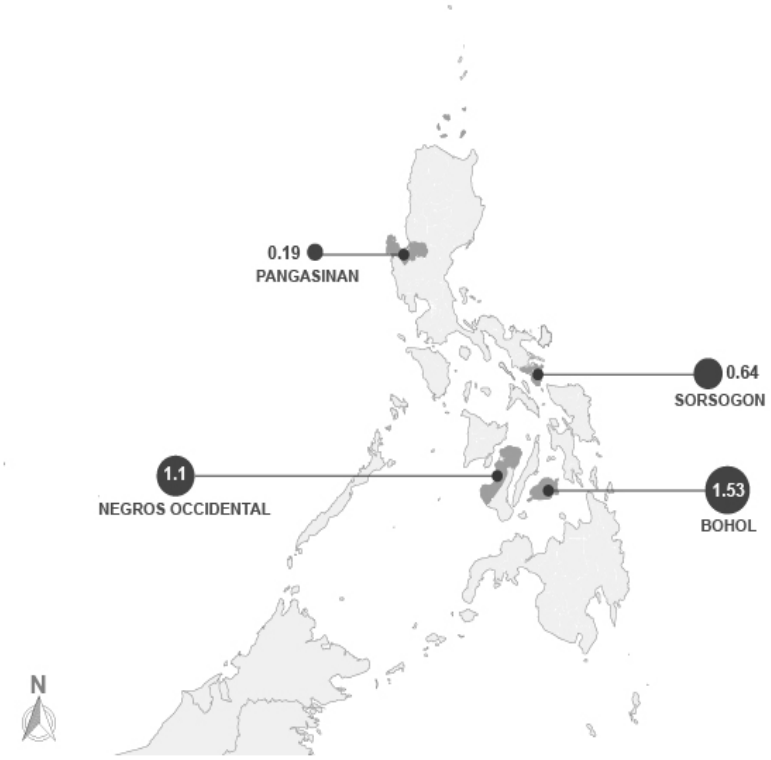

Figure 1. Percent fucoidan content (semi-purified) of Dictyota collected in Pangasinan, Sorsogon, Negros Occidental and Bohol.

Table 1. Sampling sites and GPS coordinates

		Sample Collection		
Genera	**Site**	**Date**	**Latitude**	**Longitude**
Sargassum	Patar, Bolinao, Pangasinan	17-19 May 2010	16°19'59.11"N	119°47'13.95"E
	Patar, Bolinao, Pangasinan	17-19 May 2010	16°19'59.11"N	119°47'13.95"E
	Trensiera, Bolinao, Pangasinan	17-19 May 2010	16°26' 24.84"N	119°56' 45.87"E
	Lucero, Bolinao, Pangasinan	17-19 May 2010	16°24'10.50"N	119°54'22.91"E
	Villa Manzano Norte, Alabat, Quezon	25-30 Nov 2011	14°1'43.17"N	122°5'17.56"E
	Sabang, Alabat, Quezon	25-30 Nov 2011	14°3'28.52"N	122°9'33.78"E
	Gonzaga, Cagayan	25-29 July 2010	18°17'16.30"N	121°59'24.89"E
	Sta. Ana, Cagayan	25-29 July 2010	18°28'49.06"N	122°8'26.09"E
	Sta. Ana, Cagayan	25-29 July 2010	18°28'49.06"N	122°8'26.09"E
	Blue Lagoon, Ilocos Norte	25-29 July 2010	18°37'22.49"N	120°51'34.16"E
	Burgos, Ilocos Norte	25-29 July 2010	16°2'44.93"N	119°45'13.97"E
	Burgos, Ilocos Norte	25-29 July 2010	16°2'44.93"N	119°45'13.97"E
	Burgos, Ilocos Norte	25-29 July 2010	16°2'44.93"N	119°45'13.97"E
	Lioes, Ilocos Norte	25-29 July 2010	18°0' 59.68"N	120°29' 11.37"E
	Pangil, Ilocos Norte	25-29 July 2010	18°0'24.19"N	120°29'20.19"E
	Bgy Nailon, Bogo City, Cebu	10-16 Aug 2010	11°2'52.02"N	124°2'28.96"E
	Bgy Nailon, Bogo City, Cebu	10-16 Aug 2010	11°2'52.02"N	124°2'28.96"E
	Alcoy, Cebu	10-16 Aug 2010	9°40'25.97"N	123°30'18.65"E
	Alcoy, Cebu	10-16 Aug 2010	9°40'25.97"N	123°30'18.65"E
	Maribago, Mactan, Cebu	10-16 Aug 2010	10°17'8.17"N	124°0'26.30"E
	Catmon, Cebu	10-16 Aug 2010	10°43'20.72"N	124°1'4.35"E
	Dalaguete, Cebu	10-16 Aug 2010	9°45'54.64"N	123°32'10.47"E
	Dalaguete, Cebu	10-16 Aug 2010	9°45'54.64"N	123°32'10.47"E
	Bgy. Paypay, Daanbantayan, Cebu	10-16 Aug 2010	11°13'20.67"N	123°58'56.78"E
	Ubojan East, Garcia-Hernandez, Bohol	10-16 Aug 2010	9°36'32.40"N	124°18'7.14"E
	Larapan, Jagna, Bohol	10-16 Aug 2010	9°38'55.90"N	124°22'7.31"E
	Pamilacan Island, Baclayon, Bohol	10-16 Aug 2010	9°29'25.84"N	123°54'59.53"E
	Pamilacan Island, Baclayon, Bohol	10-16 Aug 2010	9°29'25.84"N	123°54'59.53"E
	Sitio Basdio, Loon, Bohol	10-16 Aug 2010	9°48' 2.22"N	123°47' 20.61"E
	Punta-Cruz, Maribojoc, Bohol	10-16 Aug 2010	9°43'56.69"N	123°47'54.99"E
	Sitio Daorong, Bgy. Danao, Panglao, Bohol	10-16 Aug 2010	9°32'41.70"N	123°46'1.16"E
	Bgy. Lawis, Panggangan Island, Calape, Bohol	10-16 Aug 2010	9°54'13.80"N	123°50'27.84"E
	Bgy. Lawis, Panggangan Island, Calape, Bohol	10-16 Aug 2010	9°53' 40.86" N	123°50' 29.37"E
	Pungtod Island, Panglao, Bohol	10-16 Aug 2010	9°40'41.37"N	123°51'0.69"E
	Sitio Hoyohoy, Bgy. Tawala, Panglao, Bohol	10-16 Aug 2010	9°33'23.51"N	123°48'32.91"E
	Sto. Domingo, (Bicol)	8-13 Nov 2010	13°23'42.40"N	123°11'29.20"E
	Sto. Domingo, (Bicol)	8-13 Nov 2010	13°23'42.40"N	123°11'29.20"E
	Pasacao, (Bicol)	8-13 Nov 2010	13°30'30.59"N	123°0'27.70"E
	Bulusan, Sorsogon	8-13 Nov 2010	12°44'52.69"N	124°8'33.59"E
	Bulusan, Sorsogon	8-13 Nov 2010	12°44'52.69"N	124°8'33.59"E
	Sangay, Sorsogon	8-13 Nov 2010	13°36'22.02"N	123°32'51.26"E
	Matnog, Sorsogon	8-13 Nov 2010	12°35'59.45"N	124°6'24.24"E
	Pinagtigasan, Sorsogon	8-13 Nov 2010	14°9'56.41"N	122°58'34.42"E
	Poblacion, Oroqueta City, Misamis Occidental	18-24 Oct 2010	8°28'55.05"N	123°49'37.89"E
	Poblacion, Oroqueta City, Misamis Occidental	18-24 Oct 2010	8°28'55.05"N	123°49'37.89"E
	Talisayan, Poblacion, Misamis Oriental	18-24 Oct 2010	9°0'53.98"N	124°52'15.25"E
	Cantaan, Guinsilaban, Camiguin	18-24 Oct 2010	9°5'36.28"N	124°47'29.84"E
	Tagcatong, Carmen, Misamis Oriental	18-24 Oct 2010	9°5'36.28"N	124°47'29.84"E
	Tagcatong, Carmen, Misamis Oriental	18-24 Oct 2010	8°31'8.56"N	124°37'48.51"E
	Gingoog, Misamis Oriental	18-24 Oct 2010	8°49'57.16"N	125°5'49.66"E
	Kauswagan, Lanao del Norte	18-24 Oct 2010	8°12'3.60"N	124°4'57.57"E
	Liangan, Maigo, Misamis Oriental	18-24 Oct 2010	8°9'36.72"N	123°56'20.24"E
	Bgy. Roque, Mantigue Island, Camiguin	18-24 Oct 2010	9°10'14.48"N	124°49'26.41"E
	San Jose, Negros Occidental	17-20 Sept 2010	9°25'10.65"N	123°14'36.85"E
	Sipalay City, Negros Occidental	17-20 Sept 2010	9°44'47.75"N	122°23'50.14"E
	Dumaguete, Negros Oriental	17-20 Sept 2010	9°18'17.53"N	123°18'40.40"E

Table 1. Sampling sites and GPS coordinates (Cont.)

		Sample Collection		
Genera	**Site**	**Date**	**Latitude**	**Longitude**
	Hinobaan 2, (Negros)	17-20 Sept 2010	9°32'23.05"N	122°30'56.19"E
	San Juan, (Negros)	17-20 Sept 2010	10°36'32.86"N	122°54'36.25"E
	Bais City, (Negros)	17-20 Sept 2010	9°34'44.33"N	123°10'19.55"E
	Hinobaan 1, (Negros)	17-20 Sept 2010	9°35'57.65"N	122°27'50.81"E
	Sta. Catalina, (Negros)	17-20 Sept 2010	9°19'40.42"N	122°51'54.28"E
	Lazi, (Negros)	17-20 Sept 2010	9°19'21.00"N	123°19'33.01"E
	Maria 2, (Negros)	17-20 Sept 2010	10°43'52.81"N	122°56'2.08"E
Turbinaria	Trensiera, Bolinao, Pangasinan	17-19 May 2010	16°26' 24.84"N	119°56' 45.87"E
	Villa Manzano Norte, Alabat, Quezon	25-30 Nov 2011	14°1'43.17"N	122°5'17.56"E
	Gonzaga, Cagayan	25-29 July 2010	18°17'16.30"N	121°59'24.89"E
	Blue Lagoon, Ilocos Norte	25-29 July 2010	18°37'22.49"N	120°51'34.16"E
	Maribago, Mactan, Cebu	10-16 Aug 2010	10°17'8.17"N	124°0'26.30"E
	Punta-Cruz, Maribojoc, Bohol	10-16 Aug 2010	9°44' 4.20" N	123°47' 26.04" E
	Sitio Hoyohoy, Bgy. Tawala, Panglao, Bohol	10-16 Aug 2010	9°32' 57.91"N	123°46' 52.84"E
	Sangay, Sorsogon	8-13 Nov 2010	13°36'22.02"N	123°32'51.26"E
	Talisayan, Poblacion, Misamis Oriental	18-24 Oct 2010	9°0'53.98"N	124°52'15.25"E
	Bgy. Balite, Sagay, Camiguin	18-24 Oct 2010	9°6'14.35"N	124°42'48.10"E
	Bgy. Roque, Mantigue Island, Camiguin	18-24 Oct 2010	9°10' 16.99"N	124°49' 22.38"E
	Sipalay City, Negros Occidental	17-20 Sept 2010	9°44'47.75"N	122°23'50.14"E
	Hinobaan 2, (Negros)	17-20 Sept 2010	9°32'23.05"N	122°30'56.19"E
	San Juan, (Negros)	17-20 Sept 2010	10°36'32.86"N	122°54'36.25"E
Padina	Patar, Bolinao, Pangasinan	17-19 May 2010	16°19'59.11"N	119°47'13.95"E
	Perez, Alabat, Quezon	25-30 Nov 2011	14°10'48.33"N	121°55'27.49"E
	Gonzaga, Cagayan	25-29 July 2010	18°17'16.30"N	121°59'24.89"E
	Sta. Ana, Cagayan	25-29 July 2010	18°28'49.06"N	122°8'26.09"E
	Burgos, Ilocos Norte	25-29 July 2010	16° 2'44.93"N	119°45'13.97"E
	Alcoy, Cebu	10-16 Aug 2010	9°40'25.97"N	123°30'18.65"E
	Maribago, Mactan, Cebu	10-16 Aug 2010	10°17'8.17"N	124°0'26.30"E
	Bgy. Paypay, Daanbantayan, Cebu	10-16 Aug 2010	11°13'20.67"N	123°58'56.78"E
	Pamilacan Island, Baclayon, Bohol	10-16 Aug 2010	9°29'25.84"N	123°54'59.53"E
	Sitio Basdio, Loon, Bohol	10-16 Aug 2010	9°47'51.87"N	123°47'1.22"E
	Sto. Domingo, (Bicol)	8-13 Nov 2010	13°23'42.40"N	123°11'29.20"E
	Bulusan, Sorsogon	8-13 Nov 2010	12°44'52.69"N	124°8'33.59"E
	Sipalay City, Negros Occidental	17-20 Sept 2010	9°44'47.75"N	122°23'50.14"E
	Dumaguete, Negros Oriental	17-20 Sept 2010	9°18'17.53"N	123°18'40.40"E
	Caliling, (Negros)	17-20 Sept 2010	9°59'32.31"N	122°28'14.94"E
	Hinobaan 1, (Negros)	17-20 Sept 2010	9°35'57.65"N	122°27'50.81"E
Hormophyza	Patar, Bolinao, Pangasinan	17-19 May 2010	16°19'59.11"N	119°47'13.95"E
	Trensiera, Bolinao, Pangasinan	17-19 May 2010	16°26' 24.84"N	119°56'45.87"E
	Lucero, Bolinao, Pangasinan	17-19 May 2010	16°24'10.50"N	119°54'22.91"E
	Maribago, Mactan, Cebu	10-16 Aug 2010	10°17'8.17"N	124°0'26.30"E
	Dalaguete, Cebu	10-16 Aug 2010	9°45'54.64"N	123°32'10.47"E
	Sto. Domingo, (Bicol)	8-13 Nov 2010	13°23'42.40"N	123°11'29.20"E
	Bulusan, Sorsogon	8-13 Nov 2010	12°44'52.69"N	124° 8'33.59"E
	Talisayan, Poblacion, Misamis Oriental	18-24 Oct 2010	9°0'53.98"N	124°52'15.25"E
	Hinobaan 2, (Negros)	17-20 Sept 2010	9°32'23.05"N	122°30'56.19"E
	San Juan, (Negros)	17-20 Sept 2010	10°36'32.86"N	122°54'36.25"E
Hydroclathrus	Patar, Bolinao, Pangasinan	17-19 May 2010	16°19'59.11"N	119°47'13.95"E
	Patar, Bolinao, Pangasinan	17-19 May 2010	16°19'59.11"N	119°47'13.95"E
Dictyota	Lucero, Bolinao, Pangasinan	17-19 May 2010	16°24'10.50"N	119°54'22.91"E
	Ubojan East, Garcia-Hernandez, Bohol	10-16 Aug 2010	9°36'32.40"N	124°18'7.14"E
	Pamilacan Island, Baclayon, Bohol	10-16 Aug 2010	9°29'25.84"N	123°54'59.53"E
	Bulusan, Sorsogon	8-13 Nov 2010	12°44'52.69"N	124°8'33.59"E
	Hinobaan 2, (Negros)	17-20 Sept 2010	9°32'23.05"N	122°30'56.19"E
	San Juan, (Negros)	17-20 Sept 2010	10°36'32.86"N	122°54'36.25"E
	Maria, (Negros)	17-20 Sept 2010	10°20'58.91"N	122°50'54.02"E

the same locations. The type of seaweeds collected varied among sampling sites. Samples were washed with distilled water to remove salt and epiphytes, air dried, and milled for extraction. Voucher specimens were dried, identified, labeled, and kept at the GT Velasquez Phycological Herbarium. Study collection sites were limited by geopolitical and accessibility considerations.

Extraction of fucoidan

Milled samples were used for extraction following the methods presented by Ale et al. (2011) with slight modifications. Fifty grams of dried and milled seaweed thalli were briefly acid-treated using dilute hydrochloric acid, heated, allowed to cool, and centrifuged. Residues were discarded afterwards. The solution was neutralized to pH 7.0 using sodium hydroxide pellets, forming brown precipitate of crude fucoidan. Partial purification was performed by fractional precipitation using 30% and 60% ethanol, in order to remove alginate contamination and to precipitate semi-pure fucoidan. Semi-pure fucoidan extracts were subjected to infrared spectroscopy to verify signature peaks of functional groups of fucoidan from *Fucus vesiculosus*. Using FT-IR spectrophotometer, dry fucoidan was mounted to the attenuated total reflectance (ATR) accessory sample holder and scanned from 400 cm^{-1} to 4000 cm^{-1}. Fucoidan from *F. vesiculosus* (Sigma Aldrich: F5631) was used as standard for structure elucidation.

Data analyses

Percent fucoidan content of the sampled seaweeds from different sites were pooled within respective provinces. Percent fucoidan content was calculated using the weight of the semi-purified fucoidan (in grams) divided by the dried and milled biomass (50 g) of seaweeds. The resulting value was then multiplied by 100. The average value of the percent fucoidan content from its corresponding seaweed sources were plotted on the Philippine map through QGIS, an open-source geographic information software. There were differences in the occurrence of seaweeds per sampling site. Statistical analyses on the percent content were conducted via one-way ANOVA and Tukey's Multiple Comparison Test.

RESULTS

The diversity and occurrence of brown seaweeds varied significantly among sampling sites. Samples were grouped and pooled up to genus level. Of the major

groups, *Sargassum* was consistently present and collected in all of the 14 provinces, *Turbinaria* in 11 provinces, *Padina* in 10 provinces, *Hormophysa* in six provinces, *Dictyota* in four provinces, and *Hydroclathrus* in only one province (Figures 1-6). Crude fucoidan content varied from 10.23% to 24.55% (*Sargassum* spp., *Turbinaria ornata*), whereas partially-purified fucoidan yield were at 1.89% to 7.03% (*Padina* sp., *T. ornata*) based on dry weight. *Sargassum* samples from Camiguin had the highest fucoidan content (4.3%) among the provinces while samples from Pangasinan had the lowest content (1.89%). *Turbinaria* from the northern Philippine provinces of Cagayan and Ilocos had the highest content (7.03% and 6.85%, respectively),

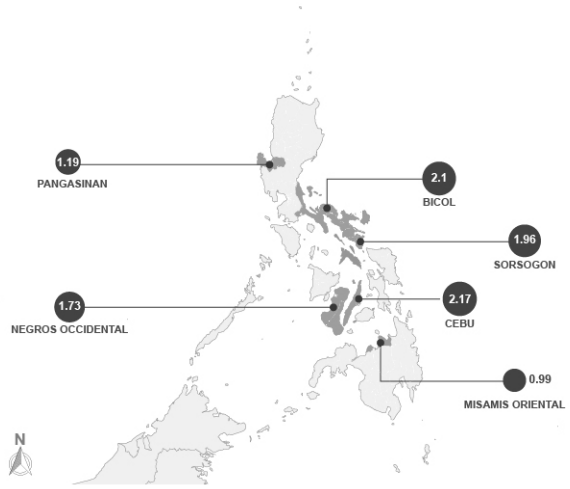

Figure 2. Percent fucoidan content (semi-purified) of the brown seaweed *Hormophysa* collected in six provinces in the Philippines.

Figure 3. Percent fucoidan content (semi-purified) of *Hydroclathrus*. *Hydroclathrus* was only observed in Pangasinan.

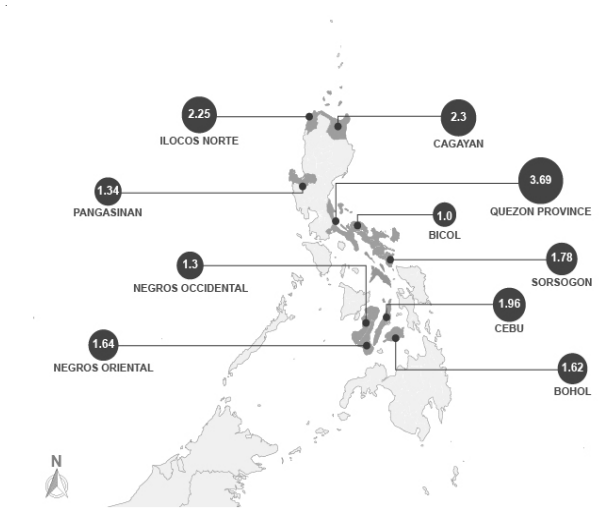

Figure 4. Percent fucoidan content (semi-purified) of *Padina* collected in 10 provinces in the Philippines.

Figure 5. Percent fucoidan content (semi-purified) of *Sargassum*. Samples were collected in 14 provinces in the Philippines. Highest fucoidan yield was observed in Camiguin.

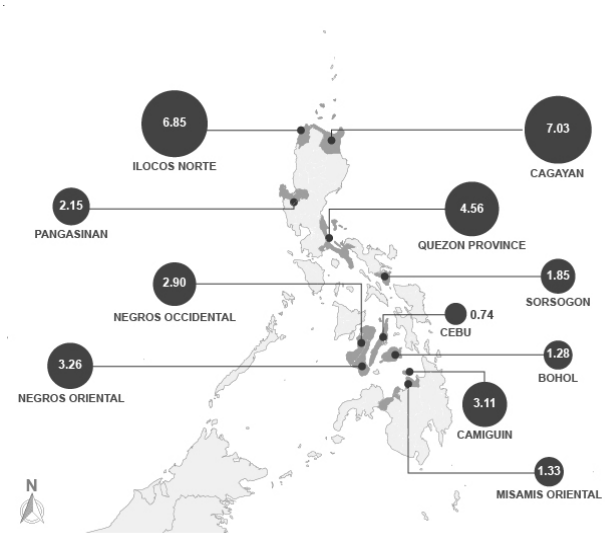

Figure 6. Percent fucoidan content (semi-purified) of *Turbinaria* collected in 11 provinces in the Philippines. Samples from Cagayan obtained the highest fucoidan yield.

while those obtained in Cebu had the lowest fucoidan content at 0.74%. *Padina* from the Quezon Province had the highest content at 3.69%, while the Negros Occidental samples had the lowest content at 1.3%. *Hormophysa* from Cebu had the highest content at 2.17%, while the Misamis Oriental samples obtained the lowest content at 0.99%. *Dictyota* from Bohol had the highest content at 1.53%, while the Pangasinan samples had the lowest content at 0.19%. *Hydroclathrus* from Pangasinan averaged at 2.23% fucoidan content.

Fucoidan percent content among the genus were also compared. There was no significant difference between the contents of *Sargassum,* and *Hormophysa, Hydroclathrus, Padina*, and *Turbinaria* ($p \leq 0.05$). However, the percent content of *Sargassum* compared to *Dictyota* was significantly higher ($p \geq 0.05$). Percent content from *Turbinaria* was significantly higher compared to *Dictyota*, *Hormophysa,* and *Padina* ($p \leq 0.05$). There was no significant difference between the yields of *Sargassum* and *Turbinaria* ($p \leq 0.05$). Additionally, there was no significant difference between the fucoidan contents of *Padina* and *Hormophysa, Hydroclathrus* and *Dictyota*, and *Hormophysa* against *Hydroclathrus* and *Dictyota* (Figure 7).

Representative data on the semi-purified Fucoidan from *Sargassum*, *Turbinaria,* and *Padina* showed peaks similar to the standard fucoidan from *F. vesiculosus* (Figure 8). There were broad bands at 3321–3415 cm^{-1} and small peaks at 2941-2945 cm^{-1}, indicating signature vibrations of OH groups and CH of pyranoid rings, and C6 of fucose and galactose, respectively (Kim et al. 2010). A peak at 1732 cm^{-1} indicates the O-acetyl group (Chandia and Matsuhiro 2008; Kim et al. 2010; Synytsya et al. 2010). Sulfate stretch was observed at 1241–1242 cm^{-1}, which are peaks unique to ester sulfates. Finally, centered peaks were observed between 830–842cm^{-1}, corresponding to C-O-S with sulfate at equatorial and/or axial positions (Bilan et al. 2004; Kim et al. 2010).

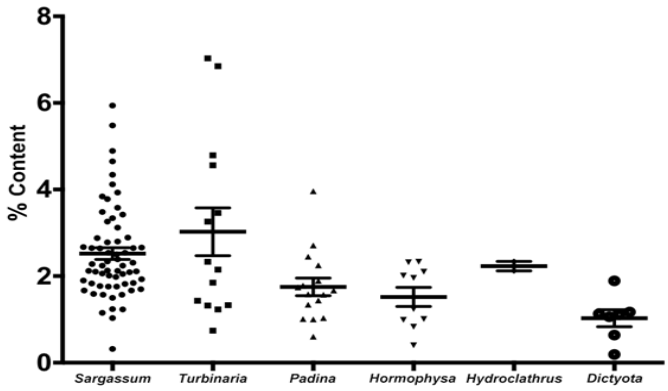

Figure 7. Percent fucoidan content of brown seaweeds in the Philippines. Comparison of the fucoidan yield of samples gathered from different provinces in the country from 2010-2011. Significant differences between the following comparisons were observed at 95% confidence interval: *Sargassum* and *Dictyota*, *Turbinaria* and *Padina*, *Turbinaria* and *Hormophysa,* and *Turbinaria* and *Dictyota*.

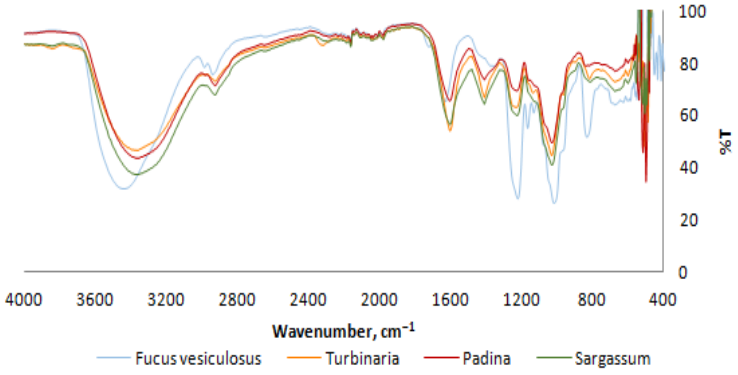

Figure 8. IR spectra of semi-purified fucoidan from different brown seaweed species and *F. vesiculosus*.

DISCUSSION

In this study, we sampled six genera of brown macroalgae from more than 50 sites within 14 provinces in the Philippines. Some seaweeds were at minimal distribution, if not absent, in sampling sites; hence, it was not feasible to extract sufficient fucoidan for analyses. All samples were not collected in the same sites at the same time during the year. Seasonal differences and varying distribution patterns could account for the absence or presence of certain species in the sampling sites. For instance, *Dictyota* is known to be widely distributed in the Luzon and Visayas regions (Trono 1997), but it was not found during certain collection periods in sampling sites in Mindanao. On the other hand, *Sargassum* was collected in all provinces because it is widely distributed and grows during wet and dry seasons. Trono (1997) detailed the distribution and seasonal variation of brown seaweeds in the Philippines. Thus, the differences in their distribution affect the comparison of fucoidan content among the provinces. As a consequence of this irregularity, we pooled the data collected in each genus or species per provinces. This gives us an estimate of how much content can be obtained in seaweeds from representative sites per province.

At present, there is no standardized purification procedure for fucoidans. Classical methods of extracting fucoidan involve a multi-step aqueous extraction using an acid which is usually hydrochloric acid (Ale et al. 2012). Fucoidan extracted using HCl is similar to the fucoidan supplied by Sigma-Aldrich. It is important to note that the characteristics of fucoidan are dependent on the extraction technique. Different extraction methods and purification treatments of fucoidans have resulted to varied compositional results and structural suggestions for fucoidan and other polysaccharides (Ale and Meyer 2013).

Among the seaweeds sampled, *Dictyota* had the lowest fucoidan content while *Sargassum* and *Turbinaria* had the highest. It is expected that Dictyota will have the lowest fucoidan content because of its fleshy and soft fronds. Fucoidan yield and monosaccharide composition are also affected by plant age or maturity (Skriptsova et al. 2010). Aside from differences in fucoidan content, seaweeds are also reported to exhibit a relatively large variation in composition and structural properties, even those belonging to the same order or family (Ale et al. 2011), resulting to an array of varied intensities of bioactivities. The amount and composition of algal metabolites are influenced by complex exogenous factors and endogenous biological and biochemical processes. Mature and reproductive stages of the macrophyte reportedly produce significant amounts of fucoidan compared to young thalli (Zvyagintseva et al. 2003; Skriptsova et al. 2010). Fucoidan content of reproductive

tissues of five macroalgal species were 1.3-1.5 times higher compared to their sterile counterparts. Fucoidan generally accumulates in the reproductive structures of brown seaweeds, whose reproduction cycle also affect the changes in fucoidan monosaccharide composition (Skriptsova et al. 2012).

Geographical location, seaweed species, and seasonal variations may also influence the differences in polysaccharide composition and their chemical structure. In a study conducted by Sinurat et al. (2016), *Sargassum polycystum* from three different sampling sites in Indonesia exhibited differences in their fucoidan and ash contents.

The maturation cycle of the seaweed also influences the changes in fucoidan content. This cycle is primarily influenced by the changes in season. In temperate countries, the increase in water temperature influences the growth and maturity of the seaweeds. This was observed in the brown seaweed *Undaria pinnatifida* collected from September-October 2011 in three different mussel farms in New Zealand, wherein seaweed samples exhibited low fucoidan content on July, an increase in the content on September, and a drastic drop on October 2011. Aside from the changes in the fucoidan content, uronic, sulphate, fucose, and protein contents of the seaweeds were also affected by the month of harvest. The study also suggested that there were variations in the crude fucoidan content and composition between the two different sampling sites (Mak et al. 2013).

Sargassum and *Turbinaria* are potential sources of fucoidan because of their greater fucoidan content and wide distribution in the Philippines. For future studies, it is recommended that the relationships between the fucoidan content of the seaweeds, and the seasonal variations and the reproductive cycles should be investigated. It is also recommended to fine scale the sampling sites, and to focus on locations where there is a high chance of collecting the same type of species in certain months. For example, the preliminary results of this study suggest that the provinces of Camiguin, Negros Oriental, and Pangasinan are possible locations for establishing multiple collection sites for *Sargassum*. For Turbinaria, possible sampling sites can be established in Cagayan, Ilocos Norte, and Quezon Province. By establishing multiple sites in these provinces, researchers and investors can be assisted in deciding which areas should be prioritized for collection and which months the seaweeds should be collected. It is recommended to further study the life cycle and physiology of these fucoidan-yielding species. It is also important to develop culture techniques for local brown seaweeds to prevent the overharvesting of these species in the wild and to create a steady supply of brown seaweeds in the

market. For instance, culture techniques for brown seaweeds *Undaria* and *Laminaria* were already developed (Tseng and Fei 1986). Possible investors and farmers may culture the brown macroalgal species in the sites identified.

ACKNOWLEDGEMENTS

This study was funded by the Department of Agriculture-Biotech Program Implementation Unit through the Bureau of Agricultural Research of the Department of Agriculture, Republic of the Philippines. We thank Ms. Hannah Faith Dormido for making the maps presented in this study. This is contribution no. 452 of the Marine Science Institute, University of the Philippines.

REFERENCES

Ale MT, Meyer AS. 2013. Fucoidans from brown seaweeds: an update on structures, extraction techniques and use of enzymes as tools for structural elucidation. Royal Chemistry Society Advances. 3:8131-8141.

Ale MT, Mikkelsen JD, Meyer AS. 2011. Important determinants for fucoidan bioactivity: a critical review of structure-function relations and extraction methods for fucose-containing sulphated polysaccharides from brown seaweeds. Marine Drugs. 9(10):2106-2130.

Ale MT, Mikkelsen JD, Meyer AS. 2012. Designed optimization of a single-step extraction of fucose-containing sulfated polysaccharides from *Sargassum* sp. Journal of Applied Phycology. 24(4):715-723

Ang PO, Leung SM, Choi MM. 2013. A verification of reports of marine algal species from the Philippines. Philippine Journal of Sciences. 142:5-49

Berteau O, Mulloy B. 2003. Sulfated fucans, fresh perspectives: structures, functions, bioactivities, and biological properties of sulphated fucans and an overview of enzymes active toward the class of polysaccharides. Glycobiology. 13(6):29R-40R.

Bilan MI, Grachev AA, Ustuzhanina NE, Shashkov AS, Nifantiev NE, Usov AI. 2004. A highly regular fraction of a fucoidan from the brown seaweed *Fucus distichus* L. Carbohydrate Research. 339:511–517.

Chandia N, Matsuhiro B. 2008. Characterization of a fucoidan from *Lessonia vadosa* (Phaephyta) and its anticoagulant and elicitor properties. International Journal of Biological Macromolecules. 42:235-240.

Kim EJ, Park SY, Lee JY, Park JHY. 2010. Fucoidan present in brown algae induces apoptosis of human colon cancer cells. BMC Gastroentorology. 10:96.

Li B, Lu F, Wei X, Zhao R. 2008. Fucoidan: Structure and bioactivity. Molecules. 13:1671-1695.

Mak W, Hamid N, Liu T, Lu J, White WL. 2013. Fucoidan from New Zealand *Undaria pinnatifida*: Monthly variations and determination of antioxidant activities. Carbohydrate Polymers. 95(1):606-614.

Sinurat E, Saepudin E, Peranginangin R, Hudiyono S. 2016. Characterization of fucoidan extracted from *Sargassum polycystum* different habitats. International Journal of Chemical, Environmental and Biological Sciences. 4(1):96-99.

Skriptsova AV, Shevchenko NM, Zvyagintseva TN, Imbs TI. 2010. Monthly changes in the content and monosaccharide composition of fucoidan from *Undaria pinnatifida* (Laminariales, Phaeophyta). Journal of Applied Phycology. 22:79–86.

Skriptsova AV, Shevchenko NM, Tarbeeva DV, Zvyagintseva TN. 2012. Comparative study of polysaccharides from reproductive and sterile tissues of five brown seaweeds. Marine Biotechnology. 14:304-311.

Synytsya A, Kim W, Kim S, Pohl R, Synytsya A, Kvasnicka F, Park Y. 2010. Structure and antitumour activity of fucoidan isolated from sporophyll of Korean brown seaweed *Undaria pinnatifida*. Carbohydrate Polymers. 81:41-48.

Trono GC. 1997. Field guide and atlas of the seaweed resources of the Philippines. Makati: Bookmark.

Tseng CK, Fei XG. Macroalgal commercialization in the Orient. In: Ragan MA, Bird CJ, editors. Proceedings of the Twelfth International Seaweed Symposium. Twelfth International Seaweed Symposium; July 27-August 1, 1986; Sao Paolo, Brazil. Netherlands: Springer. 1986. pp 167-172.

Zvyagintseva TN, Shevchenko NM, Chizhov AO, Krupnova TN, Sundukova EV, Isakov VV. 2003. Water-soluble polysaccharides of some far eastern brown seaweeds. Distribution, structure, and their dependence on the developmental conditions. Journal of Experimental Marine Biology and Ecology. 294(1):1-13.

Joemark T. Narsico is a graduate of the Marine Science Institute under the Marine Biology program. He is currently a Ph.D. student at Hokkaido University in Japan. His dissertation focuses on the biochemical studies of polysaccharide lyases from a marine bacterium. His research interests include microbial biotechnology and algal polysaccharides.

Joyce A. Nieva is a graduate of the Marine Science Institute under the Marine Biotechnology program. She is currently pursuing ecological chemistry for her Ph.D. in Alfred Wegener Institute in Bremerhaven, Germany.

Alper James Alcaraz is currently a Ph.D. Research Fellow on Molecular and Environmental Toxicology at the University of Saskatchewan, Canada. He was a research associate at the Marine Science Institute working on inland macroalgal farming techniques and seaweed polysaccharide chemistry. He also lead an ecotoxicology research project that was used in the development of offshore effluent standards, partnering with government and private sectors. He graduated with a Bachelor's degree in Chemistry and an M.S. in Environmental Science in UP where he also worked with leading scientists in the marine sciences.

Eladio G.M. Anino V was one of the research assistants in Dr. Montaño's team, working on algal polysaccharides from brown and red seaweeds during his time in the Seaweed Chemistry Laboratory of the Marine Science Institute. He is currently a fourth year medical student in the University of the Philippines College of Medicine. His research interests include biomedical applications of marine natural products and drug delivery systems.

Norchel Corcia Gomez is a graduate student in the Marine Science Institute under the program Marine Biotechnology. As a research assistant in the Seaweed Chemistry Lab, she has worked with algal polysaccharides from brown and red seaweeds under the supervision of Dr. Montaño. Her research interests include marine natural products, and marine pollution. She plans to study about microplastics in the marine environment for her MS thesis.

Marco Nemesio E. Montano, Ph.D. is a retired professor from the Marine Science Institute. He is a member of the National Academy of Science and Technology of the Philippines. He was awarded by the Integrated Chemists of the Philippines as the Most Outstanding Chemist Award for the year 2012 for his dedication and professional excellence in supporting the seaweed industry in the Philippines. He has published numerous papers and spearheaded projects on various research topics on algal polysaccharides, marine pollution and marine natural products.

Science Diliman (January-June 2018) 30:1, 60-73

Staphylococcus aureus and Methicillin-resistant *S. aureus* (MRSA) carriage in Public Computer Service Providers and Utility Jeepneys in UP Diliman

Jann Eldy L. Daquioag
Ricardo Benedict C. Almirol
Mary Grace B. Ayala
Ma. Socorro Edden P. Subejano
Gil M. Penuliar*
Institute of Biology
College of Science
University of the Philippines Diliman

ABSTRACT

Staphylococcus aureus is a Gram-positive bacterium that causes minor skin infections to life-threatening diseases. It is transmitted through direct contact with fomites, such as computer peripherals and handrails. Treatment of *S. aureus* infections is generally straightforward, but is complicated by drug-resistant strains, particularly methicillin-resistant *S. aureus* (MRSA). The University of the Philippines Diliman (UP Diliman) has hundreds of computer service providers (CSPs) and public utility jeepneys (PUJs) regularly used by faculty, students, staff, and visitors. While no outbreaks of *S. aureus* and MRSA have been reported, the possibility of infection with this pathogen through CSPs and PUJs is very likely. The objectives of this study are to determine the carriage rates of *S. aureus* and MRSA in CSPs, computer peripherals, and handrails of PUJs inside UP Diliman, and to identify the risk factors associated with *S. aureus* and MRSA contamination. A total of 162 computer peripherals from 27 CSPs and 196 PUJ handrails were swabbed. *S. aureus* isolates were identified using colony morphology, biochemical tests, and amplification of the *nuc* gene, whereas MRSA isolates were identified using the cefoxitin challenge and amplification of the *mecA* gene. *S. aureus* was identified in 92.6% of CSPs, 36.4% of computer peripherals, and

*Corresponding Author

ISSN 0115-7809 Print / ISSN 2012-0818 Online

7.1% of PUJs, while MRSA carriage was 3.1% in CSPs and 2% in PUJs. No significant associations between *S. aureus*/MRSA contamination and the assessed risk factors were observed ($p > 0.05$). Results indicate that while *S. aureus* prevalence is relatively high, MRSA carriage is low in CSPs and PUJs in UP Diliman.

Keywords: Staphylococcus aureus, MRSA, computer peripherals, handrails

INTRODUCTION

Staphylococcus aureus is a Gram-positive, coccus-shaped bacterium belonging to the phylum Firmicutes and the family Staphylococcaceae. It is a facultative anaerobe which can ferment mannitol and produce enzymes, such as catalase, coagulase, and deoxyribonuclease (Plata et al. 2009; Kateete et al. 2010). It asymptomatically colonizes the skin and nose in humans, and is able to survive in fomites like plastic and steel surfaces (Chiller et al. 2001; Kusumaningrum et al. 2003).

S. aureus is the causative agent of several diseases, ranging from mild skin infections like impetigo and folliculitis, to toxin-mediated conditions like food poisoning and toxic shock syndrome, and severe infections like staphylococcal bacteremia and endocarditis (Lowy 1998; Chiller et al. 2001). Staphylococcal infections are common and can generally be treated without complications. However, methicillin-resistant strains of *S. aureus* (MRSA), usually mediated by the *mecA* gene, are recently becoming more frequent in the community. In the Philippines, 30% of community-acquired *S. aureus* (CASA) and 38% of hospital-acquired *S. aureus* (HASA) infections are caused by MRSA (Song et al. 2011). According to the Antimicrobial Resistance Surveillance of the Philippines (ARSP), the prevalence of MRSA in the country is 31%. Dicloxacillin remains as the antibiotic of choice for methicillin-susceptible *S. aureus* (MSSA) infections, whereas MRSA infections are treated with vancomycin or teicoplanin (Rayner and Munckhof 2005).

Transmission of *S. aureus* commonly occurs through hand contact with fomites like computer peripherals and handrails contaminated by *S. aureus* (Alkhezali and Taha 2013). According to Yahoo-Nielsen (2009), 20% of Filipinos in urban areas access the internet using public computer service providers (CSPs). The Land Transportation Franchising and Regulatory Board listed 210,840 public utility jeepneys (PUJs) nationwide in 2012, with 58,000 operating in Metro Manila (Ronda 2012). CSPs and PUJs are the dominant access points and mode of transportation, respectively,

for users from lower socio-economic classes. Despite this, there is very little published data on the prevalence of *S. aureus* and MRSA in CSPs and PUJs in the country.

The objectives of this study are the following: to determine the prevalence of *S. aureus* and MRSA in computer peripherals in CSPs and handrails of PUJs in the University of the Philippines Diliman (UP Diliman), and to analyze the risk factors associated with contamination. Findings from this study may be used to influence university policies regarding the regular sanitation in CSPs and PUJs to prevent or reduce further contamination.

MATERIALS AND METHODS

Sample Size

The number of CSPs in UP Diliman was obtained from two sources: the Business Permit Licensing Office of the Quezon City Hall for Department of Trade and Industry-accredited internet cafés, and the website www.mainlib.upd.edu.ph (University Library Diliman 2010) for libraries affiliated with UP Diliman. The number of PUJs was obtained from the UP Diliman Police through the Office of the Vice-Chancellor for Community Affairs. Only CSPs with at least three computers units, signed the consent forms, and allowed unannounced sampling dates were included in the study. The PUJs per route were randomly sampled. The sample size was determined from each population with a 95% confidence level and a confidence interval of 10 (Creative Research Systems 2014). A total of 162 computer peripherals from 27 CSPs and 196 PUJ handrails were sampled.

Consent and Survey Forms

An introductory letter and consent form explaining the purpose of the study and rights regarding participation were provided to the participants. Head librarians and owners of internet cafés were given survey forms for the assessment of the following risk factors: years in service, service hours, comfort room availability, number of computer units, number of clients per day, usual gender of clients, duration of computer use, consumption of food and drink, frequency of cleaning the facility, frequency of cleaning the peripherals, and availability of hand sanitizers.

Sample Collection

Three computers were selected from each CSPs: the computers nearest to the door, furthest to the door, and in the middle of the facility. Sample collection in CSPs was performed on weekdays between 1:00 PM and 4:00 PM. Sterile cotton swabs dipped into 0.9% sterile saline were swabbed on the entire surface of keyboards and mice. The number of PUJs sampled per route is indicated in Table 1. Sampling of PUJs was performed every Thursday from 2:30 PM to 5:30 PM. For each handrail, a 10-cm length was swabbed with 10 sweeps of consistent length. The plate number of each PUJ was recorded to prevent duplication. The location and distribution of the CSPs are shown in Figure 1. The cotton swabs were placed into 15-mL tubes of mannitol salt broth (MSB) and delivered to the Medical Microbiology Laboratory of the Institute of Biology, UP Diliman within 4 hours of collection for incubation at 37°C for 18-24 hours.

Table 1. Prevalence of *S. aureus* and MRSA in PUJs

Route	*S. aureus* Prevalence	MRSA Prevalence
Ikot	2.9% (1/35)	ND
Katipunan	11.6% (5/43)	2.3% (1/43)
Pantranco	6.4% (3/47)	4.3% (2/47)
Philcoa	3.3% (1/30)	ND
SM North EDSA	ND (0/28)	ND
Toki	30.8% (4/13)	7.7% (1/13)
Total	**7.1% (14/196)**	**2% (4/196)**

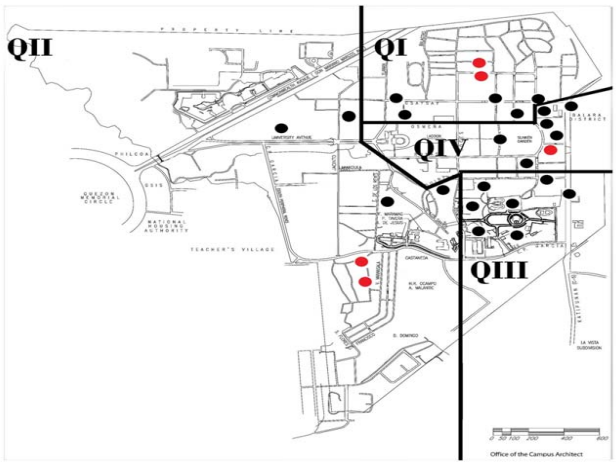

Figure 1. Location and distribution of CSPs that participated in the study. Red dots indicate CSPs where MRSA isolates were obtained.

Isolation

Samples positive for mannitol fermentation were streaked on mannitol salt agar (MSA) plates and incubated at 37°C for 18-24 hours. Medium-sized yellow colonies with smooth surfaces were purified in MSA plates, and the resulting isolated colonies were subcultured on nutrient agar (NA) slants for maintenance.

S. aureus Identification

Gram staining, KOH test, catalase test, coagulase test, and DNase test were used to identify *S. aureus*. Identification was confirmed through the PCR amplification of the *nuc* gene. Genomic DNA was extracted using the microwave lysis method (Ahmed et al. 2014). The cell pellets were briefly washed and resuspended in 100 µL TE buffer. Fifty (50) µL of 10% SDS was added to the mixture for incubation at 65°C for 30 minutes. The lysates were centrifuged at 10,000 x g for 10 minutes. Supernatants were discarded and the cell pellets were heated three times for 1 minute at the high setting of a microwave oven (3D, model no. WP-70B17-65, input: 230V ~60 Hz 1200 W, output: 700 W 2450 MHz). The pellets were dissolved in 200 µL TE buffer. An equal volume of phenol/chloroform/isoamyl alcohol (25:24:1) was added to extract the DNA, followed by overnight absolute ethanol precipitation at -20°C. DNA was recovered by centrifugation at 10,000 x g for 10 minutes, air-dried, and resuspended in 30 µL TE buffer. DNA yield and purity were determined using the Nanodrop™ 2000c Spectrophotometer (Thermo Scientific, USA).

PCR was performed as previously reported with slight modifications (Brakstad et al. 1992) using the forward primer SA-01F 5'-GCGATTGATGGTGATACGGTT-3' and the reverse primer SA-02R 5'-AGCCAAGCCTTGACGAACTAAAGC-3'. Each 25 µL reaction mixture was composed of 5 µL DNA (48 to 50 ng), 3.5 µL sterile water, 2.0 µL of each primer (0.8 µM), and 12.5 µL 2X GoTaq® master mix (Promega, USA). PCR amplifications were performed in a MyCycler™ Thermal Cycler (Bio-Rad, USA) using the following conditions: 94°C for a 2-minute initial denaturation; 37 cycles of 94°C for 1 minute, 42°C for 30 seconds, 72°C for 1 minute; and 72°C for a 7-minute final extension. *S. aureus* BIOTECH 1350 and *S. epidermidis* BIOTECH 10098 were used as controls. PCR products were electrophoresed in 1.3% agarose gel pre-stained with 0.5 µg/mL ethidium bromide using the PowerPac Basic electrophoresis system (Bio-Rad, USA) at 100 V for 22 minutes. The gel was viewed using a White/2UV transilluminator (Thermo Scientific, USA).

PCR amplification of the 16S rDNA was performed as internal control, in order to rule out false-negative results (Amit-Romach et al. 2004). Amplification of the 16S rDNA was performed using the forward primer Unibac-F 5'-CGTGCCAGCCGCGGTAATACG-3' and the reverse primer Unibac-R 5'-GGGTTGCGCTCGTTGCGGGACTTAACCCAACAT-3' under the following conditions: 94°C for 3-minute initial denaturation; 37 cycles of 94°C for 30 seconds, 60°C for 1 minute, 68°C for 2 minutes; and 68°C for a 7-minute final extension. PCR products were electrophoresed and visualized as previously described.

MRSA Identification

S. aureus isolates were challenged with 30 µg cefoxitin using the Kirby-Bauer disk diffusion assay as described in the Clinical and Laboratory Standards Institute (2014). Isolates were identified as MRSA if the zone of inhibition was less than or equal to 21 millimeters. MRSA identification was confirmed by PCR amplification of the *mecA* gene. PCR was performed as described above using the forward primer mecA1F 5'-AAAATCGATGGTAAAGGTTGGC-3' and the reverse primer mecA2R 5'-AGTTCTGCAGTACCGGATTTGC-3'. PCR was performed using the following conditions: 94°C for a 4-minute initial denaturation; 30 cycles of 94°C for 30 seconds, 53°C for 30 seconds, 72°C for 1 minute; and 72°C for a 7-minute final extension (Murakami et al. 1991). MRSA BIOTECH 10378 and *S. aureus* BIOTECH 1350 were used as controls. PCR products were electrophoresed and visualized as previously described.

Statistical Analysis

The prevalence of *S. aureus* and MRSA was determined using the data from samples that yielded positive results. The association of potential risk factors in *S. aureus* and MRSA contamination was performed using the Chi-square test in the IBM SPSS software (IBM Corporation, 2013). P-values less than 0.05 were considered to be statistically significant. Otherwise, the null hypothesis was failed to be rejected, and the risk factor in question was concluded to play no role in contamination.

Waste Disposal

All materials that were contaminated with *S. aureus,* MRSA, and reference microorganisms were decontaminated using an autoclave prior to disposal (CDC 2009).

RESULTS

Prevalence of *S. aureus* and MRSA among CSPs

A total of 162 samples (81 keyboards and 81 mice) were collected from 27 CSPs, which were artificially categorized into four quadrants based on their locations (Figure 1). The prevalence of *S. aureus* among CSPs was 92.6% (Table 2). *S. aureus* was detected in all CSPs located in Quadrants II and III, while only 85.7% of the CSPs in Quadrants I and IV were contaminated. The prevalence of *S. aureus* among keyboards was 40.7%, with more than half (56%) of the keyboards in Quadrant II contaminated with *S. aureus*. Keyboards of the CSPs in Quadrant IV were the least contaminated (24%). The prevalence of *S. aureus* among mice was 32.1%, which is lower compared to the keyboards. Mice of the CSPs in Quadrant II were the least contaminated. The difference in contamination between quadrants was not statistically significant ($p > 0.05$). MRSA had a prevalence of 3.1% and was isolated from one keyboard in Quadrant I, 2 keyboards in Quadrant IV, and one keyboard and one mouse in Quadrant III.

Table 2. Prevalence of *S. aureus* and MRSA in CSPs

Quadrant	*S. aureus* Prevalence in CSPs	*S. aureus* Prevalence in Keyboards	*S. aureus* Prevalence in Mice	Total	MRSA Prevalence
I	85.7% (6/7)	38.1% (8/21)	33.3% (7/21)	35.7% (15/42)	ND
II	100% (6/6)	55.6% (10/18)	27.8% (5/18)	41.7% (15/36)	2.8% (1/36)
III	100% (7/7)	47.6% (10/21)	38.1% (8/21)	42.9% (18/42)	4.8% (2/42)
IV	85.7% (6/7)	23.8% (5/21)	29.6% (6/21)	26.2% (11/42)	4.8% (2/42)
Total	**92.6% (25/27)**	**40.7% (33/81)**	**32.1% (26/81)**	**36.4% (59/162)**	**3.1% (5/162)**

Prevalence of *S. aureus* and MRSA among PUJs

Samples were collected from a total of 196 PUJ handrails designated in 6 different routes (Table 1). The prevalence of *S. aureus* among PUJs was 7.1%. *S. aureus* was detected in all routes except for PUJs traveling to SM North EDSA. PUJs traveling to Katipunan had the highest prevalence of 11.6%. The difference in contamination between routes was not statistically significant ($p > 0.05$). MRSA had a prevalence of 2% and was isolated from PUJs traveling along the Katipunan, Pantranco, and Toki routes.

Risk factor analysis

None of the risk factors assessed in this study was found to have a significant effect on the contamination of *S. aureus* and MRSA on computer peripherals and handrails (Table 3).

Table 3. Statistical analysis of risk factors assessed in the study

Risk factor assessed	X^2	df	*P* value
Years in service	0.270	2	0.874
Service hours	0.909	2	0.635
Comfort room availability	0.173	1	0.678
Number of computer units	2.70	2	0.259
Number of clients per day	0.513	3	0.163
Usual gender of clients	0.376	1	0.540
Duration of use of computer	1.392	4	0.846
Food consumption in facility	0.376	1	0.540
Drinking inside the facility	0.003	1	0.957
Frequency of cleaning the facility	0.756	3	0.860
Frequency of cleaning the peripherals	1.121	4	0.891
Availability of hand sanitizers	0.270	1	0.603

DISCUSSION

The University of the Philippines Diliman has 59 CSPs and 324 PUJs, which cater to faculty, students, administrative staff, and visitors. Computer peripherals, such as keyboards and mice, and PUJ handrails can serve as fomites for the transmission of pathogenic bacteria like *S. aureus*. In the absence of clear sanitation guidelines and regular cleaning of computer peripherals and handrails, contaminated keyboards and mice in CSPs and handrails in PUJs pose a risk to the health of computer users and commuters, respectively.

The inclusion and exclusion criteria of the study specified that only CSPs with at least three computer units may participate, reducing the number of qualified CSPs in calculating our sample size. Some internet cafés also refused to sign the consent forms on grounds of possible bad publicity despite a clause on the confidentiality of the study. In order to have a representation of UP Diliman, the effective sampling sizes were 21 libraries and 5 internet cafés. In this study, 22 libraries and 5 internet cafés were sampled.

Among the 27 CSPs, 25 were positive for *S. aureus* contamination, resulting to a prevalence of 92.6%. No significant difference in the prevalence was observed among quadrants ($p > 0.05$) because most of the CSPs had at least one computer peripheral contaminated with *S. aureus*. Out of the 162 peripherals sampled, 36.4% were positive for *S. aureus* contamination. The high prevalence observed among the CSPs is likely due to the lack of disinfection policies before and after use of the computers. Library computers are high-traffic computer units with high-contact surfaces. Given the large number of students accessing these computers on a daily basis, contamination rates must be intuitively high. The lack of routine disinfection, coupled with the absence of hand sanitizers near the computer terminals, likely contribute to the high prevalence observed. *S. aureus*, including MRSA, has been reported to be a persistent pathogen because it can survive for months on dry surfaces. If no regular surface disinfection is performed, these dry surfaces can be a source of transmission (Kramer et al. 2006). *S. aureus* and other pathogenic microorganisms have also been demonstrated to persist on non-porous surfaces, such as keyboards and mice, even in the absence of enrichment. Unwashed moist or sweaty hands and a room temperature that favor the growth of *S. aureus* can also be factors in the high prevalence observed. *S. aureus* can survive in a salt environment, and sweat is a hospitable environment for the carriage and transfer of the bacterium onto various surfaces (Kahanov et al. 2015).

The prevalence of *S. aureus* was higher in keyboards (40.7%) compared to mice (32.1%), although the difference was not statistically significant ($p > 0.05$). The total surface area of a keyboard is larger than that of a mouse, allowing for the colonization by a greater number of microorganisms. Keyboards also have spaces between keys where dirt and food particles can accumulate. Moreover, both hands are in contact with the keyboard.

The prevalence of *S. aureus* in CSPs observed in this study is lower compared to a similar study conducted in Kogi State University in Nigeria, where *S. aureus* was isolated from all CSPs (Enemuor et al. 2012). It should be noted, however, that in their study, only 30 samples were collected from five sampling sites. By contrast, the prevalence of *S. aureus* among keyboards and mice in this study is higher compared to a study in Al-Mustansiriya University in Iraq, where *S. aureus* had a prevalence of 18.6% among computer peripherals (Alkhezali and Taha 2013). The difference is likely due to the larger number of samples and sampling sites used in this study (162 versus 50 samples). Understandably, a study conducted in Ebonyi State University in Nigeria observed a higher prevalence of 42.6% after sampling 250 keyboards and mice in three campuses (Chukwudi et al. 2013), because it only

included internet cafés, where food and drinks are generally allowed, unlike in school libraries.

The prevalence of *S. aureus* in PUJs in UP Diliman is surprisingly low at 7.1%, considering the heavy traffic of commuters PUJs encounter during school days. However, previous studies on public transportation have reported prevalence values ranging from 8% in London (Otter and French 2009) to 68% in the United States (Lutz et al. 2014), or to even the absence of *S. aureus* (Yeh et al. 2011). The prevalence of *S. aureus* in PUJs is dependent on the nature of the fomite surveyed for the study. The handrails of PUJs are made of smooth steel. The lack of rough surface limits the amount of dirt or organic material that *S. aureus* may use for attachment or nutrient, unless the turnover of passengers using the handrails is high.

PUJs along the Toki route had the highest contamination of *S. aureus* at 30.8%, while PUJs along the SM North EDSA route had no contamination of *S. aureus*. The differences in the prevalence of *S. aureus* across PUJ routes is multifactorial and may be due to the following: passenger profile, personal hygiene of the passengers, bacterial contamination from paper bills and coins used as payment or change, and eating and drinking inside the PUJs. Different numbers and profiles of passengers (students versus non-students) per PUJ were observed during sample collection.

In this study, methicillin resistance was detected through the cefoxitin disk diffusion test and the PCR amplification of the *mec*A gene. The cefoxitin disk test was used as a surrogate test for oxacillin and methicillin test because cefoxitin can better detect heteroresistant strains or strains that carry the resistance gene but express different levels of resistance (CDC 2015). Furthermore, cefoxitin can better induce the *mec*A gene and produce more reproducible and accurate results than oxacillin and methicillin. Based on the results, the prevalence of MRSA in UP Diliman CSPs and PUJs were low at 3.1% and 2%, respectively. Different studies have varied reports on the prevalence of MRSA isolated from public transportation. Stepanoviæ (2008) reported the presence of methicillin-resistant coagulase-negative Staphylococci in the handrails of public buses in Belgrade, Serbia, but no MRSA was detected. A study in Portugal reported a prevalence of 36.2% for MRSA in public buses (Conceição et al. 2013). Based on our search in published literature, no points of comparison could be found for MRSA colonization in CSPs and PUJs in universities in other countries, but it would seem that MRSA prevalence is low in CSPs and PUJs in UP Diliman. However, the isolation of MRSA from these places indicates a potential risk for the transmission of these bacteria in an out-hospital environment.

Based on the risk factor analysis, no correlation was observed between any of the risk factors considered and the contamination of CSPs and PUJs by *S. aureus* and MRSA (Table 3). Previous studies showed similar results (Kassem et al. 2007; Oguzkaya et al. 2015). Such observation could be due to the ubiquitous nature of *S. aureus,* its easy mode of transmission by hand contact, and its status as a normal microflora of the body, allowing *S. aureus* contamination of fomites to be prevalent and unnoticed.

Understanding the spread of infectious diseases involves gaining insight into its complex spatial diffusion through a network of people. Individuals in a given population participate in various activities that may either be mobile or stationary. Mobile activities include commuting through the PUJs, while stationary activities take place at fixed locations such as CSPs. Tracking disease transmission not only involves the individual members of the population but also the physical environment, where these activities are carried out. The epidemiologic model of infectious disease propagation in the work by Perez and Dragicevic (2009) revealed that dynamic spatial interactions within a population lead to high numbers of exposed individuals who carried out stationary activities after moving between places within their environment. It was found that individuals at risk were concentrated in locations like universities. The findings presented in the work support the significance of public areas, such as PUJs and CSPs, in the transmission of microorganisms to commuters and computer users.

In conclusion, this study documents the prevalence of *S. aureus* and MRSA in CSPs and PUJs in UP Diliman, and emphasizes the potential of computer peripherals and handrails as environmental vehicles for the transmission of potentially pathogenic bacteria within the university. The isolation of MRSA, in particular, calls for a need to increase public awareness among computer users and commuters to disinfect hands after being in CSPs and PUJs.

ACKNOWLEDGEMENTS

The results of this study were presented in a poster paper during the 45th Annual Convention and Scientific Meeting of the Philippine Society for Microbiology, Inc. in Vigan City, 2016. This study was supported by the Office of the Vice-Chancellor for Research and Development of the University of the Philippines Diliman through the Ph.D. Incentive Award (Project No. 151505 PhDIA).

REFERENCES

Ahmed OB, Asghar AH, Elhassan MM. 2014. Comparison of three DNA extraction methods for polymerase chain reaction (PCR) analysis of bacterial genomic DNA. African Journal of Microbiology Research. 8(6):598-602.

Alkhezali KAO, Taha BM. 2013. Bacterial contamination of computer keyboards and mice in a university setting. Journal of Biology, Agriculture and Healthcare. 3(18):11-14.

Amit-Romach E, Sklan D, Uni Z. 2004. Microflora ecology of the chicken intestine using 16S ribosomal DNA primers. Poultry Science. 83:1093-1098.

Brakstad OG, Aasbakk K, Maeland JA. 1992. Detection of *Staphylococcus aureus* by polymerase chain reaction amplification of the *nuc* gene. Journal of Clinical Microbiology. 30(7):1654-1660.

[CDC] Centers for Disease Control and Prevention. 2009. Biosafety in Microbiological and Biomedical Laboratories (BMBL), 5th ed. USA: US Department of Health and Human Services. [cited 2015 Sep 1]. Available from www.cdc.gov/biosafety/publications/bmbl5/bmbl.pdf.

[CDC] Centers for Disease Control and Prevention (CDC). 2015. Laboratory Testing for MRSA. USA: US Department of Health and Human Services. [cited 2015 August 11]. Available from www.cdc.gov/mrsa/lab/.

Chiller K, Selkin BA, Murakawa GJ. 2001. Skin microflora and bacterial infections of the skin. The Society for Investigative Dermatology. 6(3):170-174.

Chukwudi A, Ilang DC, Okonkwo EC. 2013. Bacteriological examination of computer keyboards and mouse devices and their susceptibility patterns to disinfectants. American Journal of Bioscience and Bioengineering. 1(3):36-43.

[CLSI] Clinical and Laboratory Standards Institute (CLSI). 2014. Performance standards for antimicrobial susceptibility testing; Twenty-fourth informational supplement. Wayne (PA): CLSI. CLSI document M100-S24, 34(1).

Conceição T, Diamantino F, Coelho C, de Lencastre H, Aires-de-Sousa M. 2013. Contamination of public buses with MRSA in Lisbon, Portugal: A possible transmission route of major MRSA clones within the community. PLoS ONE. 8(11):e77812.

Creative Research Systems, Inc. 2014. Sample Size Calculator. [cited 2015 Nov 22]. Available from: http://www.surveysystem.com/sscalc.htm.

Enemuor SC, Apeh TA, Oguntibeju OO. 2012. Microorganisms associated with computer keyboards and mice in a university environment. African Journal of Microbiology Research. 6(20):4424-4426.

IBM Corporation. 2013. IBM SPSS Statistics for Windows, Version 22.0. New York: IBM Corp.

Kahanov L, Kim YK, Eberman L, Dannelly K, Kaur H, Ramalinga A. 2015. *Staphylococcus aureus* and Community-Associated Methicillin-Resistant *Staphylococcus aureus* (CAMRSA) in and around therapeutic whirlpools in College Athletic Training Rooms. Journal of Athletic Training. 50(4):432-4437.

Kassem II, Sigler V, Esseili MA. 2007. Public computer surfaces are reservoirs for methicillin-resistant staphylococci. The ISME Journal. 1(3):265-268.

Kateete DP, Kimani CN, Katabazi FA, Okeng A, Okee MS, Nanteza A, Joloba ML, Najjuka FC. 2010. Identification of *Staphylococcus aureus*: DNase and Mannitol salt agar improve the efficiency of the tube coagulase test. Annals of Clinical Microbiology and Antimicrobials. 9(1):23-29.

Kramer A, Schwebke I, Kampf G. 2006. How long do nosocomial pathogens persist on inanimate surfaces? A systematic review. BMC Infectious Diseases. 6:130-137.

Kusumaningrum HD, Riboldi G, Hazeleger WC, Beumer RR. 2003. Survival of foodborne pathogens on stainless steel surfaces and cross-contamination to foods. International Journal of Food Microbiology. 85(3):227-236.

Lowy FD. 1998. *Staphylococcus aureus* infections. The New England Journal of Medicine. 339(8):520-532.

Lutz JK, van Balen J, Mac Crawford J, Wilkins JR, Lee J, Nava-Hoet RC, Hoet AE. 2014. Methicillin-resistant *Staphylococcus aureus* in public transportation vehicles (buses): another piece to the epidemiologic puzzle. American Journal of Infection Control. 42(12):1285-1290.

Murakami K, Minamide W, Wada K, Nakamura E, Teraoka H, Watanabe S. 1991. Identification of methicillin-resistant strains of staphylococci by polymerase chain reaction. Journal of Clinical Microbiology. 29(10):2240–2244.

Oguzkaya-Artan M, Baykan Z, Artan C, Avsarogullari L. 2015. Prevalence and risk factors for methicillin-resistant *Staphylococcus aureus* carriage among emergency department workers and bacterial contamination on touch surfaces in Erciyes University Hospital, Kayseri, Turkey. African Health Sciences. 15(4):1289-1294.

Otter JA, French GL. 2009. Bacterial contamination on touch surfaces in the public transport system and in public areas of a hospital in London. Letters in Applied Microbiology. 49(6):803-805.

Perez L, Dragicevic S. 2009. An agent-based approach for modeling dynamics of contagious disease spread. International Journal of Health Geographics. 8:50.

Plata K, Rosato AE, Wegzryn G. 2009. *Staphylococcus aureus* as an infectious agent: overview of biochemistry and molecular genetics of its pathogenicity. Acta Biochimica Polonica. 56(4):597-612.

Rayner C, Munckhof WJ. 2005. Antibiotics currently used in the treatment of infections caused by *Staphylococcus aureus*. Internal Medicine Journal. 35(s2):S3-S16.

Ronda RA. 2012. "Too many vehicles slowing down traffic", group says. Manila: The Philippine Star. [cited 2014 Nov 20]. Available from http://www.philstar.com/metro/2012/07/23/830576/too-many-vehicles-slowing-down-traffic-group-says.

Song JH, Hsueh PR, Chung DR, Ko KS, Kang CI, Peck KR, Yeom JS, Kim SW, Chang HH, Kim YS, Jung SI, Son JS, So TM, Lalitha MK, Yang Y, Huang SG, Wang H, Lu Q, Carlos CC, Perera JA, Chiu CH, Liu JW, Chongthaleong A, Thamlikitkul V, Van PH,on behalf of the ANSORP Study Group. 2011. Spread of methicillin-resistant *Staphylococcus aureus* between the community and the hospitals in Asian countries: an ANSORP study. Journal of Antimicrobial Chemotherapy. 66(5):1061-1069.

Stepanović S, Ćircović I, Djukić D, Vuković D, Švabić-Vlahović M. 2008. Public transport as a reservoir of methicillin-resistant staphylococci. Letters in Applied Microbiology. 47(4):339-341.

University Library Diliman. 2010. The University Library, University of the Philippines Diliman. [cited 2016 May 15]. Available from http://www.mainlib.upd.edu.ph.

Yahoo-Nielsen. 2009. Yahoo-Nielsen net index highlights. [cited 2016 May 15]. Available from http://www.scribd.com

Yeh PJ, Simon DM, Millar JA, Alexander HF, Franklin D. 2011. A diversity of antibiotic-resistant *Staphylococcus* spp. in a public transportation system. Osong Public Health and Research Perspectives. 2(3):202-209.

Gil M. Penuliar <gil.penuliar@upd.edu.ph> is an Assistant Professor of the Institute of Biology. He has a Ph.D. in Medical Science and is a Specialist Microbiology certified by the Philippine Academy of Microbiology.

Jann Eldy L. Daquioag is a graduate student of the Institute of Biology. He is enrolled in the MS Microbiology Program and is affiliated with the Medical Microbiology Laboratory. His current research interests include bioprospecting for natural products against *Staphylococcus aureus*.

Ricardo Benedict C. Almirol is a graduate of the B.S. Biology Program of the Institute of Biology. He was the first undergraduate student of the Medical Microbiology Laboratory to work on *Staphylococcus aureus*.

Mary Grace B. Ayala is a graduate of the M.S. Microbiology Program of the Institute of Biology. She spearheaded the work on *Staphylococcus aureus* in the Medical Microbiology Laboratory.

Ma. Socorro Edden P. Subejano is a graduate student of the Institute of Biology. She is enrolled in the M.S. Microbiology Program and is currently a University Research Associate.

Science Diliman (January-June 2018) 30:1, 74-81

Population Structure of the Krill Prey of the Spinetail Devil Ray *Mobula japanica* (Chondrichthyes, Mobulidae) from Southeastern Bohol Sea, Philippines

Shirlamaine Irina G. Masangcay
Caraga State University

Ephrime B. Metillo*
Mindanao State University-Iligan Institute of Technology

Shuhei Nishida
University of Tokyo

In our recent study on the feeding biology of the Spinetail Devil Ray *Mobula japanica* Müller and Henle, 1841 from Butuan Bay, Southeastern Bohol Sea (Figure 1) (Masangcay et al. 2018), we observed the predominance of euphausiids or krill in the stomach content of the ray. The Norwegian term 'krill' refers to holoplanktonic shrimp-like crustaceans that belong to the Order Euphausiacea (Mauchline 1980).

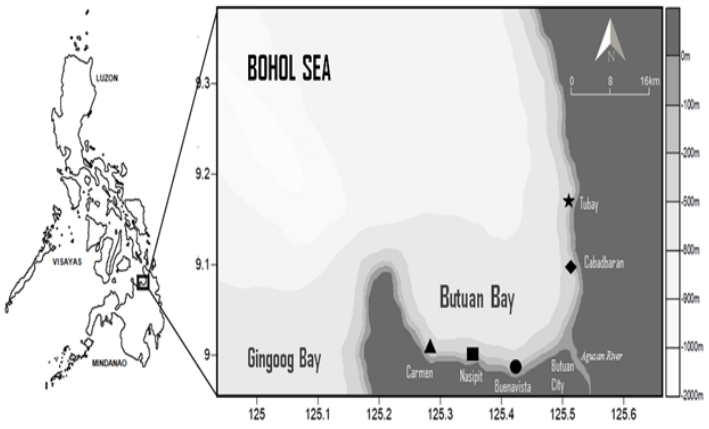

Figure 1. Geographical location of Butuan Bay in Northeastern Mindanao (Southeastern Bohol Sea) and collection sites of landed Spinetail Devil Ray *Mobula japanica* off the Municipality of Carmen (triangle), Nasipit (square), Buenavista (dot), Cabadbaran (diamond), and Tubay (star) in the Province of Agusan del Norte. Inset is the map of the Philippines with the study site enclosed in a square.

*Corresponding Author

ISSN 0115-7809 Print / ISSN 2012-0818 Online

Having an adult body size range of about 1 to 6 cm long, the 86 known species and 11 genera of krill (Baker et al. 1990) usually form dense swarms, and dwell exclusively in oceans and seas at depths of 73 to 220 m (Mauchline 1980). They generally graze upon phytoplankton and detritus, and prey on small zooplankton at surface layers, and through their instinctive diel vertical migration, krill help shunt tons of carbon down to the greater depths of the ocean (Sameoto et al. 1987). Krill are widely known as food of baleen whales, seals, fish, and marine birds (Mauchline 1969, 1980), but recent studies include whaleshark and manta and devil rays in the list of animals feeding on krill (Notarbatolo-di-Sciara 1988; Wilson et al. 2001; Wilson and Newbound 2001; Jarman and Wilson 2004; Sampson et al. 2010; Masangcay et al. 2018). Population structure analysis, which is a major aspect of demography, provides data on the proportions of different life stages, sex ratio, individual size-frequency, and reproductive state of individuals—information that have important ramifications on the species interactions and the population itself (Ranta et al. 2006). Demographic studies of tropical krill species are very limited, but most warm water species are small, mature and breed in 10-12 months, reach 16 to 20 mm in total length of infinity, and a life span of 1 year (Mauchline 1980). Krill are difficult to collect using conventional conical plankton nets (Masangcay 2016), but their high abundance in the stomach of *M. japanica* provided the opportunity to characterize the size structure of intact krill individuals from Butuan Bay. The objective of this study is to describe the population structure of these ingested krill from January to May 2016, during the peak season period of *M. japanica* fishing in Butuan Bay, Southeastern Bohol Sea, Philippines.

Krill samples were obtained from the stomachs of bycatch *M. japanica* individuals (n = 16; for ray body lengths, see Masangcay et al. 2018) caught monthly from January to May 2016 in Butuan Bay, Southeastern Bohol Sea, Philippines (Figure 1). Krill were carefully identified following the descriptions of Weigmann (1971) and Brinton (1975). In order to determine krill size-structure, a sub-sample was randomly collected from the entire *M. japanica* stomach content samples. Since stomach samples contain >1000 individuals per stomach, $1/10^{th}$ sub-sample was obtained for krill size-structure analysis (Brinton 1975). Intact individuals of juvenile and adult male and female stages were meticulously sorted out since partially digested individuals were common in the sub-samples. We made sure that, apart from juveniles, at least 50 males and 50 females were obtained from the sub-sample, with the total number of sorted individuals greater than the 100 mentioned by Watkins (1986). Krill were measured individually based on their total length (from the medial tip of the rostral plate to the end of the telson excluding any setae) using a Vernier caliper with an accuracy of 0.01 mm (Juáres et al. 2017). The size of every krill individual was recorded, and size-frequency histograms were constructed

for different body length categories. Variation of sizes of *Pseudeuphausia latifrons (P. latifrons*) in the stomach population structure analysis based on the influence of size, sex, and sampling month was examined using multifactorial ANOVA (SPSS 2002).

We identified the krill as *Pseudeuphausia latifrons* (G.O. Sars, 1883) (Figure 2). The population structure of ingested *P. latifrons* from each of the 16 ray individuals are shown in Figure 3. Krill total lengths ranged between 4.0 mm and 10.9 mm for

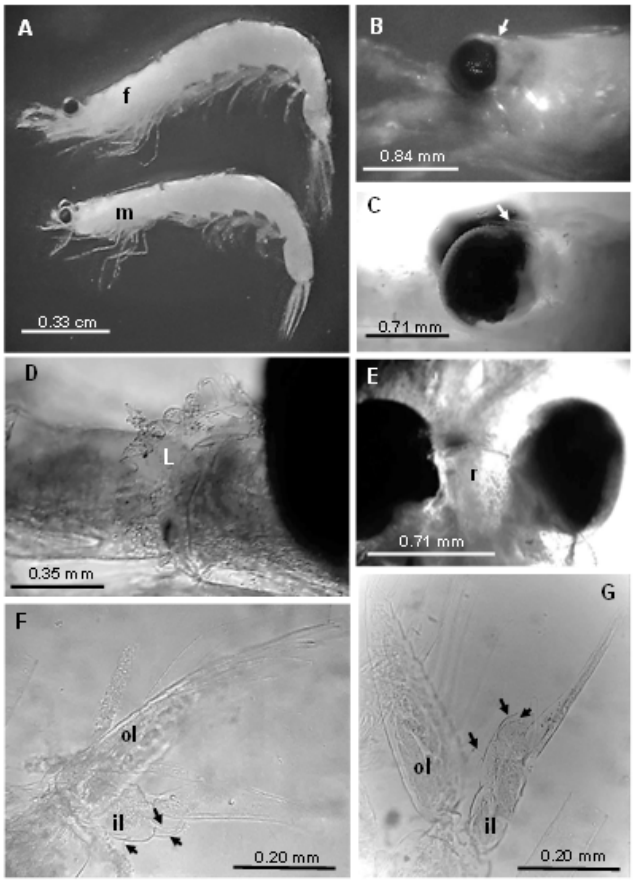

Figure 2. *P. latifrons* (G.O. Sars, 1883), the krill species dominating the ingested prey of the Spinetail Devil Ray *Mobula japanica* from Butuan Bay, Southeastern Bohol Sea. A: Adult female (f) and male (m) individuals. Lateral view of anterior cephalothorax of male (B) and female (C) showing the frontal plate (white arrows). D: Lateral view of the lappet (L) on the left antennular peduncle of an adult female. E: Dorsal view of frontal plate (r) in female. F: Left adult male petasma with processes (black arrows) on the inner lobe (il); ol – outer lobe. G: Right adult male petasma with processes on the inner lobe (il); ol – outer lobe.

both sexes. Individuals that were within the range of 4.0 mm – 6.9 mm were classified as juveniles, while those larger than 7.0 mm were adults. Sizes of prey differed according to the monthly collection of predator (F = 5.52, df = 24, p = 0.00), with males larger than females (F = 2.25, df = 6, p = 0.04). Ingested krill between January to early March ranged between 4.0 mm and 9.9 mm, and the juveniles were abundant until late March. Towards the end of March, the sizes of krill were definitely larger by 1 mm for both sexes (F = 21.83, df = 6, p = 0.00), and a switch in frequency

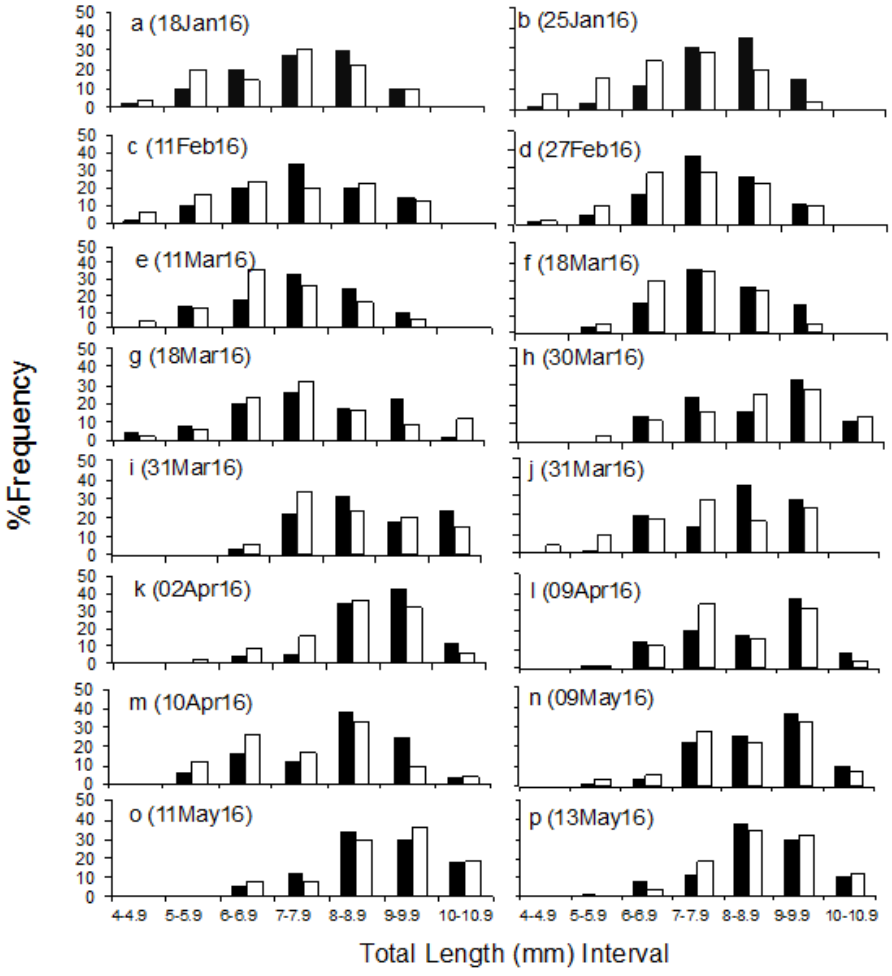

Figure 3. Length-frequency distribution of *P. latifrons* (G.O. Sars, 1883) collected from the stomach contents of the Spinetail Devil Ray *Mobula japanica* individuals (a-p) from Butuan Bay, Southeastern Bohol Sea, Philippines. Solid bar - males; open bar - females. Dates indicate day of collection of the Spinetail Devil Ray.

values with less juvenile krill and more adult krill was observed (F = 20.72, df = 1, p = 0.00). By April and May, both adult male and female prey were noticeably larger, ranging between 5.0 mm and 10.9 mm, than the preceding months which visibly show fewer juvenile prey (F = 18. 06, df = 1, p = 0.05).

The length-frequency histograms clearly show changes in the size-structure of *P. latifrons*, reflecting the individual growth from January to May (Figure 3). Except in January when there were no significant differences in krill sizes between sexes, we observed that male krill were generally larger than female, which agree with the findings of Hanamura et al. (2003) on stranded *P. latifrons* in Western Japan. The histograms show a decrease in the number of juveniles as evidenced by the absence of krill of the smallest length interval and only a few second to the smallest length interval during the warm months of April and May. There was also an increase in the number of adult individuals from the largest length interval in the same warm months. The data on krill lengths show that, towards the warm month of April, body size of krill was bigger and the number of egg-carrying females was greater. This can be related to reproduction, as the tropical krill *P. latifrons* tends to be smaller before warmer months (April and May in Butuan Bay) and becomes larger in warmer months due to mature females carrying eggs (Wilson et al. 2003). If we assume that the minimum maturity length of *P. latifrons* is at 8mm (Wilson et al. 2003), our data indicate that the breeding of this krill species occurs from January to May, with the peak of breeding season occurring in the warmer months of April and May, on account of the many large egg-carrying females during these months. Moreover, for *P. latifrons*, larger females were found to carry more eggs (Wilson et al. 2003). Our findings seem to slightly differ from the report that *P. latifrons* peak in spawning at the end of the Northeast monsoon in Vietnam waters in the South China Sea (Brinton 1975). Our study provides evidence that spawning can also occur during the intermonsoon months of April and May for *P. latifrons* in Butuan Bay.

The temporal change in the size structure of Spinetail Devil Ray-ingested populations of *P. latifrons* indicates that juvenile and adult male and female individuals are present from January to May in Butuan Bay. While juveniles became rare, the largest male and female individuals appeared during the warmer months of April and May. These females bore eggs, indicating spawning in April and May. Krill species *P. latifrons* dominated the ingested food of *M. japonica* from January to May in Butuan Bay. The January to May window is within the fishing season of the Spinetail Devil Ray *M. japanica* in Bohol Sea (Alava et al. 2002; Acebes 2013; Freeman 2014) and Butuan Bay (Metillo and Masangcay 2016), which fall on

September to May, with peak season during February to April. It remains to be studied if there is a link between the temporal pattern of *P. latifrons* abundance and the upwelling events associated with a strong northeast monsoon and the estuarine plume formation during highest river discharge in Butuan Bay (Cabrera et al. 2011; Villanoy et al. 2011).

ACKNOWLEDGEMENTS

We are very grateful for the financial support of the Department of Science and Technology- Science Education Institute, the Office of the Vice-Chancellor for Research and Extension of Mindanao State University-Iligan Institute of Technology, the Manta Trust UK, and the Japan Society for the Promotion of Science (JSPS) (the Asian CORE and the Core-to-Core Programs); the field assistance by local fisherfolks of Buenavista, Agusan del Norte; the copyediting help of Dr. MTRD Sanchez-Metillo; and constructive comments of anonymous reviewers.

REFERENCES

Acebes JMV. 2013. Hunting "Big Fish": A marine environmental history of a contested fishery in the Bohol Sea [Doctoral dissertation]. Western Australia: Murdoch University.

Alava MNR, Dolumbalo ERZ, Yaptinchay AA, Trono RB. 2002. Fishery and trade of whale sharks and manta rays in the Bohol Sea, Philippines. In: Fowler SL, Reed TM, Dipper FA, editors. Elasmobranch biodiversity, conservation and management: Proceedings of the international seminar and workshop; Sabah, Malaysia: Occasional paper of the IUCN Species Survival Commission No. 25. p. 132-148.

Baker A, De C, Boden BP, Brinton E. 1990. A practical guide to the euphausiids of the world. London: British Museum (Natural History). 96 pp.

Brinton E. 1975. Euphausiids of the Southeast Asian waters. Scientific results of marine investigations of the South China Sea and the Gulf of Thailand 1959-1961, Volume 4. USA: University of California. Naga Report. p. 1-287.

Cabrera OC, Villanoy CL, David LT, Gordon AL. 2011. Barrier layer control of entrainment and upwelling in the Bohol Sea, Philippines. Oceanography. 24:130-141.

Freeman AL. 2014. Mobulidae fishery in Bohol, Philippines: An assessment of its sustainability [MRes thesis]. UK: Swansea University.

Hanamura Y, Saito N, Hayashi KI. 2003. Shore stranding of the neritic euphausiid *Pseudeuphausia latifrons* (G.O. Sars, 1883) in Western Japan. Crustaceana. 76(9):1147-1152.

Jarman SN, Wilson SG. 2004. DNA-based species identification of krill consumed by whale sharks. Journal of Fish Biology. 65:586-591.

Juáres MA, Casaux R, Corbalán A, Blanco G, Pereira GA, Perchivale PJ, Coria NR, Mercedes Santos MM. 2018. Diet of Adélie penguins (*Pygoscelis adeliae*) at Stranger Point (25 de Mayo/King George Island, Antarctica) over a 13-year period (2003–2015). Polar Biology. 4(2):303-311.

Masangcay SI. 2016. Feeding biology of devil rays (Mobulidae, Chondrichthyes) in Butuan Bay, Northeastern Mindanao, Philippines [MSc Thesis]. Iligan City, Philippines: Mindanao State University-Iligan Institute of Technology.

Masangcay SI, Metillo EB, Hayashizaki K, Tamada T, Nishida S. 2018. Feeding habits of *Mobula japanica* (Chondrichthyes, Mobulidae) in Butuan Bay, Mindanao Is., Philippines. Science Diliman. 30(1):24-44.

Mauchline J, Fisher LR. 1969. The biology of euphausiids. Advances in Marine Biology. 7:1-454.

Mauchline J. 1980. The biology of mysids and euphausiids. Advances in Marine Biology. 18:1-681.

Metillo EB, Masangcay SIG. 2016. Rapid assessment of rays (Mantas and Mobulids) in Sulu Sea and Bohol Sea. Technical Report submitted to the Manta Trust Fund, UK; Save Our Seas and Mindanao State University-Iligan Institute of Technology.

Notarbartolo-di-Sciara G. 1988. Natural history of the rays of the genus *Mobula* in the Gulf of California. Fishery Bulletin. 86(1):45-66.

Ranta E, Lundberg P, Kaitala V. 2006. Ecology of populations. London: Cambridge University Press. 373 p.

Sameoto DL, Guglielmo L, Lewis MK. 1987. Day/night vertical distribution of euphausiids in the Eastern Tropical Pacific. Marine Biology. 96:235-245.

Sampson L, Galván-Magaña F, De Silva-Dávila R, Aguíñiga-García S, O'Sullivan JB. 2010. Diet and trophic position of the devil rays *Mobula thurstoni* and *Mobula japanica* as inferred from stable isotope analysis. Journal of the Marine Biological Association of the United Kingdom. 90(5):969-976.

SPSS. 2002. SPSS for Windows version 11. Chicago, IL: SPSS Inc.

Villanoy C, Cabrera O, Yniguez A, Camoying M, de Guzman A, David L, Flament P. 2011. Monsoon-driven coastal upwelling off Zamboanga Peninsula, Philippines. Oceanography. 24(1):156-165.

Watkins JL. 1986. Variations in the size of Antarctic krill, *Euphausia superba* Dana, in small swarms. Marine Ecology Progress Series. 31(1):67-73.

Weigmann R. 1971. Eine isolierte Population von *Pseudeuphausia latifrons* (Crustacea: Euphausiacea) im Persischen Golf. Marine Biology. 8(4):351-355.

Wilson SG, Newbound DR. 2001. Two whale shark faecal samples from Ningaloo Reef, Western Australia. Bulletin of Marine Science. 68(2):361-362.

Wilson SG, Meekan M, Carleton J, Stewart T, Knott B. 2003. Distribution, abundance and reproductive biology of *Pseudeuphausia latifrons* and other euphausiids on the southern North West Shelf, Western Australia. Marine Biology. 142(2):369-379.

Wilson SG, Pauly T, Meekan MG. 2001. Daytime surface swarming by *Pseudeuphausia latifrons* (Crustacea, Euphausiacea) off Ningaloo Reef, Western Australia. Bulletin of Marine Science. 68(1):157-162.

Shirlamaine Irina G. Masangcay is a graduate of B.S. Marine Biology from Mindanao State University-Iligan Institute of Technology. She graduated M.S. Marine Biology from Mindanao State University-Iligan Institute of Technology on time as a DOST-ASTHRDP scholarship in 2016, and was hired immediately after graduation as Instructor at the Caraga State University, Butuan City, Philippines.

Ephrime B. Metillo <ephrime.metillo@g.msuiit.edu.ph> is B.S. Zoology graduate at the Mindanao State University Marawi City. He was University Research Assistant at the Marine Science Institute of the University of the Philippines Diliman before doing a straight Ph.D. Program at the University of Tasmania at Hobart, Australia under the Australian International Development Assistance Bureau (AIDAB) Equity and Merit Scholarship Scheme. He is now Professor at the Mindanao State University-Iligan Institute of Technology, Iligan City, Philippines.

Shuhei Nishida is a recently retired Professor at the Atmosphere and Ocean Research Institute of the University of Tokyo, Japan. He has published more than 110 papers in the field of marine biology and became Editor of the Springer journal Marine Biology. His main field of interest is marine zooplankton biology and ecology.

Guidelines for Expanding Conference Papers for Submission to *Science Diliman*

Science Diliman welcomes conference paper submissions provided they have been updated and expanded. Below is a checklist of required and suggested actions for authors.

Mandatory Actions

- ✓ If changes are made, choose a new title for the paper.
- ✓ Use feedback obtained at the conference to update, revise, and rewrite the paper as appropriate to improve its overall quality.
- ✓ Reference your conference paper in the appropriate locations.
- ✓ Include a footnote in the submitted manuscript stating, e.g., "An earlier version of this paper was presented at the 20XX Technical Conference and was published in its proceedings."
- ✓ Indicate in a letter (upload as a supporting document during the submission process) whether the conference paper was peer-reviewed and clearly state what has been changed.
- ✓ Provide the original conference paper (upload a PDF file during the submission process).
- ✓ If the conference organizers or professional society hold the copyright for your conference paper, obtain permission to reprint figures and tables that are used in the expanded paper.

Recommended Actions

- ✓ Expand the background section and include additional references.
- ✓ Include novel scientific content and expanded descriptions of procedures.
- ✓ Provide data that was not published at the conference.
- ✓ Revise and update figures and text to avoid exact duplication of the conference proceedings.

(Adapted with permission from the Editors of IEEE Sensors Journal)

UNIVERSITY OF THE PHILIPPINES DILIMAN

Office of the Vice-Chancellor for Research and Development

Call for Papers

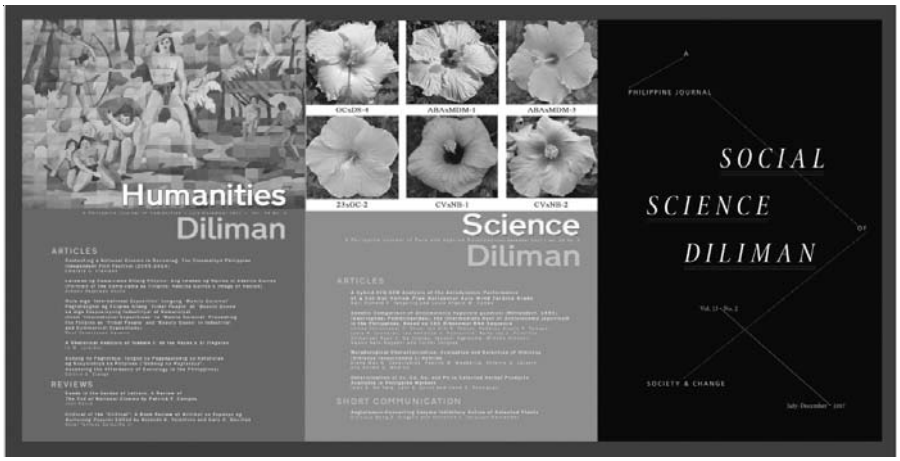

Humanities Diliman, Science Diliman* and *Social Science Diliman

are peer-reviewed journals published biannually (in June and December) by the University of the Philippines Diliman through the Office of the Vice-Chancellor for Research and Development (OVCRD).

Papers are accepted year-round.

For more information, please visit the OVCRD website <www.ovcrd.upd.edu.ph>

Journal Cover images courtesy of (l-r) Vargas Museum & Magdalita et al.

RESEARCH DISSEMINATION AND UTILIZATION OFFICE
OFFICE OF THE VICE-CHANCELLOR FOR RESEARCH AND DEVELOPMENT
Lower Ground Floor, PHIVOLCS Bldg., C.P. Garcia Ave., UP Diliman 1101 Quezon City
☎(02) 436-8720 Fax (02) 927-2568 ✉ research.dissemination1@upd.edu.ph

JOURNAL SUBSCRIPTION FORM

NOTE: This Subscription Form is for the three journals published by UP Diliman through its Office of the Vice-Chancellor for Research and Development (OVCRD), as follows: *Humanities Diliman, Science Diliman,* and *Social Science Diliman.* Each journal is published twice a year. **The subscription price for each journal (vols. 1 and 2) is Php650.00. (Subscription price is subject to change without prior notice.)**

I/We would like to subscribe to the following journal/s:

JOURNAL TITLE (please check)	**NUMBER OF SUBSCRIPTIONS** (for each journal, please indicate desired number of copies)	**TOTAL AMOUNT** (number of subscriptions x Php650)
☐ HUMANITIES DILIMAN		
☐ SCIENCE DILIMAN		
☐ SOCIAL SCIENCE DILIMAN		
	GRAND TOTAL	

METHOD OF PAYMENT (Please check one)

☐ PAY CASH at the OVCRD (See address above)

☐ PAY IN CHECK (Please make check payable to the University of the Philippines Diliman-OVCRD)

☐ MONEY REMITTANCE (Payable to NARITA E.C. DE LAS ALAS, c/o OVCRD Research Dissemination and Utilization Office, with office address as indicated above and mobile phone no. 09209605857)

SUBSCRIBER DETAILS

NAME/INSTITUTION _____

CONTACT PERSON
(For Institutional Subscribers) _____

MAILING ADDRESS _____ EMAIL ADDRESS _____

_____ TELEPHONE NO. _____

_____ FAX NO. _____

Please send accomplished Subscription Form to the RDUO-OVCRD via email or fax (please see above for contact details). If mode of payment is through money remittance, please send proof of remittance together with the accomplished Subscription Form.

Journal Policy on Research Misconduct[1] (Final March 13, 2009)[2]

PRINCIPLES

The journals[3] published by the Office of the Vice-Chancellor for Research and Development, University of the Philippines Diliman (OVCRD, UP Diliman) uphold the highest standards of excellence and ethics in the conduct of research. These being publications of the flagship campus of the only National University of the Philippines, the editorial boards consider the maintenance of such standards part of their commitment to public trust and the pure pursuit of new knowledge. As such, research misconduct shall never be tolerated.

PURPOSE

This document defines research misconduct, specifies the internal controls the journals have formulated to prevent such misconduct, describes the process for responding to allegations of research misconduct, and identifies appropriate disciplinary actions.

DEFINITIONS

Scientific misconduct or research misconduct (henceforth these shall be used interchangeably) is the fabrication, falsification, or plagiarism in proposing, performing, or reviewing research or in reporting research results.[4]

Fabrication is making up data or results and recording or reporting them.[5]

Falsification is manipulating research materials, equipment or processes, or changing or omitting data or results such that the research is not accurately represented in the research record.

Plagiarism is the appropriation of another person's ideas, processes, results or words without giving appropriate credit.

Research misconduct does not include honest error or differences of opinion.

INTERNAL CONTROLS

Appointments to the editorial boards are based on track records of scholarship and research integrity.

The journals strictly follow a double-blind refereeing process in which at least two experts in the research area concerned review any manuscript submission.

Three mechanisms ensure adequate safeguards against research misconduct. The "Notes to Contributors" stipulates that "all articles must have a high degree of scholarship," that "all articles must be original" and that "all allegations of research misconduct shall be pursued assiduously." The "Manuscript Submission Form" includes a certification from the corresponding author on the veracity of the presentations of the co-authors. The Publication Agreement which the author signs before the article is published includes among others, a provision allowing wide latitude in responding to research misconduct: "The Author warrants that the articles is original and does not infringe upon any proprietary or intellectual property right…."

RESPONSE TO ALLEGATIONS OF RESEARCH MISCONDUCT

Upon receipt of a written allegation of research misconduct, the editor-in-chief shall convene the editorial board to review the allegation. The editorial board shall seek to establish if the complaint a.) is an instance of research misconduct as defined above and; b.) is specific and substantiated. If these requirements are not met, the editor-in-chief writes the complainant of the board's decision to dismiss the complaint and the bases for such dismissal. If these are met, the board consults with the referees of the article and may opt to consult with another expert in the research area concerned, to further determine the substance of the allegation. In both instances, the respondent shall be advised in writing of the receipt of such allegation and shall be allowed to respond.

If the manuscript in question has not yet been published in the journal, the board shall return the article to the author with the specific advice on how to rework the article; the author is also given the option to withdraw the manuscript. If the manuscript has already been published in the journal, and research misconduct is proven, the editor-in-chief shall notify the author and the institution to which the

author is affiliated as well as the funding agency that supported the research. The board shall ensure correction of the literature in the succeeding issue through various methods as defined by the board. These may include errata, retractions, and apologies to be written by the author concerned.

Moreover, the Board can opt to impose the following sanctions: 1. disallow the contributor concerned from refereeing a manuscript submission; 2. ban the contributor from publishing in the journal for a period the Board shall determine.

DISCIPLINARY ACTION

The editorial board does not consider it within its purview to impose disciplinary sanctions against the contributors concerned. However, in the case of faculty, researchers, and students from UP Diliman, it shall adhere to the protocol in processing written complaints against the faculty and employees and support appropriate disciplinary action stipulated in the Rules and Regulations on the Discipline of Faculty Members and Employees of the UP Diliman Faculty and Administrative Manual.

FOOTNOTES

[1] Based on discussions in the meetings held on February 2, 2009 and February 24, 2009 at the OVCRD Conference Room in response to Dean Saloma's request for *Science Diliman* to formulate a scientific misconduct policy. In attendance were: Dr. Corazon D. Villareal, RDUO Director, presiding; Dr Henry J. Ramos, PMRGO Director and Professor, NIP; Atty. Vyva Victoria Aguirre, OVCRD Legal Consultant; Editors-in-Chief Dr. Maricor Soriano (*Science Diliman*) and Dr. Maria Mangahas (*Social Science Diliman*). Ms. Nanie Domingo and Ms. Dercy Mararac, editorial assistants for OVCRD journals took down the minutes.

[2] As approved in the meeting of the above discussants on February 24, 2009 at the OVCRD Conference Room.

[3] *Science Diliman, Social Science Diliman,* and *Humanities Diliman*

[4] Federal Policy on Research Misconduct, United States of America.

[5] These definitions of the forms of research misconduct are quoted verbatim from the policy of the Office of Research Integrity of the United States Public Health Service. Similar phrasings of definitions are adopted in the references listed at the end of this document.

REFERENCES

Council of Science Editors. "White Paper on Promoting Integrity in Scientific Journal Publications, As Approved by the CSE Board of Directors on September 3, 2006." www.Council ScienceEditors.org. Accessed on January 26, 2009.

"Policy on Scientific Misconduct: University of Southern California. http://policies.usc.edu/plicies/scientific misconduct070108.pdf

"Scientific Misconduct Policy: New York University, The Office of Sponsored Programs. https://www.nyu.edu/osp/policies/scientific misconduct.php

"Manuscript Submission." *Optical and Quantum Electronics*. http://www.springer.com/physics/optics/journall/11082

"Manuscript Submission Procedures." *American Journal of Physics*. http://www.kzoo.edu/ajp/submit.html

Information for Authors

1. Science Diliman is a journal of pure and applied sciences published by the University of the Philippines through the Office of the Vice-Chancellor for Research and Development (OVCRD). Considered for publication are primary and original papers. Review articles and short communications may occasionally be accepted. In all other cases, papers should present new and previously unpublished material.

2. Contributions must be in English and should not have been submitted for publication elsewhere.

3. Manuscripts are selected for publication according to editorial assessment of their suitability and reviews of independent referees. They will be sent to two or three reviewers, chosen for their expertise. Contributors may suggest reviewers.

4. Submission of a manuscript implies: that the work described has not been published before (except in the form of an abstract or as part of a published lecture, review, or thesis); that it is not under consideration for publication elsewhere; that its publication has been approved by all co-authors, if any, as well as by the responsible authorities at the institute where the work has been carried out.

   The letter to the editor usually contains these: that, if and when the manuscript is accepted for publication, the authors agree to the automatic transfer of the copyright to the publisher; that the manuscript will not be published elsewhere in any language without the consent of the copyright holders; that written permission of the copyright holder is obtained by the authors for material used from other copyrighted sources; and that any costs associated with obtaining this permission are the authors' responsibility.

5. Authors must submit electronically prepared manuscripts in Microsoft Word.

6. Manuscripts should be formatted for A4 paper, double-spaced, with 1" margins on all sides. Each page of the manuscript must include continuous line numbers in the margin. All pages should be numbered consecutively on the upper right hand corner of the page.

7. Page 1 should contain the article title, author(s), affiliation(s), and the name and complete mailing address (and telephone number, fax number, and e-mail) of the person to whom correspondence should be sent.

8. Page 2 should contain a short abstract of not more than 250 words. The abstract should contain facts and conclusions, rather than citation of the areas and subjects that have been treated or discussed. The abstract should start with the hypothesis or a statement of the problem to be solved, followed by a description of the method or technique utilized to solve the problem. The abstract should end with a summary of the results that were obtained and their implications. It is to be followed by a maximum of six key words. The author must also submit a layman's abstract of not more than 200 words.

9. The paper should be organized as follows:

   Abstract and Layman's Abstract
   Introduction
   Materials and Methods
   Results and Discussion (or Results separate from Discussion)
   Acknowledgments
   References

10. Reference lists, figures, tables, and figure/list captions should all be on separate sheets, all of which should be double-spaced, and numbered. Standard nomenclature should be used. Unfamiliar terms, abbreviations, and symbols must be defined at first mention.

11. References to the literature citations in the text should be by author and year; where there are two authors, both should be named; with three or more only the first author's name plus "et al." need to be given.

    References in the text should follow the Council of Science Editors (CSE) Scientific Style and Format, 7th Edition, 2006.

Examples:

Articles from Journals: Print (Section 29.3.7.1 p. 518-527)

Format: Author(s). Date. Article title. Journal title. Volume(issue):location.

Example: Smart N, Fang ZY, Marwick TH. 2003. A practical guide to exercise raining for heart failure patients. J Card Fail. 9(1):49-58.

Articles from Journals: Online (Section 29.3.7.13 p. 557-558)

Format: Author(s) of article. Date of publication. Title of article. Title of journal (edition) [medium designator]. [date updated; date cited]; Volume(issue):location. Notes.

Example: Savage E, Ramsay M, White J, Beard S, Lawson H, Hunjan R, Brown D. 2005. Mumps outbreaks across England and Wales in 2004: observational study. BMJ [Internet]. [cited 2005 May 31]; 330(7500):1119-1120. Available from: http://www.bmj.bmjjournals.com/cgi/reprting/330/7500/1119 doi:10.1136/bmj.330.7500.1119.

Articles from Newspapers: Print (Section 29.3.7.8 p. 543)

Format: Author(s). Date. Title of article. Title of newspaper (edition). Section:beginning page of article (column no.).

Example: Weiss R. 2003 Apr 11. Study shows problems in cloning people: researchers find replicating primates will be harder than other mammals. Washington Post (Home Ed.). Sect. A:12 (col. 1).

Books: Print (Section 29.3.7.2 p. 527-534)

Format: Author(s). Date. Title. Edition. Place of publication: publisher. Extent. Notes.

Example: Schott J, Priest J. 2002. Leading antenatal classes: a practical guide. 2nd ed. Boston (MA): Books for Midwives.

Books: Online (Section 29.3.7.13 p. 556-564)

Format: Author(s). Date of publication. Title of book [medium designator]. Edition. Place of publication: publisher; [date updated; date cited]. Notes.

Example: Griffiths AJF, Miller JH, Suzuki DT, Loweontin RC, Gelbart WM. c2000. Introduction to genetic analysis [Internet]. 7th ed. New York (NY): W. H. Freeman & Co.; [cited 2005 May 31]. Available from: http://www.ncbi.nlm.nih.gov/books/bv.fcgi?call=bv.View..ShowTOC&rid=iga.TOC.

Book Chapter (Section 29.3.7.2.10 p. 533)

With Editors

Format: Author(s). Title of article. In: Editors. Title of book. Edition. Place of publication: publisher; Date of Publication. Notes.

Example: Anderson RJ, Schrier RW. Acute renal failure. In: Braunwald E, Isselbacher KJ, Petersdorf RD, editors. Harrison's principles of internal medicine. 15th ed. New York (NY); McGraw-Hill; c2001. p. 1149-1155.

Without Editors

Format: Author(s). Title of article. In: Title of book. Edition. Place of publication: publisher; Date of Publication. Notes.

Example: Hazeltine WA. AIDS. In: The encyclopedia Americana. International ed. Danbury (CT): Grolier Incorporated; 1990. p. 365-366.

Conference Proceedings/Papers (Section 29.3.7.3 p. 534)

Published without author(s)

Format: Editor(s). Date. Title of book. Number and name of conference; date of conference; place of conference. Place of publication: publisher. Extent. Notes.

Example: Callaos N, Margenstern M, Zhang J, Castillo O, Doberkat EE, editors. c2003. SCI 2003. Proceedingsof the 7th World Multiconference on Systemics, Cybernetics and Informatics; Orlando, FL. Orlando (FL): International Institute of Informatics and Systematics.

Published with author(s)

Format: Author(s) of Paper. Date. Title of paper. In: Editor(s). Title of book. Number and name of conference; date of conference; place of conference. Place ofpublication: publisher. Location. Notes.

Example: Lee DJ, Bates D, Dromey C, Xu X, Antani S. c2003. An imaging system correlating lip shapes with tongue contact patterns for speech pathology research. In: Krol M, Mitra S, Lee DJ, editors. CMS 2003. Proceedings of the 16th IEEE Symposium on Computer-Based Medical Systems; New York. Los Alamitos (CA): IEEE Computer Society. p. 307-313.

Unpublished (Section 29.3.7.15 p. 566-568)

Format: Authors(s). Date of conference. Title of paper. Paper presented at: Title of conference. Number and Name of the conference; place of the conference.

Example: Antani S, Long LR, Thomas GR, Lee DJ. 2003. Anatomical shape representation in spine x-ray images. Paper Presented at: VIIP 2003: Proceedings of the 3rd IASTED International Conference on Visualization, Imaging and Image Processing; Benalmadena, Spain.

Technical Reports (Section 29.3.7.4 p. 537)

Format: Author(s). Date. Title of report. Edition. Place of publication: Publisher. Extent. Report No.: Notes.

Example: Feller BA. 1981. Health characteristics of persons with chronic activity limitation, United States, 1979. Hyattsville (MD): National Center for Health Statistics (US). Report NO.: VHS-SER-10/137. Available from: NTIS, Springfield, VA; PB88-228622.

Dissertations and Theses (Section 29.3.7.5 p. 539-541)

Format: Authors(s). Date. Title of dissertation and thesis [content designator]. Place of publication: publisher. Extent. Notes.

Example: Lutz M. 1989. 1903: American nervousness and the economy of cultural change [dissertation]. Stanford (CA): Stanford University.

Group/Corporate Author (Section 29.2.1.2.5 p. 494)

Format: [Abbreviation of group] Name of group (Country). Date. Title. Place of publication: Publisher. Notes.

Example: [IOM] Institute of Medicine (US). 1975. Legalized abortion and the public health; report of a study by a committee of the Institute of Medicine. Washington (DC): National Academy of Sciences.

Other Internet Materials (Section 29.3.7.13 p. 556-564)

Homepage

Format: Title of Homepage [medium designator]. Date of publication. Edition. Place of publication: publisher; [date updated; date cited]. Notes.

Example: APS*net*: plant pathology online [Internet]. c1994-2005. St Paul (MN): American Phytopathological Association; [cited 2005 Jun 20]. Available from:http://www.apsnet.org/.

For more detailed examples please refer to the CSE Manual 7th Edition.

12. The list of references at the end of the paper should include only works mentioned in the text and should be arranged alphabetically by the name of the author.

13. Responsibility for the accuracy of bibliographic references rests entirely with the author, who is requested to use as few "in press" citations as possible. "In press" citations must include the name of the journal that has accepted the paper.

14. Footnotes in the text should be numbered consecutively. Footnotes to the title or authors of the article are marked by asterisks and placed on the title page.

15. Figures and graphs should always be mentioned in the text and numbered with Arabic numerals. A brief descriptive caption should be provided for each figure or table on a separate page. At the lower hand corner, the name of the author and the figure number should be indicated.

16. Illustration hard copy should comprise:

    Line drawing should be of good quality and should not exceed 8 1/2" x 11" size paper, with clearly legible inscriptions, even if reduced to 85% of their size.

    Photographs/Illustrations: Well-constructedphoto-graphic prints (not photocopies), trimmed at right angles and in the final size desired by the author.

17. When possible, all organisms must be identified by the scientific binomen.

18. Mathematical equations should be clearly presented so that they can be interpreted properly.

19. Obscure primes, symbols, and dots must be brought to the attention of the printer. Distinguish very clearly number 1 and letter l. Use fractional exponents instead of root signs and the solidus (/) for fractions wherever their use will save vertical space.

20. All equations must be numbered sequentially in Arabic numerals in parentheses on the right-hand side of the equations.

21. The authors should follow internationally accepted abbreviations, symbols, units, etc., especially those adopted by the Council of Science Editors (CSE) Scientific Style and Format, 7th Edition, 2006.

22. Less common abbreviations may be printed as footnotes.

23. Short communications must be guided by the following points:

    - Short communications are reports of limited data or important findings that warrant publication before the completion of the study;

    - Short communications are reports of significant new data arising from problems with narrow, well defined limits before broader studies are completed; and results have not been published in print elsewhere, except as partial communications or posters in conference proceedings;

- Short communications should not be divided into conventional sections like Introduction, Methodology, etc. but should be provided with keywords, full names and addresses of all authors, current addresses, email addresses, and contact person to whom queries and proofs should be sent;

- Abstracts will be required on submission but not to be part of the Short Communication but for potential reviewers;

- Author must also submit a Layman's Abstract of not more than 200 words;

- Short communications are 3 to 4 print pages (about 6 to 10 manuscript pages) in length with simple layout, a maximum of two tables and two figures, and a small number of citations;

- Authors should make it clear that their work is to be treated as Short Communication.

24. Authors may opt to submit their typeset manuscripts as an email attachment to <science.updiliman@up.edu.ph>. Submissions should be addressed to:

    The Editor in Chief
    SCIENCE DILIMAN
    Office of the Vice-Chancellor for Research and Development
    University of the Philippines
    Lower Ground Floor, Phivolcs Bldg., C.P. Garcia Avenue
    UP Campus, Diliman, Quezon City 1101, Philippines

    Camera-ready illustrations must accompany the manuscript.

Science Diliman: A Philippine Journal of Pure and Applied Sciences is an awardee of the Journal Incubation Grant through the Journal Incubation Program of the Commission on Higher Education (CHED).

WEB OF SCIENCE™

Science Diliman has been selected for coverage in the Emerging Sources Citation Index of Clarivate Analytics (formerly Thomson Reuters Intellectual Property and Science Business).

Science Diliman is listed in ASEAN Citation Index and is available via www.doaj.org and www.ebsco.com